THE REVERSAL OF DOPAMINE TRANSPORTER FUNCTION IS GOVERNED BY PLASMA MEMBRANE INTERACTIONS AND DISRUPTED BY GENETIC VARIATIONS

By

Peter J. Hamilton

Dissertation

Submitted to the Faculty of the

Graduate School of Vanderbilt University

in partial fulfillment of the requirements

for the degree of

DOCTOR OF PHILOSOPHY

in

Neuroscience

December, 2014

Nashville, Tennessee

Approved:

Laurence J. Zwiebel, Ph.D.
Kevin P. Currie, Ph.D.
Hassane S. Mchaourab, Ph.D.
David A. Jacobson, Ph.D.
Aurelio Galli, Ph.D.

For Grace

ACKNOWLEDGMENTS

First, I must acknowledge my mentor, Dr. Aurelio Galli. I am extremely fortunate to have trained with such a driven scientist, and I would not be where I am today without him. I learned a great deal from him during my tenure in the lab, and for that I am truly grateful. I would also like to recognize my thesis committee members Drs. Larry Zwiebel, Kevin Currie, Hassane Mchaourab, David Hachey, and David Jacobson, for their helpful suggestions and guidance throughout my graduate career. Additionally, the members of the Galli lab have helped make this experience instructive and enjoyable. I would specifically like to recognize Dr. Kevin Erreger for training me in electrophysiology, Dr. Christine Saunders for training me in biochemistry, and Dr. Heiner Matthies for being an invaluable scientific resource and spearheading the *Drosophila* behavior experiments. Also, a big thanks to Nicole Bibus-Christianson and Amanda Poe for holding the lab together.

The work presented herein would not have been possible without the funding that helped support it. This includes a National Science Foundation graduate research fellowship (DGE0909667) and a predoctoral NRSA fellowship (DA035535).

Also, I am extremely grateful to my friends and family for their support and encouragement. The friends I made here in Nashville are friends for life. My parents and brothers have been a constant source of support and following their examples has allowed me to maintain perspective throughout this process. Lastly, I am sincerely appreciative to my wife, Grace. She is my inspiration and the foundation of my success.

TABLE OF CONTENTS

LIST OF FIGURES

Figure **Page**

LIST OF ABBREVIATIONS

5-HT	**Serotonin**
ACh	**Acetylcholine**
ADE	**Anomalous DAT-mediated DA efflux**
ADIR	**Autism Diagnostic Interview Revised**
ADOS	**Autism Diagnostic Observational Session**
ADHD	**Attention-deficit hyperactivity disorder**
AMPH	**Amphetamine**
ANOVA	**Analysis of variance**
ASD	**Autism spectrum disorder**
BoNT/C	**Botulinum toxin serotype C**
CaMKII	**Calcium/calmodulin-dependent kinase II**
CHO	**Chinese hamster ovary**
CK2	**Casein kinase 2**
CNS	**Central nervous system**
CNV	**Copy number variation**
COC	**Cocaine**
CTR	**Control**
DA	**Dopamine**

DAG	**Diacylglycerol**
DAT	**Dopamine transporter**
dDAT	***Drosophila melanogaster* dopamine transporter**
DEER	**Double electron electron resonance**
DR	**Dopamine receptor**
ECL	**Extracellular loop**
EPI	**Electrostatic potential isosurfaces**
EPR	**Electron paramagnetic resonance**
ERK	**Extracellular signal-regulated kinase**
GAT	**γ-aminobutyric acid transporter**
GFP	**Green fluorescent protein**
GST	**Glutathione S-transferase**
hDAT	**Human dopamine transporter**
HEK	**Human embryonic kidney**
HFA	**High functioning autism**
hM1R	**Human muscarinic acetylcholine receptor M1**
IP_3	**Inositol trisphosphate**
LeuT	**Leucine transporter**
MD	**Molecular dynamics**
MPH	**Methylphenidate**

NET	**Norepinephrine transporter**
NSS	**Neurotransmitter:sodium symporters**
PET	**Positron emission tomography**
PH	**Pleckstrin homology**
PI3K	**Phosphatidylinositol 3-kinase**
PIP_2	**Phosphatidylinositol (4,5)-bisphosphate**
PIP_3	**Phosphatidylinositol (3,4,5)-trisphosphate**
PKA	**Protein kinase A**
PKC	**Protein kinase C**
PKCβ	**Protein kinase C β**
PLC_δ	**Phospholipase C_δ**
POPC	**Phosphatidylcholine**
POPE	**Phosphatidylethanolamine**
RFP	**Red fluorescent protein**
SCG	**Superior cervical ganglion**
SCMFM	**Self-consistent mean-field model**
SERT	**Serotonin transporter**
SLC6	**Solute carrier 6**
SNARE	**Soluble NSF attachment receptor**
SNP	**Single nucleotide polymorphism**

SNV	**Single nucleotide variation**
SRS	**Social Responsiveness Scale**
STX1	**Syntaxin 1**
TBB	**4,5,6,7-tetrabromobenzotriazole**
TH	**Tyrosine hydroxylase**
TMD	**Transmembrane domain**
VMAT	**Vesicular monoamine transporter**
VTA	**Ventral tegmental area**
WES	**Whole exome sequencing**
WPPSI	**Wechsler Preschool and Primary Scale of Intelligence**
WT	**Wild type**

CHAPTER I

INTRODUCTION AND LITERATURE REVIEW

Overview of the Dopaminergic System

Dopamine (3,4-Dihydroxyphenethylamine; DA) is a catecholamine neurotransmitter that plays several important roles in the human central nervous system (CNS). Within the CNS, there are four major dopaminergic pathways: the tuberoinfundibular pathway, the nigrostriatal pathway, the mesocortical pathway, and the mesolimbic pathway (**Fig. 1**). The tuberoinfundibular pathway consists of DA neurons that project from the hypothalamus to the pituitary gland. These neurons mediate the secretion of prolactin, a hormone that stimulates lactation(Fitzgerald and Dinan, 2008). The nigrostriatal pathway consists of DA neurons that project from the substantia nigra to the striatum, which play an important role in voluntary motor control. Interestingly, these neurons are vulnerable to damage, and their death results in a Parkinsonian syndrome(Beitz, 2014). The mesocortical pathway consists of DA neurons that project from the ventral tegmental area (VTA) to the frontal lobes of the cerebrum, particularly the prefrontal cortex. The mesocortical pathway is involved in cognitive processing, motivation, and emotion(Miller and Cohen, 2001). Lastly, the mesolimbic pathway consists of DA neurons that originate in the VTA and project to the nucleus accumbens. The mesolimbic pathway is important in mediating reward and pleasure(Wise, 1998).

Within these dopaminergic pathways, DA neurotransmission modulates the physiological and behavioral processes of executive function, movement, motivation, mood, and reward(Bjorklund and Dunnett, 2007). Alterations in DA neurotransmission are thought to contribute to the

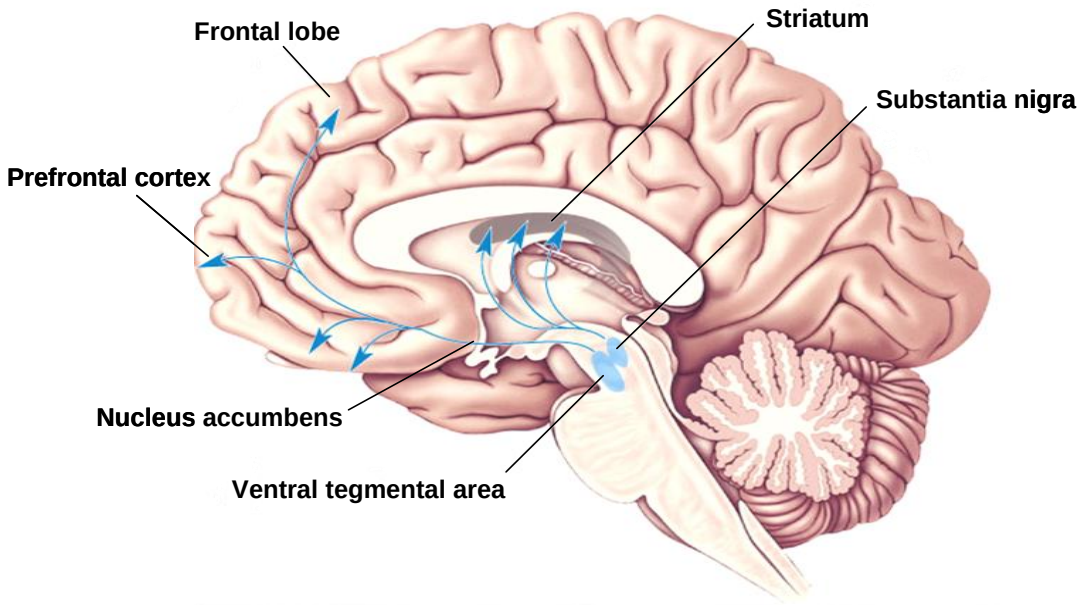

Figure 1. Schematic illustration of dopaminergic pathways. Dopaminergic neurons in the ventral tegmental area project to the nucleus accumbens and prefrontal cortex to form the mesolimbic and mesocortical pathways, respectively. Dopaminergic neurons in the substantia nigra project to the striatum to form the nigrostriatal pathway. The tuberoinfundibular pathway is not depicted. Image adapted from Neuroscience Exploring the Brain Third Edition by Mark F. Barry, Barry Connor, and Mark. F. Paradiso.

pathogenesis of neuropsychiatric disorders, including schizophrenia, bipolar disorder, attention-deficit hyperactivity disorder (ADHD), and drug abuse(Seeman and Niznik, 1990, Volkow *et al.*, 2007, Cousins *et al.*, 2009, Kristensen *et al.*, 2011). More recently, dysfunctional DA neurotransmission has been implicated in the etiology of autism spectrum disorder (ASD)(Hamilton *et al.*, 2013, Bowton *et al.*, 2014, Nguyen *et al.*, 2014) .

DA neurotransmission occurs at the synapse and is shaped by synaptic features, which include the amount of DA released, the signaling of pre- and postsynaptic DA receptors, and the time that DA spends in the synaptic space. The DA transporter (DAT) is a presynaptic protein that mediates the high affinity re-uptake of DA from the synaptic space, thereby controlling the post-synaptic exposure to DA(Kristensen *et al.*, 2011). The DAT regulates the intensity and duration of the dopaminergic response, making it a crucial regulator of DA neurotransmission. Therefore, a more complete understanding of the events that regulate DAT function in health and disease may yield an improved understanding of the etiology of these disorders and result in more appropriately targeted pharmacotherapies.

Dopamine Transporter Structure

The DAT is member of the solute carrier 6 (SLC6) gene family of Na^+/Cl^- symporters, which includes other monoamine transporters, such as the serotonin transporter (SERT) and norepinephrine transporter (NET). In the early 1990s, molecular cloning experiments revealed a highly conserved amino acid sequence across SLC6 transporters, suggesting a shared general structure(Blakely *et al.*, 1991). Indeed, the DAT and other SLC6 transporters consist of a membrane topology with 12 transmembrane domain (TMD) helices with intracellular N- and C-termini and a large glycosylated loop between transmembrane helices III and IV (**Fig. 2**). This topology has been confirmed by the high resolution structure of LeuT, a prokaryotic sodium-

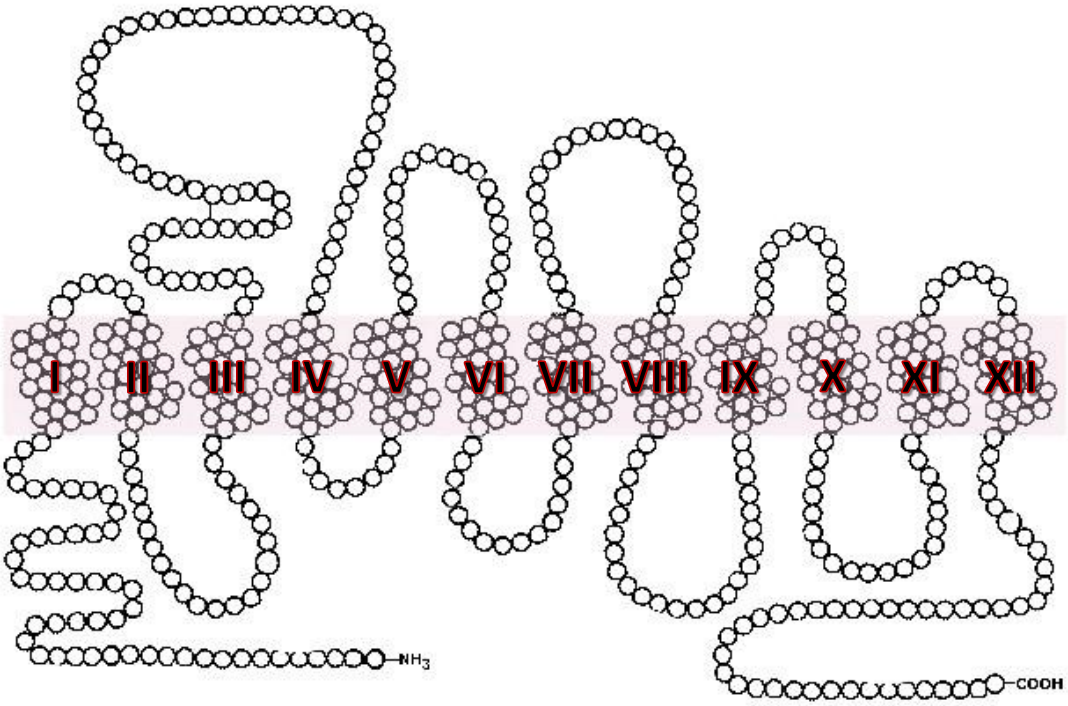

Figure 2. Topology of the dopamine transporter (DAT). The DAT is predicted to have twelve transmembrane helices with cytoplasmic N- and C-termini.

dependent leucine transporter with significant homology to DAT(Yamashita *et al.*, 2005), and, more recently, by the high resolution structure of the *Drosophila melanogaster* DAT ($dDAT_{cryst}$) (**Fig. 3**)(Penmatsa *et al.*, 2013). The N-terminus of the DAT has proved difficult to include in a DAT crystal structure, thus there are a scarcity of structural insights to this functional domain. However, the N-terminus of the DAT is recognized as a major regulator of DAT function. The N-terminus contains numerous putative phosphorylation sites, including Ser residues located at position 2, 4, 7, 12, and 13. The phosphorylation of these Ser residues are thought to regulate specific aspects of DAT function, particularly DAT-mediated reverse transport of DA(Khoshbouei *et al.*, 2004, Fog *et al.*, 2006, Bowton *et al.*, 2010).

Dopamine Transporter Function

A characteristic of the transporters in the SLC6 gene family is the use of the ion concentration gradient as the driving force for transporter-mediated re-uptake of their respective substrate(Gu *et al.*, 1994). In the case of the DAT, the uptake of DA is coupled with the translocation of two Na^+ ions and one Cl^- ion, resulting in a net movement of two positive charges per DA molecule (since DA is positively charged at physiological pH)(Krueger, 1990). In the LeuT, a Cl^- independent transporter, two distinct sites were discovered to be occupied by Na^+ ions, designated Na1 and Na2(Yamashita *et al.*, 2005). In $dDAT_{cryst}$, the resolution of the Cl^- binding site was resolved in addition to the two Na^+ binding sites(Penmatsa *et al.*, 2013). The amino acids that comprise these ion binding sites are conserved across phylogeny and SLC6 transporters, underscoring their importance in DAT function. Both Na^+ binding sites and the Cl^- binding site are believed to play a role in stabilizing the DAT in the presence of substrate, thereby allowing substrate translocation *via* a conformational change in the transporter.

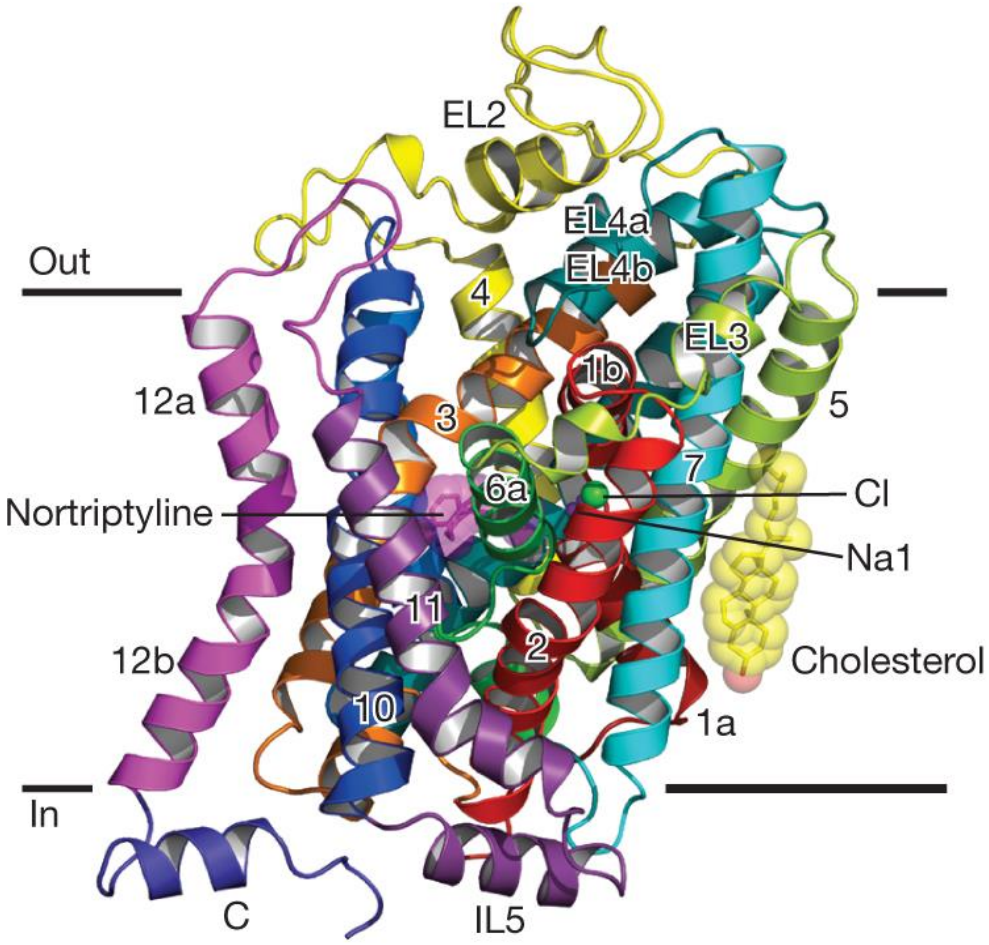

Figure 3. Structure of *Drosophila* dopamine transporter ($dDAT_{cryst}$). Architecture of $dDAT_{cryst}$ viewed parallel to membrane. Nortriptyline (a tricyclic antidepressant), sodium ions, a chloride ion, and a cholesterol molecule co-crystallized with the $dDAT_{cryst}$ are shown in sphere representation in magenta, purple, green and yellow, respectively. Image adapted from Penmatsa *et al. Nature* **503**, 85-90 (2013).

The concept that the DAT assumes conformations required for substrate translocation is reinforced by studies exploring zinc regulation of DAT. The DAT contains three endogenous, extracellular-facing amino acids (His193, His375, and Gln396) that coordinate zinc binding(Norregaard *et al.*, 1998, Loland *et al.*, 1999)(**Fig. 4**). Zinc binding to these DAT residues results in an inhibition of DA transport but not an inhibition of substrate binding(Norregaard *et al.*, 1998), suggesting that conformational changes in extracellular loops (ECLs) 2 and 4 are necessary for substrate translocation. A Tyr to Ala mutation in the third intracellular loop of hDAT (hDAT Y335A) (seen in **Fig. 4**) converts the inhibitory action of zinc into a zinc-dependent activation of transporter uptake(Loland *et al.*, 2002). Despite normal substrate affinity and surface expression, hDAT Y335A displays a dramatic decrease in the V_{max} for DA uptake that can be partially recovered in the presence of zinc(Loland *et al.*, 2002). Taken together, the dichotomous actions of zinc are consistent with a shift in the distribution of conformational states in the transport cycle.

A helpful conceptual model for understanding changes in DAT conformation in the DAT transporter cycle is the classical “alternating access” model of transporter function(Jardetzky, 1966). The model assumes the DAT is capable of an “outward-facing” conformation, in which extracellular DA, Na^+, and Cl^- are required to bind to the transporter in a fixed ratio and induce a conformational change, resulting in an “inward-facing” conformation and the dissociation of the cargo, thereby completing the transport of DA from the synaptic space into the cytosol. Thus, the conformational equilibrium between “inward”- and “outward”-facing states is determined by binding of ions and substrate and mediated by the physical movement of DAT structural domains.

Dopamine Transporter-Mediated Reverse Transport

There is an inherent asymmetry of ion and substrate concentration, membrane potential, and DAT protein structure when using the neuronal cell membrane as the axis of symmetry. This

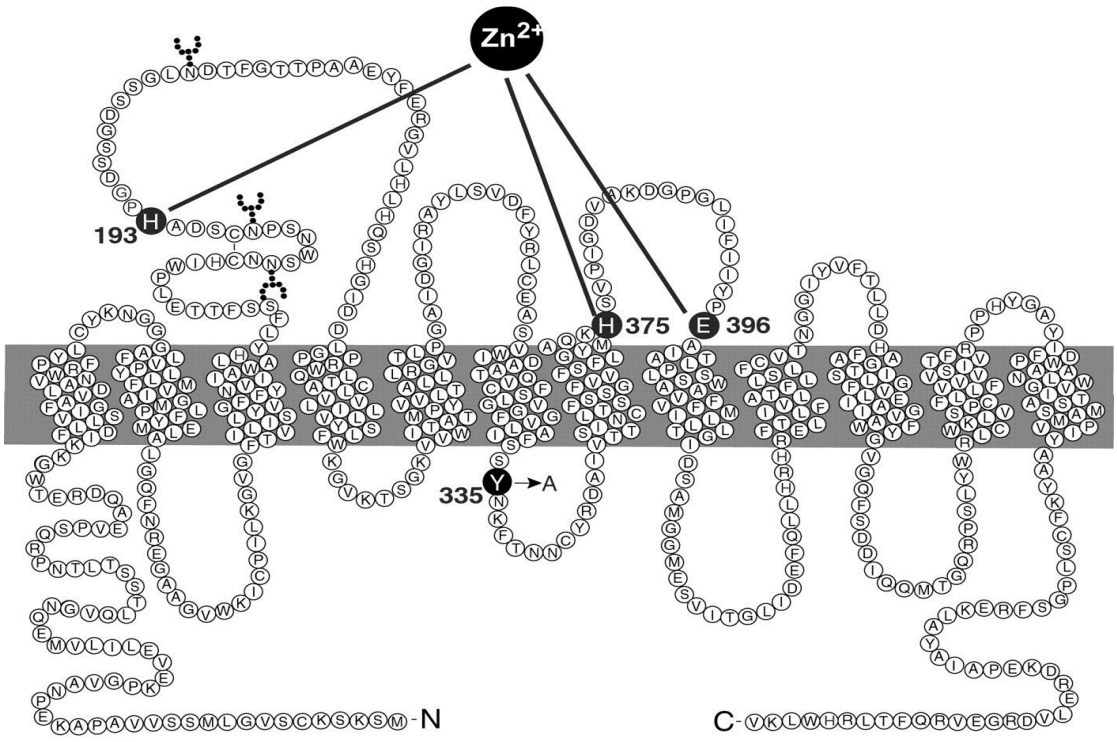

Figure 4. Endogenous zinc binding sites in the human dopamine transporter (hDAT) and hDAT Y335A. The hDAT residues that coordinate the binding of zinc are illustrated in black. His193 is located in the second extracellular loop, while His375 and Gln396 are located in the fourth extracellular loop. Additionally, mutation of the intracellular Tyr to an Ala at position 335 is highlighted here. Image from Loland *et al. PNAS* **99**, 1683-1688 (2002).

may seem to suggest that the DAT is only capable of DA re-uptake. However, there are clear and documented instances of the reversal of the DAT function, where the net flow of DA, mediated by the DAT, travels from the cell cytosol to the extracellular space(Pifl *et al.*, 1995, Wall *et al.*, 1995, Khoshbouei *et al.*, 2003). These well-documented conditions in which reverse transport is known to occur are: exposure to psychostimulants such as amphetamine (AMPH), activation of second messenger signaling pathways and proteins, and DAT coding variants identified in neuropsychiatric disease.

Reverse Transport: Amphetamines

Pharmacological substances have long been used to study the process of DAT-mediated DA efflux, not only due to the merit of understanding the molecular events that surround human abuse of these substances, but also because these substances provide a mechanism to induce the molecular events that are required for reverse transport, allowing this phenomenon to be studied. Of these pharmacological substances, AMPH is the gold standard.

AMPH is a psychostimulant that primarily exerts its pharmacological effects by altering DAT function(Jones *et al.*, 1998). AMPH and its congeners, including methamphetamine, are structurally similar to DA, and are therefore substrates for the DAT (**Fig. 5**). AMPH competitively inhibits DA re-uptake, thereby increasing synaptic DA concentration. Additionally, AMPH elicits DAT-mediated DA release in the CNS(Fischer and Cho, 1979, Jones *et al.*, 1998) and in cells expressing the DAT(Pifl *et al.*, 1995, Wall *et al.*, 1995, Sitte *et al.*, 1998, Khoshbouei *et al.*, 2003). AMPH competes with DAT substrates for interaction with the “outward-facing” conformation of the DAT. AMPH is translocated into the intracellular space, which increases the availability of “inward-facing” binding sites of the DAT(Fischer and Cho, 1979). Once inside the cell, AMPH interacts with the vesicular monoamine transporter (VMAT). AMPH is a weak base,

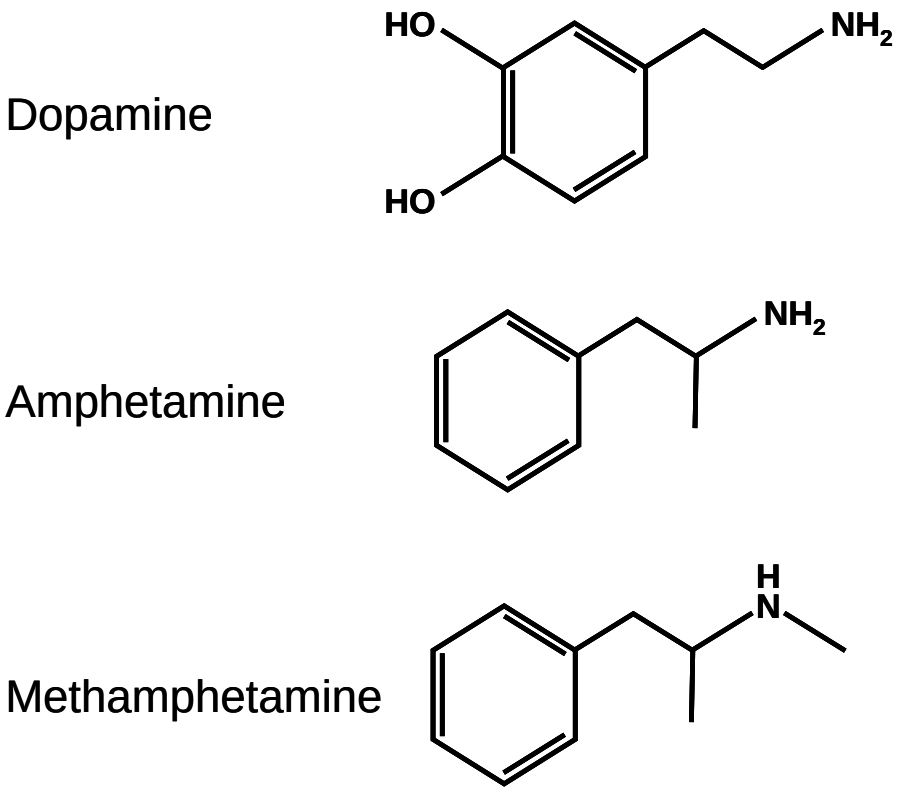

Figure 5. Chemical structure of DAT substrates. DAT substrates are depicted here, including the physiological substrate dopamine and the psychostimulant substrates amphetamine and methamphetamine.

thus it alters the pH gradient necessary for VMAT to package DA in synaptic vesicles(Sulzer *et al.*, 1995). This results in an increase in cytosolic DA concentration. This cytosolic DA has access to the "inward-facing" binding sites on the DAT, and, along with the increased intracellular Na^+ concentration promoted by AMPH translocation, it stimulates a DAT-mediated DA efflux(Fischer and Cho, 1979). This increases the synaptic DA concentration, which activates downstream signaling pathways.

Reverse Transport: Associated Proteins

The scope of AMPH's influence on DAT function is not limited to direct interactions with the DAT itself. AMPH can influence the local and transient environment surrounding the DAT, which, in turn, can influence the properties of the DAT. Ultimately, exposure to AMPH shifts the DAT from a "reluctant" state to a "willing" state, an state that favors reverse transport of DA(Khoshbouei *et al.*, 2004). These modulations in DAT function are thought to be mediated, at least in part, by the activities of DAT-interacting proteins that become catalytically active in response to AMPH exposure.

There are numerous putative phosphorylation sites within the intracellular domains of DAT, suggesting that the DAT is amenable to regulation by kinases. Indeed, the distal N-terminal region of the DAT contains crucial Ser residues that, when phosphorylated, promote reverse transport of DA without affecting DAT uptake function(Khoshbouei *et al.*, 2004). When truncated or replaced with non-phosphorylatable Ala residues, the AMPH-induced DA efflux is reduced by 80%(Khoshbouei *et al.*, 2004). Alternatively, when these Ser are replaced with Asp, which mimics phosphorylation, the ability of the DAT to efflux DA remains intact, suggesting that phosphorylation of one or more of these Ser are critical for AMPH-induced DA release(Khoshbouei *et al.*, 2004). Importantly, these N-terminal residues can be phosphorylated by protein kinase C

(PKC)(Giambalvo, 1992, Johnson *et al.*, 2005) and Ca^{2+}/calmodulin-dependent protein kinase II (CaMKII)(Fog *et al.*, 2006, Bowton *et al.*, 2010).

Both PKC and CaMKII have been revealed to be major regulators of DAT-mediated reverse transport. Researchers have discovered that AMPH exposure can induce an increase in PKC activity *in vivo*(Giambalvo, 1992). Inhibition of PKC prevents AMPH-induced DA efflux in rat striatal slices(Kantor and Gnegy, 1998, Johnson *et al.*, 2005), and exposure to phorbol esters, compounds that promote PKC activity, induces DA efflux in the absence of AMPH(Cowell *et al.*, 2000). In the rat striatum, a physical interaction was observed between the DAT and one of the PKC family isozymes, PKCβII(Johnson *et al.*, 2005), highlighting tight regulation of the DAT by PKC. A physical interaction between CaMKII and the DAT C-terminus has been observed, as well(Fog *et al.*, 2006). Disruption of this interaction or inhibition of CaMKII reduces reverse transport of DA in both *in vitro* and *in vivo* preparations(Fog *et al.*, 2006). Interestingly, AMPH treatment increases CaMKII activity in striatal synaptosomes, an effect that can be blocked in the absence of extracellular Ca^{2+} or in the presence of nomifensine, a DAT inhibitor(Iwata *et al.*, 1997). This suggests that both Ca^{2+} and DAT activity are required for AMPH to potentiate CaMKII activity. Importantly, AMPH has been shown to increase intracellular Ca^{2+} in DAT expressing cells, a process mediated by DAT activity(Gnegy *et al.*, 2004) and dependent on voltage-gated N- and L-type Ca^{2+} channel activity(Kantor *et al.*, 2004). Therefore, AMPH may activate CaMKII and other second messenger signaling pathways by increasing intracellular Ca^{2+} concentration.

A potential mediator of CaMKII's influence on DAT-mediated reverse transport of DA is the protein syntaxin 1 (STX1). STX1 is a member of the soluble N-ethylmaleimide-sensitive factor attachment protein receptor (SNARE) complex, which is required for the docking and release of synaptic vesicles(Sudhof and Rothman, 2009). Aside from its role in the SNARE complex, there is a growing body of evidence to suggest that STX1 associates with and regulates the function

of ion channels and SLC6 transporters, including the DAT(Quick, 2006, Ahmed *et al.*, 2007, Dipace *et al.*, 2007, Binda *et al.*, 2008). STX1 was revealed to directly interact with the distal region of the DAT N-terminus in both a yeast-two hybrid system(Lee *et al.*, 2004) and in a glutathione S-transferase (GST) pull-down assay(Binda *et al.*, 2008). These STX1/DAT interactions have been observed to mediate a decrease in the V_{max} of DA transport in both rat striatal tissues and in heterologous expression systems(Cervinski *et al.*, 2010). The STX1/DAT interactions are demonstrated to increase in response to AMPH and play an important role in the regulation of AMPH-induced DA efflux, as well(Dipace *et al.*, 2007, Binda *et al.*, 2008). STX1/DAT interaction promotes the ability of the DAT to efflux DA(Binda *et al.*, 2008). This indicates an asymmetric relationship in the ability of STX1 to regulate DAT uptake and efflux, where STX1/DAT interactions inhibit DAT uptake function and potentiate DAT efflux function. Moreover, the activity of the CaMKII mediates the STX1/DAT association, the interaction can be inhibited through the use of CaMKII inhibitors, and CaMKII inhibition reduces AMPH-induced DA efflux preferentially in STX1 expressing cells(Dipace *et al.*, 2007, Binda *et al.*, 2008). These data reveal the complexity of the events surrounding reverse transport of DA, including activation of protein kinases, DAT N-terminal phosphorylation, and subsequent alterations in N-terminal interactions. The sequence and the delineation of the molecular regulators of these events have yet to be elucidated.

Reverse Transport: DAT Coding Variants

In the previous examples of DAT-mediated reverse transport of DA, the efflux of DA was stimulated pharmacologically (e.g. by AMPH or phorbol esters) and modulated by key associated proteins (e.g. STX1). However, in recent years, there has been a proliferation of data outlining instances of DAT coding variations, identified in neuropsychiatric disease populations that promote alterations in DAT function, including a constitutive release of DA.

One well characterized mutation identified in multiple neuropsychiatric disease populations is the hDAT A559V, where an inherited missense mutation induces an Ala to Val substitution at site 559. Expressing the hDAT A559V in heterologous cells revealed that the DAT variant exhibited normal protein and cell surface expression, as well as normal DA uptake, yet an anomalous DA efflux (ADE) that occurred under basal conditions(Mazei-Robison *et al.*, 2008). The hDAT A559V variant was more sensitive to intracellular Na^+ and cell depolarization than hDAT, as seen by increased magnitude of DAT-mediated reverse transport under these conditions(Mazei-Robison *et al.*, 2008). Interestingly, both AMPH and methylphenidate (MPH), a DAT blocker, inhibited the hDAT A559V-mediated ADE(Mazei-Robison *et al.*, 2008). It was further revealed that tonic activation of DAT-associated D_2 receptors promoted an activation of CaMKII and subsequent DAT N-terminal phosphorylation of Ser residues which, in turn, supported hDAT A559V-mediated ADE(Bowton *et al.*, 2010). Most recently, it was observed that although hDAT A559V has normal transport of the substrate DA(Mazei-Robison and Blakely, 2005, Mazei-Robison *et al.*, 2008, Bowton *et al.*, 2010), the hDAT A559V has reduced ability to transport AMPH, suggesting that conformational dynamics of the transporter are altered in the A559V variant(Bowton *et al.*, 2014). The hDAT A559V is resistant to AMPH-induced cell surface redistribution(Bowton *et al.*, 2014), a phenomenon commonly observed in the hDAT(Chen *et al.*, 2010). This is thought to be linked to the chronic phosphorylation of the five most distal N-terminal Ser residues and stem from constitutively elevated PKCβ activity(Bowton *et al.*, 2014). Interestingly, hDAT A559V was identified in multiple separate disease populations including: a bipolar individual, two brothers diagnosed with ADHD, and, importantly, in two probands with ASD(Grunhage *et al.*, 2000, Mazei-Robison *et al.*, 2005, Bowton *et al.*, 2014). In all subjects with known inheritance, hDAT A559V was transmitted from an unaffected mother to a male child with a neurodevelopmental disorder, raising the possibility of a sex effect on penetrance. Interestingly, these three neuropsychiatric disorders share specific characteristics, particularly the

DA-related trait of hyperactivity. Indeed, ADHD is frequently comorbid with pediatric onset bipolar disorder(Faraone and Tsuang, 2003), and a co-occurrence of ADHD symptoms is common in ASD(Matson *et al.*, 2013). These shared traits between bipolar disorder, ADHD, and ASD suggest dysregulation of common pathways across these neurodevelopmental disorders, with DAT regulation as a mediator of one such potential pathway.

Separate studies have identified an adult male with both early-onset parkinsonism and ADHD who possesses a *de novo* missense mutation in the hDAT gene, resulting in Asp to Asn substitution at site 421(hDAT D421N)(Hansen *et al.*, 2014). The patient suffered from progressive dopaminergic neurodegeneration over the span of eight years, according to DAT single-photon emission computed tomography scans and a fluoro-deoxy-glucose-PET/MRI scan(Hansen *et al.*, 2014). When the hDAT D421N variant was expressed in heterologous cells, it displayed increased levels of total and cell surface expression, yet reduced DA uptake capacity and a constitutive ADE, similar to that observed in hDAT A559V(Hansen *et al.*, 2014). The dramatically altered function was thought to be due to disrupted Na^+ binding at Na2, since Asp421 participates in the Na^+ coordination at that site(Penmatsa *et al.*, 2013, Hansen *et al.*, 2014). These data reinforce the important role that Na^+ binding plays in substrate translocation and in normal DAT function. Furthermore, it highlights the role that DAT genetic variation may play in neuropsychiatric disorders, and it supports the notion that DA dysfunction, promoted by altered DAT function, can contribute to the pathogenesis of brain disorders.

Dopamine and Autism Spectrum Disorder

ASD is a neurodevelopmental disorder defined by impairments in social interactions, including verbal and non-verbal communication, impairments in social reciprocity, as well as restricted interests and repetitive behaviors. Individuals with ASD may display a spectrum of these

symptoms and may vary in symptom severity, with some individuals demonstrating above average intelligence and others with profound intellectual disability. Currently, no biological test for ASD exists. Instead, researchers and clinicians depend on highly sensitive and specific behavioral tests involving standardized interviews and psychometric and cognitive assessments(Lord *et al.*, 1994, Lord *et al.*, 2000, Wall *et al.*, 2012). ASD is considered one of the most common neuropsychiatric diseases in the United States, with a current prevalence estimated at 1 in 88(Baio, 2012). While no age of onset is required for a diagnosis, the symptoms often present early in life, thus the public health impact of ASD is substantial, since support and services are often required throughout the individual's lifetime. Currently, there is no curative treatment or broadly effective pharmacotherapy for the treatment of the multifarious symptoms of ASD. Therefore, a more complete understanding of the etiology of ASD may improve the rational design of pharmacotherapies and reduce the burden of the disorder.

ASD is one of the most heritable brain disorders(Crawley, 2012), and heritable genetic factors are established as important components in the etiology of ASD(Devlin and Scherer, 2012). Concordance rates for an ASD diagnosis are estimated at 10% for dizygotic twins and 92% for monozygotic twins(Bailey *et al.*, 1995, Ronald and Hoekstra, 2011). Rare genetic variation of nucleotides in protein-coding DNA, as well as rare genomic copy number variants are established as significant risk factors for ASD(Sebat *et al.*, 2007, Pinto *et al.*, 2010, Levy *et al.*, 2011, Sanders *et al.*, 2011, Devlin and Scherer, 2012, Sanders *et al.*, 2012). Aside from heritable factors, mounting evidence suggests that *de novo* genetic variation (genetic variation present in the progeny, but not either parent) contributes to ASD risk(Iossifov *et al.*, 2012, Neale *et al.*, 2012, O'Roak *et al.*, 2012, Sanders *et al.*, 2012). Multiple groups have conducted whole-exome sequencing of ASD families, and, collectively, these studies point to discrete *de novo* coding variation (single nucleotide variation or small insertion/deletion variants) as contributing factors to the genetic risk for ASD(Iossifov *et al.*, 2012, Neale *et al.*, 2012, O'Roak *et al.*, 2012,

Sanders *et al.*, 2012). By identifying the genetic locus of these *de novo* mutations and delineating the broader pathways that they function within, it may be possible to more clearly understand the risk factors that contribute to the deficits observed in ASD.

Genetic factors within the DA system are becoming increasingly important in understanding the etiology of ASD. Variations in genes encoding DA receptors(Reiersen and Todorov, 2011, Hettinger *et al.*, 2012, Qian *et al.*, 2013), enzymes important for both DA synthesis and catabolism(Yoo *et al.*, 2013, Nguyen *et al.*, 2014), and the DAT(Hamilton *et al.*, 2013, Bowton *et al.*, 2014) have been associated with ASD. Medications affecting dopaminergic neurotransmission are efficacious in the treatment of some symptoms of ASD(Hosenbocus and Chahal, 2012, Hsia *et al.*, 2014). In subjects with ASD, DA dysfunction has been demonstrated within brain regions involved in reward processing, including the nucleus accumbens(Scott-Van Zeeland *et al.*, 2010, Dichter *et al.*, 2012). The function and expression of the DAT has been linked to reward processes(Giros *et al.*, 1996, Volkow *et al.*, 1997, Volkow *et al.*, 2001). Genetic variation in the gene that encodes the human DAT alters anticipation and reception of rewards, as well as the motivational responses to social-emotional cues(Dreher *et al.*, 2009, Enter *et al.*, 2012, Hoogman *et al.*, 2013). In humans, functional polymorphisms in the DAT have been associated with neuropsychiatric disorders, including ASD(Mazei-Robison and Blakely, 2005, Mazei-Robison *et al.*, 2005, Bowton *et al.*, 2010). These data underscore the significance of the dopaminergic system in the pathogenesis of ASD and point to dysfunction in dopaminergic genes, particularly the DAT gene, as potential risk factors for ASD and related neuropsychiatric disorders.

CHAPTER II

PHOSPHATIDYLINOSITOL (4,5)-BISPHOSPHATE REGULATES PSYCHOSTIMULANT BEHAVIORS THROUGH ITS INTERACTION WITH THE DOPAMINE TRANSPORTER[*]

Preface

This chapter explores the role of DAT-PIP_2 interactions in the mechanism of AMPH actions. A complete presentation of these data can be found in Hamilton and Belovich *et al.*(Hamilton *et al.*, 2014).

Abuse of AMPH represents a major public health concern, placing a burden on both society and the individual due to its profound medical and psychological complications. AMPH's addictive properties are mediated through elevation of extracellular DA by inducing DA efflux *via* the DAT. It is now clear that in order to pharmacologically target AMPH actions, it is essential to understand how to precisely manipulate DAT to prevent elevation of extracellular DA. The work presented within this chapter demonstrates that PIP_2 directly binds, through electrostatic interactions, to positively charged DAT N-terminal residues. This interaction is required for robust AMPH-induced, DA efflux and behaviors.

PIP_2 is a minor phospholipid component of cell membranes, where it participates in signaling cascades and acts as a substrate for a number of important signaling proteins. Our data demonstrate that PIP_2 coordinates complex molecular events underlying AMPH actions, and we

[*] The work presented in this chapter is *in press* as Hamilton PJ[*], Belovich AN[*], Khelashvili G, Saunders C, Erreger K, Javitch JA, Sitte HH, Weinstein H, Matthies HJG[*], Galli A[*]. (2014). PIP2 regulates psychostimulant behaviors through its interaction with a membrane protein. *Nature Chemical Biology* 10(7):582-9

report that obstructing DAT-PIP_2 interaction impairs both DA efflux and AMPH behaviors, without altering the DAT physiological function of DA uptake. Using computational modeling, we provide the first molecular level description of the direct interaction between DAT and PIP_2 and resolve how the DAT N-terminal conformations dictate different aspects of the transport cycle.

Furthermore, this chapter presents novel findings in the introduction of the first animal model describing the behavioral consequences of disrupting PIP_2 interactions with a plasma membrane protein, here the DAT. In *Drosophila melanogaster*, we evaluated the behavioral significance of our molecular discoveries by exploring their relevance in AMPH-induced behaviors. We report that hindering the DAT-PIP_2 interaction in the dopaminergic neurons of these flies reduces the psychomotor effects of AMPH exposure, without affecting circadian locomotor activity.

The study presented within this chapter has broad implications, including: 1) presenting an *in vivo* framework in which to study the behavioral consequences of PIP_2-protein interactions; 2) defining the DAT N-terminus as a structural domain that dictates specific aspects of DAT transport cycle *via* its interaction with PIP_2, a mechanism that may be conserved across the neurotransmitter transporter family; 3) outlining DAT-PIP_2 interaction as “druggable” target for pharmacotherapies treating AMPH abuse and dependence.

Despite the well-documented role of PIP_2 as plasma membrane element that directly interacts with ion channels and transporters, before this work, there was no evidence that alterations in PIP_2 interactions play a significant role at the behavioral level. This work demonstrates this concept and presents novel molecular-level insights into the mechanisms underpinning the psychomotor effects of AMPH.

Abstract

Phosphatidylinositol (4,5)-bisphosphate (PIP_2) regulates the function of ion channels and transporters. Here, we demonstrate that PIP_2 directly binds the human dopamine (DA) transporter (hDAT), a key regulator of DA homeostasis and a target of the psychostimulant amphetamine (AMPH). This binding occurs through electrostatic interactions with positively charged hDAT N-terminal residues and is shown to facilitate AMPH-induced, DAT-mediated DA efflux and the psychomotor properties of AMPH. Substitution of these residues with uncharged amino acids reduces hDAT-PIP_2 interactions and AMPH-induced DA efflux without altering the hDAT physiological function of DA uptake. We evaluated the significance of this interaction *in vivo* using locomotion as a behavioral assay in *Drosophila melanogaster*. Expression of mutated hDAT with reduced PIP_2 interaction in *Drosophila* DA neurons impairs AMPH-induced locomotion without altering basal locomotion. We present what is to our knowledge the first demonstration of how PIP_2 interactions with a membrane protein can regulate the behaviors of complex organisms.

Introduction

The functional regulation of plasma membrane proteins by lipid molecules is an integral component of cell function and metabolism(McLaughlin and Murray, 2005, Suh and Hille, 2008). Phosphatidylinositol (4,5)-bisphosphate (PIP_2) is the phospholipid precursor of the second messengers inositol trisphosphate (IP_3), diacylglycerol (DAG), and phosphatidylinositol (3,4,5)-trisphosphate (PIP_3), and is, itself, capable of acting as a second messenger and cofactor for regulating protein function(Czech, 2000, Suh and Hille, 2008, Whorton and MacKinnon, 2011, Ben-Aissa *et al.*, 2012, Kadamur and Ross, 2013). Additionally, PIP_2 has been shown to modulate, through electrostatic interactions, the *in vitro* function of ion channels and transporters, including the serotonin transporter (SERT)(Suh and Hille, 2008, Buchmayer *et al.*,

2013). A sizeable research effort has been dedicated to determining the diversity of cellular roles for PIP_2 and defining the ubiquity of its electrostatic interactions with various plasma membrane proteins, but how these interactions might modulate the behaviors of complex organisms *in vivo* has never been studied.

The plasma membrane dopamine (DA) transporter (DAT) is a presynaptic protein that plays a pivotal role in regulating DA neurotransmission by mediating the high-affinity reuptake of synaptically-released DA. Gene knockout experiments in multiple organisms, including *Drosophila melanogaster*(Hamilton *et al.*, 2013, Pizzo *et al.*, 2013), point to the DAT as the main target for the locomotor stimulatory effects of amphetamine (AMPH)(Giros *et al.*, 1996). AMPH's addictive properties are mediated, at least in part, through elevation of extracellular DA by inducing DA efflux through the DAT(Sulzer *et al.*, 2005, Robertson *et al.*, 2009). Thus, in order to target and limit AMPH actions pharmacologically, it is essential to understand how to precisely manipulate the DAT to prevent DA efflux without altering its physiological function of DA uptake.

The DAT N-terminus is a structural domain of functional significance. AMPH targets the N-terminus to cause posttranslational modifications (e.g. phosphorylation(Cervinski *et al.*, 2005)), which are essential for AMPH to cause DA efflux(Khoshbouei *et al.*, 2004, Fog *et al.*, 2006) and behaviors(Pizzo *et al.*, 2013). Notably, DAT localization to plasma membrane lipid rafts is also vital for DA efflux(Cremona *et al.*) and AMPH-induced behaviors(Pizzo *et al.*, 2013). In this study, we elucidate how plasma membrane PIP_2, which is enriched in lipid rafts(Hope and Pike, 1996, Wang and Richards, 2012), dictates specific aspects of the transport cycle through its interactions with the N-terminus of the DAT. In terms of AMPH-induced DA efflux, our experimental and computational data demonstrate that the regulatory effect of PIP_2 stems from its electrostatic association with the N-terminus. Here, we introduce the first animal model

(*Drosophila melanogaster*) in which we evaluate the behavioral consequences of altered PIP_2 interactions with a plasma membrane protein. We reveal that DAT-PIP_2 interactions are required for AMPH-induced behaviors, thereby presenting PIP_2 and its synthetic pathway as novel regulators of AMPH abuse.

Results

DAT associates with PIP_2

In this study, we aimed to determine the modalities of the regulatory function of PIP_2 in terms of DA homeostasis and AMPH actions. We hypothesized that this regulatory function may be mediated through a physical association between DAT and PIP_2. Using live confocal imaging, we show that in hDAT cells, GFP-hDAT (green) co-localized (yellow) with a plasma membrane PIP_2 sensor (red) (**Fig. 6a**). As a PIP_2 sensor, we used the pleckstrin homology (PH) domain from phospholipase C_δ ($PHPLC_\delta$-mRFP) that binds specifically to PIP_2 at the plasma membrane and has been used to monitor pools of PIP_2(Varnai and Balla, 1998). In these cells, we further probed the association of hDAT with PIP_2 by immunoprecipitating (IP) PIP_2 with an anti-PIP_2 antibody and immunoblotting the immunoprecipitates for DAT (IB) with an anti-DAT antibody (see below). These data strongly suggest that PIP_2 associates with hDAT in this cell line. To reveal the association between PIP_2 and DAT in brain tissue, immunoprecipitations were performed from the striatal tissue of wild-type mice (WT; in presence (+) or absence (-) of the anti-PIP_2 antibody) or DAT knock out (KO) mice(Giros *et al.*, 1996) (**Fig. 6b**). In contrast to WT mice, DAT-PIP_2 association was lacking in DAT KO mice. Moreover, in the absence (-) of the PIP_2 antibody, no immunoreactivity was detected. These data demonstrate that PIP_2 associates with the DAT both in cell culture and *ex vivo*.

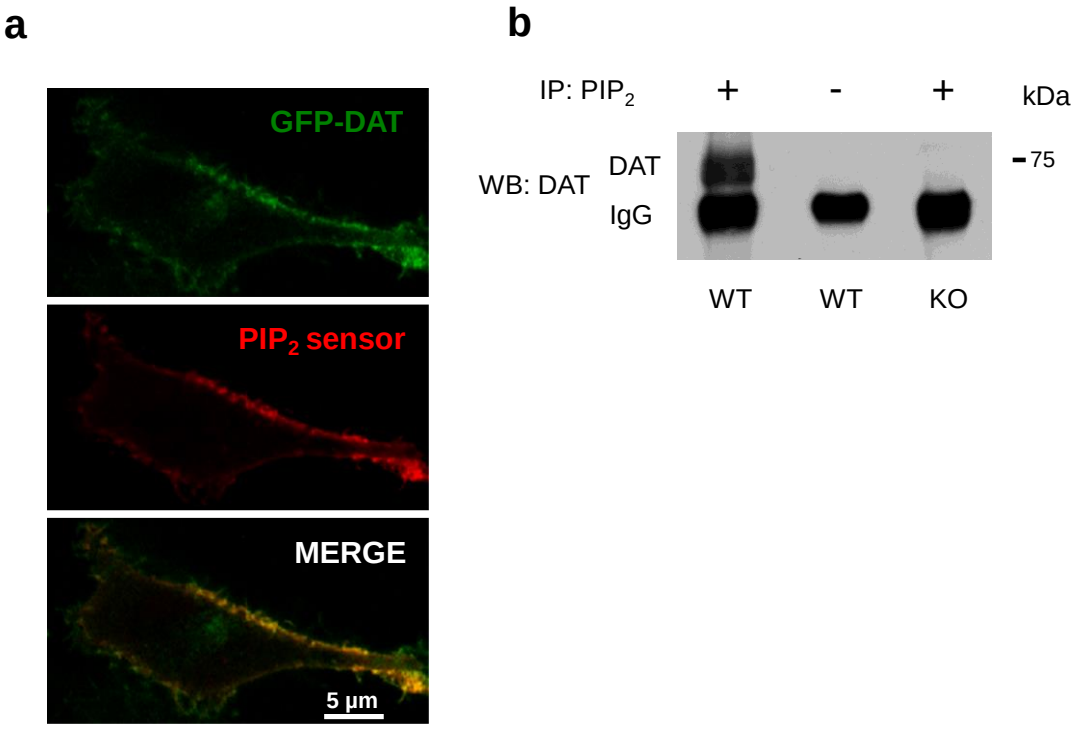

Figure 6. Phosphatidylinositol (4,5)-bisphosphate (PIP_2) interacts with hDAT. (a) hDAT and PIP_2 co-localize at the plasma membrane. In hDAT expressing cells, GFP-hDAT (green) co-localizes (yellow) at the plasma membrane with the PIP_2 sensor $PHPLC_{\delta}$-mRFP (red) (representative image from three live experiments with of 10-15 cells imaged per experiment). **(b)** PIP_2 associates with endogenous mouse DAT in striatal tissue. In striatal lysate, DAT was detected in PIP_2 immunoprecipitates using an anti-DAT antibody (+). DAT immunoreactivity was absent in the beads fraction (-) and in PIP_2 immunoprecipitates from DAT knock out (KO) animals (endogenous mouse IgG is observed) (representative of n = 3).

PIP_2 is negatively charged at physiological pH(McLaughlin and Murray, 2005). Electrostatic interactions between PIP_2 and target proteins are thought to lead to changes in protein conformation and, subsequently, their activity(Hilgemann and Ball, 1996, McLaughlin *et al.*, 2002). It is recognized that PIP_2 binds positively charged (basic) residues, such as Arg and Lys, possibly in proximity to one or more hydrophobic amino acids(Suh and Hille, 2008). Recently, residues K352 and K460 of the SERT (a DAT homolog) have been identified *in vitro* as possible sites that mediate SERT-PIP_2 association(Buchmayer *et al.*, 2013). In the DAT, the homologous amino acids to K352 and K460 are Lys at position 337 (K337) and Arg at position 443 (R443). We reasoned that these two DAT residues represent possible PIP_2 binding sites of functional significance. However, charge-neutralizing substitution of K337 and R443 to Ala (hDAT K337A-R443A), to prevent the interaction of these residues with PIP_2, caused substantial trafficking of the DAT away from the plasma membrane, as assessed by cell surface biotinylation. The amount of hDAT K337A-R443A at the cell surface was reduced by 82.6 ± 5.2% ($p \leq 0.01$ by Student's t-test; n = 7) with respect to hDAT. Therefore, in DAT, in contrast to SERT, these two residues support DAT surface expression, preventing us from determining whether their possible interaction with PIP_2 regulates any mechanistic aspect of the transport cycle.

The N-terminus of the DAT is a structural domain that has been shown to regulate specific aspects of DAT transport cycle, without altering DAT surface expression(Khoshbouei *et al.*, 2004, Fog *et al.*, 2006, Bowton *et al.*, 2010). It also contains several Lys and Arg residues (**Fig. 7**). We therefore sought to determine whether the N-terminus of the DAT directly interacts with PIP_2 *in vitro*. To this end, we generated a purified recombinant GST-fused N-terminal DAT fragment comprising the first 64 N-terminal amino acids of hDAT (GST-64 hDAT)(Binda *et al.*, 2008). The lipid binding analysis of the GST-fusion proteins was conducted using liposomes composed of mixed lipids (phosphatidylcholine, either with or without PIP_2) as previously described(Varnai *et al.*, 2002). The GST fusion proteins bound to liposomes were pelleted

hDAT

^{1}MSKSKCSVGLMSSVVAPAKEPNAVGPKEVELILVKEQNGVQLTSSTLTNPRQSPVEAQ^{58}

hSERT

^{1}METTPLNSQKQLSACEDGEDCQENGVLQKVVPTPGDKVESGQISNGYSAVPSPGAGDDTRHSIPATTT^{68}

hNET

^{1}MLLARMNPQVQPENNGADTGPEQPLRARKTAELLVVKERNGVQCLLAPRDGDAQ^{54}

hVMAT2

^{1}MALSELALVRWLQESRRSRKLILFIVFLAL^{30}

Figure 7. Sequences of the N-terminal regions of various transporters. The N-terminal regions of the human dopamine transporter (hDAT), serotonin transporter (hSERT), norepinephrine transporter (hNET), and vesicular monoamine transporter 2 (hVMAT2) are shown; positively charged residues are represented in red.

(liposome-pull down) and the binding was assessed by immunoblotting (anti-GST antibody). Figure 8a (top) shows the pull down of GST fusion proteins (GST and GST-64 hDAT) by liposomes containing (**+**) PIP_2, as compared to liposomes lacking (**-**) PIP_2. The presence (**+**) or absence (**-**) of PIP_2 did not alter pull down of GST alone (GST control). As an additional control, we "sequestered" PIP_2 by preincubating the liposomes with a basic peptide consisting of the sequence of the putative PIP_2 binding domain of the Kv7.2 channel fused to the fatty acid moiety, palmitic acid(Robbins *et al.*, 2006) (pal-HRQKHFEKRR; positively charged at physiological pH)(Robbins *et al.*, 2006). This peptide is known to interact electrostatically with the polar head groups of PIP_2 to hinder its interaction with plasma membrane proteins(Robbins *et al.*, 2006). Preincubation of PIP_2-containing liposomes with 3 μM of the basic peptide (pal-HRQKHFEKRR) inhibited pull down of GST-64 hDAT. Figure 8a (bottom) shows quantitation of immunoblots obtained from multiple experiments. Comassie stain was utilized to verify equal loading. These *in vitro* data provide the first evidence of a direct interaction between PIP_2 and a specific region of a neurotransmitter transporter, the DAT N-terminus.

Computational modeling of hDAT interaction with PIP_2

To obtain molecular level structural insights into hDAT N-terminal interactions with PIP_2-containing membranes, we generated a structural context using a previously described homology model of the hDAT(Beuming *et al.*, 2008, Kniazeff *et al.*, 2008, Bisgaard *et al.*, 2011). To this we have added a recently constructed model of the DAT N-terminus obtained with a combination of structure-prediction methods (Rosetta, Modeller) and atomistic molecular dynamics (MD) simulations (see Methods). These *in silico* modeling steps enabled the prediction of 3-dimensional folds of the N-terminal loop segment composed of hDAT residues 1-59, in the context of the complete transmembrane domain. The resulting hDAT model was used in mean-field-level calculations (SCMFM; see Methods) to quantify the electrostatic interaction

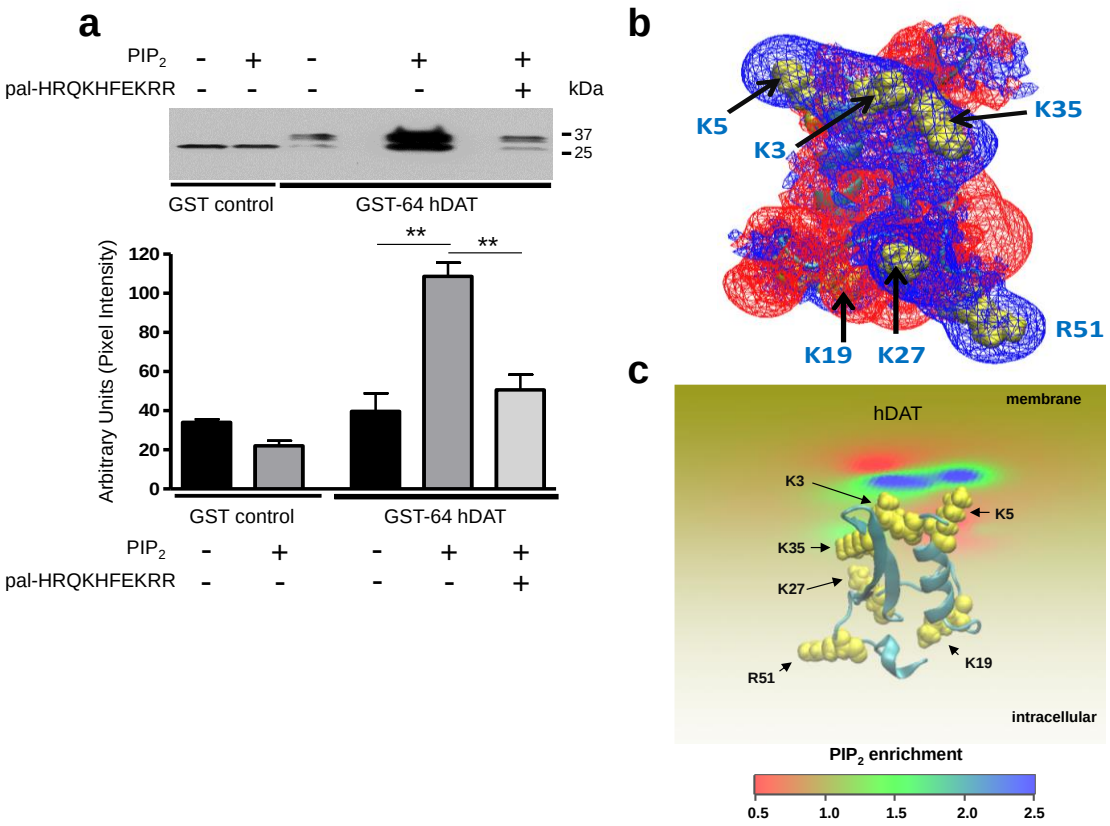

Figure 8. hDAT-PIP_2 electrostatic interactions are mediated by the hDAT N-terminus. (a) hDAT N-terminus binds directly to PIP_2. GST-64 hDAT is enriched in liposome-pull downs with liposomes containing PIP_2 (+) as compared to liposomes lacking PIP_2 (-) (** = $p \leq 0.01$ by one-way ANOVA followed by Bonferroni post-hoc test; n = 3; mean ± s.e.m.). Pull down of GST control was not altered by the presence (+) of absence (-) of PIP_2 in the liposomes ($p \geq 0.05$ by one-way ANOVA followed by Bonferroni post-hoc test; n = 3; mean ± s.e.m.). Preincubation of liposome containing PIP_2 with 3 μM of pal-HRQKHFEKRR (+) inhibited the pull down of GST-64 hDAT with liposomes containing PIP_2 (** = $p \leq 0.01$ by one-way ANOVA followed by Bonferroni post-hoc test; n = 3). Full blot is in Supplementary Figure 8. **(b)** Electrostatic potential (EP) isosurfaces (+1kT/e (+ charge)) shown as *blue wireframes* and (-1kT/e (- charge)) as *red wireframes* calculated for the predicted structure of the wild type N-terminus. **(c)** View from the intracellular side of the N-terminus (model) adsorbing on the lipid membrane. For clarity, the orientation of the N-terminus in panel (c) was obtained by a 180° rotation of the N-terminus configuration shown in panel (b). The level of the PIP_2 segregation by the N-terminus is expressed as the ratio of local and ambient lipid fraction values, and illustrated in color code (cold colors represent an enrichment of PIP_2). The positive residues in the N-terminus (yellow) that attract PIP_2 electrostatically are highlighted.

of the N-terminus with PIP_2-enriched lipid membranes.

The dominant role of the electrostatic component of the interaction energy between the hDAT N-terminus and PIP_2-containing membranes was substantiated by the shape and the values of the electrostatic potential isosurfaces (EPIs) surrounding the molecular model of the hDAT N-terminal segment shown in figure 8b. The belt-like arrangement of the Lys/Arg residues generates a region of strong positive electrostatic potential (in blue) that favors strong interaction with the negatively charged PIP_2 lipids. Energy-guided docking of this face of the N-terminus to the membrane model and solving for the steady state distributions of the charged lipid species (PIP_2) under the influence of the electrostatic forces it generates(Khelashvili *et al.*, 2008, Khelashvili *et al.*, 2009, Khelashvili *et al.*, 2012) produces a quantitative estimate of the electrostatic component of the interaction energy. Thus, the rearrangement of the PIP_2 lipids in the electrostatic field of the N-terminal segment is predicted to result in a significantly increased concentration of PIP_2 near the Lys/Arg belt (**Fig. 8c**, color coding on the membrane shows the segregation of PIP_2 (blue) to be 2.5 times larger than the PIP_2 ambient concentration (yellow/green)). Particularly notable is the strength of the PIP_2 interaction mediated by DAT residues Lys3 and Lys5. Together, these *in silico* studies suggest that the interactions between the hDAT N-terminus and PIP_2 lipids are driven by electrostatic forces.

Disrupting DAT-PIP_2 interaction inhibits reverse transport

We hypothesized that the functional consequence of DAT-PIP_2 interaction is to support reverse transport of DA. Thus, we disrupted DAT-PIP_2 associations in hDAT cells while recording AMPH-induced DA efflux with amperometry. The amperometric electrode, a carbon fiber electrode juxtaposed to the cell membrane, measures DA efflux by oxidation/reduction reactions, with DA efflux represented as a positive current. To simultaneously record DA efflux

while delivering compounds to the intracellular milieu, we combined amperometry with the whole cell patch clamp (APC) technique(Khoshbouei *et al.*, 2004, Hamilton *et al.*, 2013). The whole cell patch electrode controls the intracellular ionic composition, which includes DA(Khoshbouei *et al.*, 2004) (see Methods).

First, we perfused hDAT cells through the whole cell electrode with DA and the basic peptide pal-HRQKHFEKRR (positively charged at physiological pH and tethered to the plasma membrane through the fatty acid moiety, palmitic acid(Robbins *et al.*, 2006)) while recording DA efflux with the amperometric electrode (**Fig. 9a**). We used this peptide to compete against the DAT N-terminus for PIP_2 interactions as determined in Fig. 8a. Pal-HRQKHFEKRR (3 µM, 10 minutes of intracellular perfusion) was effective in reducing AMPH-induced DA efflux with respect to the efflux obtained with the control peptide pal-HAQKHFEAAA, in which four positive residues were substituted with Ala (**Fig. 9a**, top). Quantitation of the peak amperometric currents demonstrates that intracellular perfusion of pal-HRQKHFEKRR significantly reduced DA efflux (**Fig. 9a**, bottom). These data underscore the importance of DAT-PIP_2 interactions in the regulation of DA efflux and point to the type of interactions as electrostatic in nature. We next assessed whether DAT-PIP_2 association regulates other DAT functions (e.g. DAT-mediated inward currents). We recorded hDAT-mediated inward currents from hDAT cells voltage clamped at -60 mV with a whole-cell electrode containing either pal-HRQKHFEKRR or the control peptide pal-HAQKHFEAAA (3 µM, 10 minutes of intracellular perfusion). We stimulated the hDAT-mediated currents by perfusion of either 10 µM AMPH or DA, respectively. In contrast to DA efflux, pal-HRQKHFEKRR failed to inhibit hDAT-mediated inward currents, with respect to the control peptide, either for AMPH (109 ± 4.9% of control; $p \geq 0.8$ by Student's t-test; $n = 4$) or for DA (98 ± 16% of control; $p \geq 0.9$ by Student's t-test; $n = 4$).

To further investigate the role of DAT-PIP_2 interactions in AMPH regulation of DAT function, we

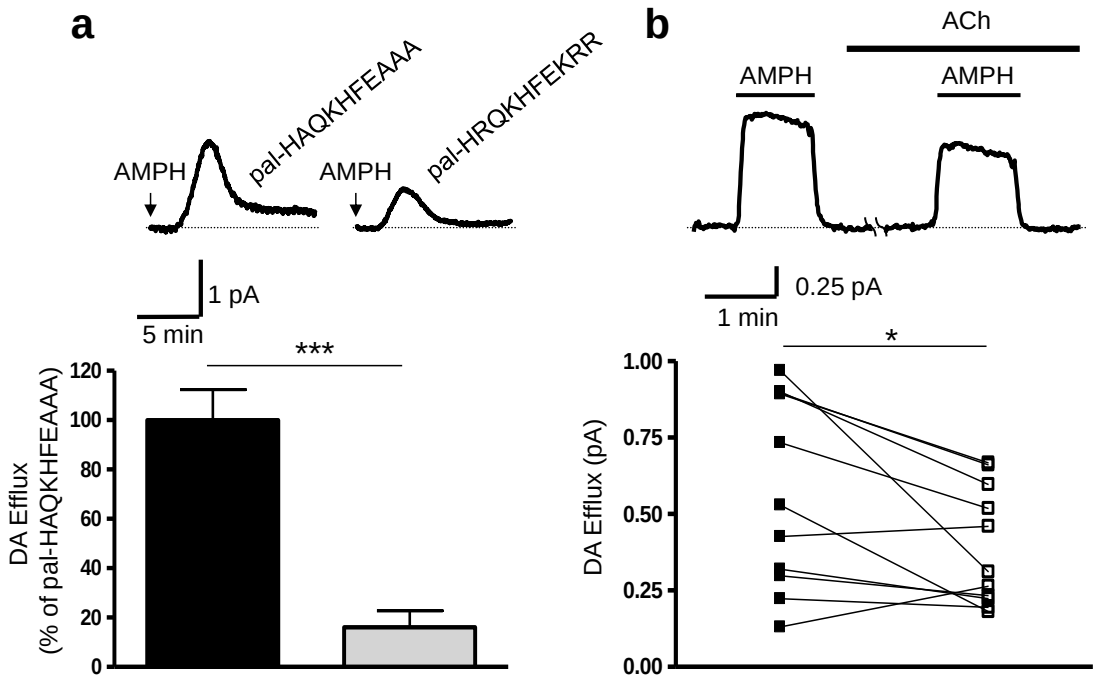

Figure 9. Sequestration or depletion of PIP_2 inhibits AMPH-induced DA efflux. (a) Sequestering PIP_2 with pal-HRQKHFEKRR decreases AMPH-induced DA efflux. Top: representative traces from stably transfected hDAT cells after patch delivery of 3 µM control peptide (pal-HAQKHFEAAA) or PIP_2 sequestering peptide (pal-HRQKHFEKRR) to the cytoplasm of the cell. Arrows indicate the application of 10 µM AMPH. Bottom: quantitation of amperometric peak currents for the two different treatments. Data are expressed as percentage of vehicle control (*** = $p \leq 0.0001$ by Student's t-test; n = 7; mean ± s.e.m.). **(b)** Depleting PIP_2 levels reduces AMPH-induced DA efflux. Top: representative trace of responses to 1 µM AMPH in stably transfected hDAT cells, co-expressing the human muscarinic acetylcholine receptor 1 (hM1R), before and after exposure to 100 µM acetylcholine (ACh). Bottom: quantitation of the amperometric peak currents representing AMPH-induced DA efflux before and after ACh-dependent PIP_2 depletion (* = $p \leq 0.05$ by Student's t-test; n = 11).

transfected hDAT cells with the human muscarinic acetylcholine (ACh) receptor M1 (hM1R), a Gαq coupled receptor. Activation of hM1R activates phospholipase C (PLC), stimulating hydrolysis of PIP_2 and effectively depleting PIP_2 stores(Kadamur and Ross, 2013). Live imaging was adopted utilizing mRFP tagged PLC-δ1 PH domain (see **Fig. 6a**) to detect changes of PIP_2 levels at the plasma membrane induced by ACh, a potent hM1R agonist(Balla *et al.*, 2009). In hDAT cells, 5 minutes of ACh (100 μM) decreased surface RFP tagged PLC-δ1 PH domain levels to 64 ± 9% of vehicle control ($p \leq 0.009$ by Student's t-test comparing ACh to vehicle; n = 16). In cells loaded with DA (see Methods), we next quantified the magnitude of AMPH-induced DA efflux before and after bath perfusion of ACh (5 minutes, 100 μM) (**Fig. 9b**, top). Quantitation of the change in AMPH-induced DA efflux induced by PIP_2 depletion within the same cell (**Fig. 9b**, bottom) demonstrates that ACh exposure significantly decreased DA efflux. This decrease was not due to a trafficking phenomenon, since exposure of ACh (5 minutes, 100 μM) in hM1R-expressing hDAT cells did not cause significant trafficking of hDAT away from the plasma membrane as compared to vehicle-treated control (**Fig. 10**). We next determined whether providing an excess of intracellular PIP_2 reduces the ability of hM1R agonism to decrease DA efflux. For this, we adopted the APC technique(Khoshbouei *et al.*, 2004, Hamilton *et al.*, 2013). Inclusion of PIP_2 (50 μM) in the whole cell patch pipette solution (10 minutes of intracellular perfusion) impaired the ability of ACh (5 minutes, 100 μM) to significantly decrease AMPH-induced DA efflux with respect to vehicle control (**Fig. 11**). Collectively, these data demonstrate that impairing the electrostatic interaction between PIP_2 and DAT selectively inhibits the ability of AMPH to cause DA efflux.

N-terminal lysine residues mediate DAT-PIP_2 association

Since our *in silico* modeling of the hDAT N-terminus indicated residues Lys3 and Lys5 to be essential in facilitating the electrostatic interaction of PIP_2 with DAT (**Fig. 8c**), we hypothesized

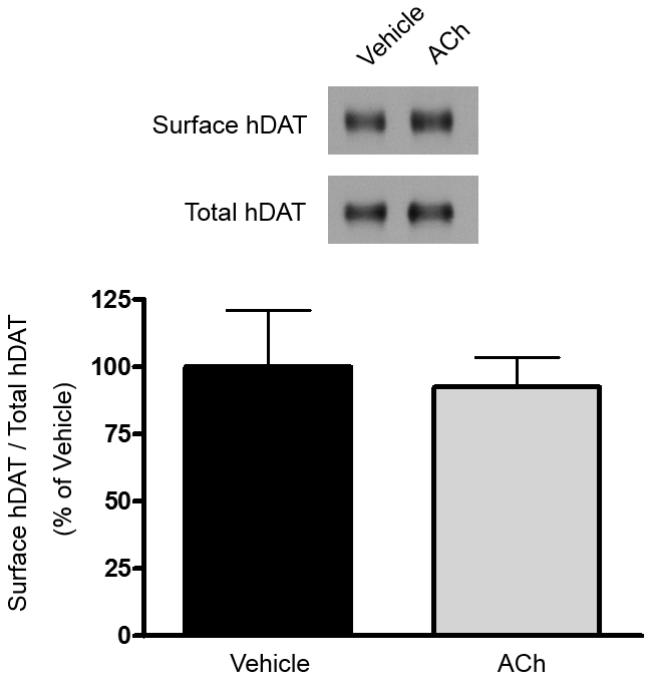

Figure 10. ACh treatment does not affect hDAT surface expression. Representative immunoblots for biotinylated (surface) and total hDAT protein fractions from stably transfected hDAT cells, co-expressing the human muscarinic acetylcholine receptor 1 (hM1R), treated either with vehicle or 100 µM ACh for 5 min. Surface fractions were quantitated, normalized to total hDAT, and expressed as a percent of vehicle treated hDAT cells ($p \geq 0.7$ by Student's t-test; n = 3 in duplicate; mean ± s.e.m.).

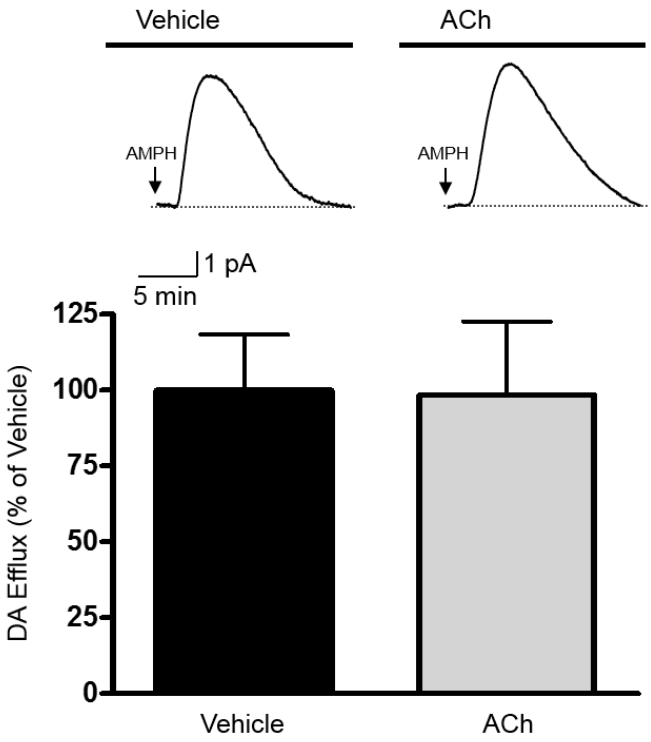

Figure 11. Excess intracellular PIP_2 levels prevent the ability of ACh to decrease AMPH-induced DA efflux. Top: representative traces of AMPH responses obtained with the APC technique in stably transfected hDAT cells, co-expressing hM1R, perfused intracellularly with 50 µM PIP_2. Cells were pre-exposed to either 100 µM ACh or vehicle for 5 minutes and DA effluxes induced by 10 µM AMPH were recorded in the continuous presence of ACh or vehicle. Bottom: quantitation of the amperometric peak currents normalized to vehicle control, and expressed as a percent of vehicle treated hDAT cells ($p \geq 0.9$ by Student's t-test; $n = 4$; mean ± s.e.m.).

that substitution of these residues with uncharged amino acids (e.g. alanine or asparagine) would disrupt DAT-PIP_2 associations. To probe this inference *in silico*, Lys3 and Lys5 were both substituted computationally with either Ala (hDAT K/A) or with Asn (hDAT K/N), and the resulting constructs (N-terminus of hDAT K/A and hDAT K/N) were evaluated for any conformational rearrangements due to the mutations. The constructs were used in the same computational protocols described for the hDAT model. The results for the mutant constructs show significantly reduced electrostatic interactions with PIP_2-containing membranes for both hDAT K/A (**Fig. 12a**, compare to **Fig. 8c**) and hDAT K/N (**Fig. 13**, compare to **Fig. 8c**).

The inferences from the computational evaluation of the N-terminus association with PIP_2 lipids *in silico* were probed biochemically by determining the effect of charge neutralizing mutations of Lys3 and Lys5. In hDAT K/A cells, we immunoprecipitated PIP_2 and immunoblotted the immunoprecipitates for DAT (IB: anti-DAT). The amount of DAT recovered in the PIP_2 immunoprecipitates was reduced in the hDAT K/A cells compared to the hDAT cells (**Fig. 12b**, top lane). In the absence of antibody against PIP_2, no signal was detected for DAT in the immunoprecipitates (**Fig. 12b**, middle lane, IP: beads). The total DAT in the hDAT K/A cells was not decreased with respect to hDAT cells (**Fig. 12b**, bottom lane; Total DAT). These data demonstrate that substitution of Lys3 and Lys5 decreases DAT-PIP_2 interaction, as predicted from the computational modeling. Quantitation of multiple experiments (n = 4) is shown in figure 12b (bottom). Next, we determined whether substitution N-terminal Lys3 and Lys5 to Ala impairs the direct interaction of DAT with PIP_2 *in vitro*. We generated a purified recombinant GST-fused N-terminal DAT fragment comprising the first 64 N-terminal amino acids of hDAT with Lys3 and Lys5 substituted to Ala (GST-64 hDAT K/A). The lipid binding analysis of the GST-fusion proteins (either GST-64 hDAT or GST-64 hDAT K/A) was conducted utilizing liposome-pull down as in figure 8. The inset in figure 12b shows the pull down of the GST fusion proteins by liposomes containing PIP_2. Quantitation of immunoblots obtained from multiple experiments

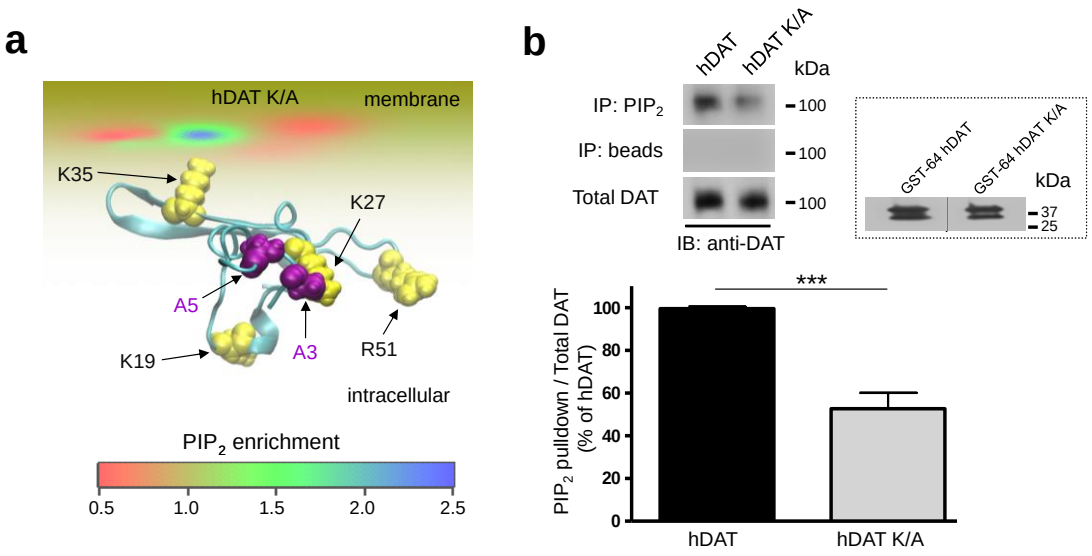

Figure 12. hDAT N-terminal Lys regulate DAT-PIP_2 interaction. (a) Mutating hDAT N-terminal residues Lys3 and Lys5 to uncharged Ala (hDAT K/A) disrupts PIP_2 segregation to the N-terminus. View from the intracellular side of the N-terminus of hDAT K/A adsorbing on the lipid membrane. The level of PIP_2 segregation by the N-terminus residues is expressed as the ratio of local and ambient lipid fraction values and illustrated in color code, with cold colors representing an enrichment of PIP_2. **(b)** N-terminal Lys residues mediate hDAT-PIP_2 interaction. Top: PIP_2 immunoprecipitates from hDAT and hDAT K/A cells were immunoblotted for DAT (top lane). The beads fraction supports absence of non-specific binding (middle lane). Bottom lane shows total DAT proteins. Full blot is in Supplementary Figure 9. Bottom: quantitation of PIP_2 pulldown band intensities normalized to the respective total DAT and expressed as a percentage hDAT (*** = $p \leq 0.001$ by Student's t-test; n = 4; mean ± s.e.m.). *Inset:* Representative blot for GST-64 hDAT and GST-64 hDAT K/A in pull downs with liposomes containing PIP_2.

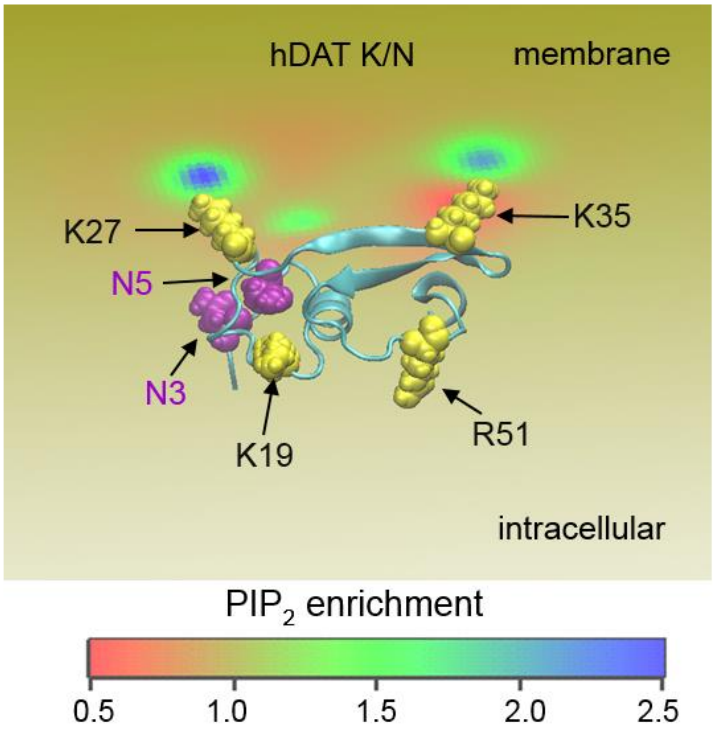

Figure 13. Mutation of hDAT N-terminal residues Lys3 and Lys5 to uncharged Asn (hDAT K/N) disrupts PIP_2 segregation to the N-terminus. View from the intracellular side of the N-terminus of hDAT K/N adsorbing on the lipid membrane. The level of PIP_2 segregation by the N-terminus is expressed as the ratio of local and ambient lipid fraction values, and illustrated in color code with cold colors representing an enrichment of PIP_2.

demonstrated that pull down of GST-64 hDAT was significantly inhibited by Lys to Ala substitution (GST-64 hDAT K/A was 45 ± 20% of GST-64 hDAT; $p \leq 0.037$ by Student's t-test; n = 4).

In order to assess whether DAT physiological function is altered by disrupting DAT-PIP_2 association, we examined radioactive [^{3}H]DA uptake in both hDAT and hDAT K/A cells. In hDAT K/A cells, the maximal velocity of DA influx (V_{max}) and the apparent DA affinity (K_m) were not significantly different from those of hDAT (**Fig. 14a**, top). A representative plot of DA uptake kinetics (in triplicate) for hDAT and hDAT K/A is shown in figure 14a (bottom), demonstrating that the uptake of substrate is not regulated by the interaction with PIP_2. Consistent with the uptake data, no significant difference was found in the whole-cell DAT-mediated inward current (recorded at -60 mV) between hDAT and hDAT K/A cells upon stimulation with 10 μM DA. The hDAT K/A inward currents were expressed as a percent of hDAT-mediated currents (103 ± 20% of hDAT; $p \geq 0.97$ by Student's t-test; n = 4).

Our pharmacological manipulations (**Fig. 9**) indicate that disrupting DAT-PIP_2 association has no effect on DAT-mediated DA uptake or DA-induced inward currents but inhibits the ability of AMPH to cause DA efflux. Consistent with this, hDAT K/A cells were found to display strikingly reduced AMPH-induced DA efflux (**Fig. 14b**, top). Quantitation of the amperometric recordings demonstrate that the Lys to Ala substitution not only decreased DAT-PIP_2 association (**Fig. 12**), but also decreased the ability of AMPH to cause DA efflux (**Fig. 14b**, bottom). The reduced AMPH-induced DA efflux was not associated with a reduction in either total or DAT surface expression as assessed by measuring changes in DAT proteins in the total and biotinylated fraction, respectively. Surface fractions were quantitated, normalized to total DAT, and expressed as a percent of hDAT (hDAT K/A was 122 ± 31% of hDAT; $p \geq 0.53$ by Student's t-test; n = 7-8). The findings in the hDAT K/A cells were mirrored by those obtained in the hDAT

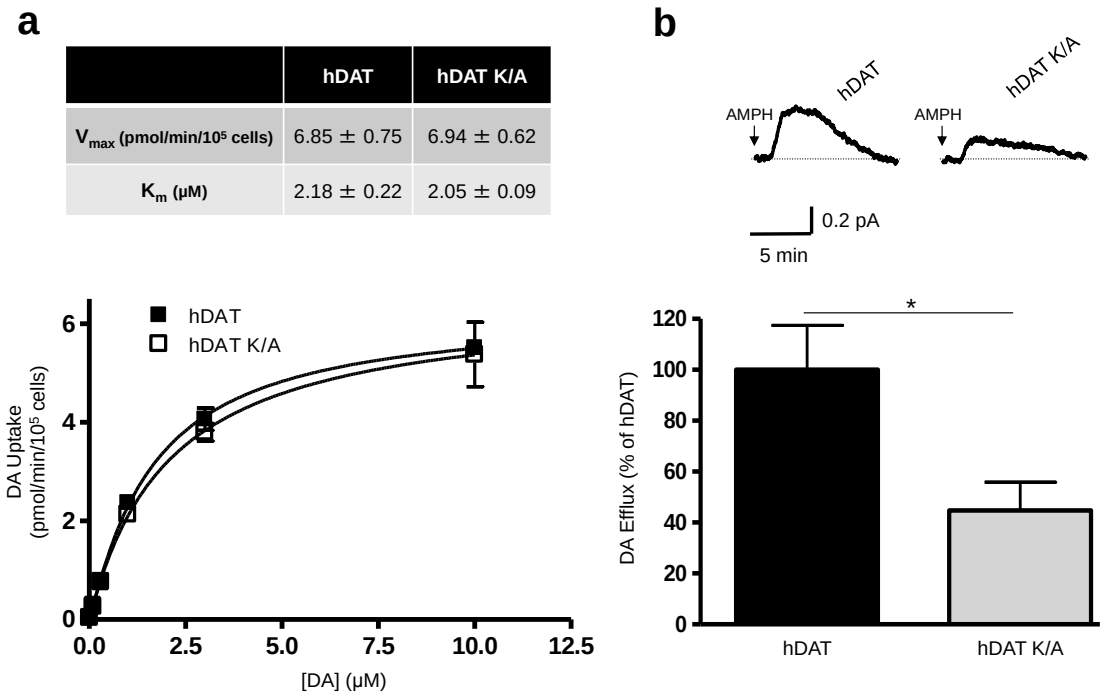

Figure 14. N-terminal Lys3 and Lys5 regulate specific modalities of hDAT function. (a) hDAT K/A exhibits normal DA uptake function. Top: kinetic parameters (V_{max} and K_m) for hDAT and hDAT K/A (V_{max}: $p \geq 0.92$ by Student's t-test; n = 3, in triplicate; K_m: $p \geq 0.62$ by Student's t-test; n = 3, in triplicate; mean ± s.e.m.). Bottom: representative plot of [^{3}H]DA uptake kinetics in hDAT (filled squares) and hDAT K/A (empty squares) cells ($p \geq 0.05$, by two-way ANOVA followed by Bonferroni post-test; in triplicate; mean ± s.e.m.). **(b)** hDAT K/A has reduced AMPH-induced DA efflux. Top: representative AMPH-induced amperometric currents recorded from hDAT and hDAT K/A cells. Arrows indicate application of 10 μM AMPH. Bottom: quantitation of AMPH-induced DA efflux. Data are represented as maximal DA efflux expressed as percent of the DA efflux recorded in hDAT controls (* = $p \leq 0.05$ by Student's t-test; n = 7-8; mean ± s.e.m.).

K/N cells in terms of both DAT-PIP_2 association and hDAT cell surface expression (**Fig. 15a** and **15b**). The hDAT K/N also displayed normal uptake (**Fig. 15c**) and, like the hDAT K/A, had a significant reduction in AMPH-induced DA efflux (**Fig. 15d**). Furthermore, AMPH uptake assays revealed that hDAT, hDAT K/A, and hDAT K/N cells displayed comparable AMPH transport (see Methods) (hDAT K/A: 101 ± 4.9% and hDAT K/N: 93.9 ± 17% relative to hDAT; $p \geq 0.88$ by one-way ANOVA; n = 3, in triplicate). These results demonstrate that the reduced ability of AMPH to cause DA efflux promoted by the Lys to Ala substitutions does not involve changes in the surface expression or changes in ability of the DAT mutants to transport AMPH. Another possibility for this decrease in DA efflux is that the N-terminal Lys substitution (hDAT K/A) perturbs the potential AMPH-induced phosphorylation of the Ser2 and Ser4 adjacent to these Lys residues by altering primary sequence requirements for phosphorylation. To explore this, we substituted Ser2 and Ser4 with Asp (to mimic phosphorylation) in the hDAT K/A background (hDAT K/A-S/D). Cells expressing hDAT K/A-S/D exhibited significantly reduced AMPH-induced DA efflux, similar to hDAT K/A cells (**Fig. 16a**, top). Quantitation of the amperometric recordings demonstrated that Ser to Asp substitution at positions 2 and 4 in the hDAT K/A background did not rescue the ability of AMPH to cause DA efflux (**Fig. 16a**, bottom). The reduced AMPH-induced DA efflux was not associated with a reduction in DA uptake (**Fig. 16b**). These data demonstrate that the reduction in DA efflux caused by substitution of Lys3 and Lys5 with uncharged amino acids cannot be attributed to impaired phosphorylation of adjacent Ser residues.

Reduced DAT-PIP_2 interaction impairs psychomotor behavior

Locomotion is an elemental behavior regulated by DA across species, including *Drosophila melanogaster*(Pendleton *et al.*, 2002, Wicker-Thomas and Hamann, 2008, Hamilton *et al.*, 2013, Pizzo *et al.*, 2013). Recently, locomotion in flies has been adopted to evaluate molecular

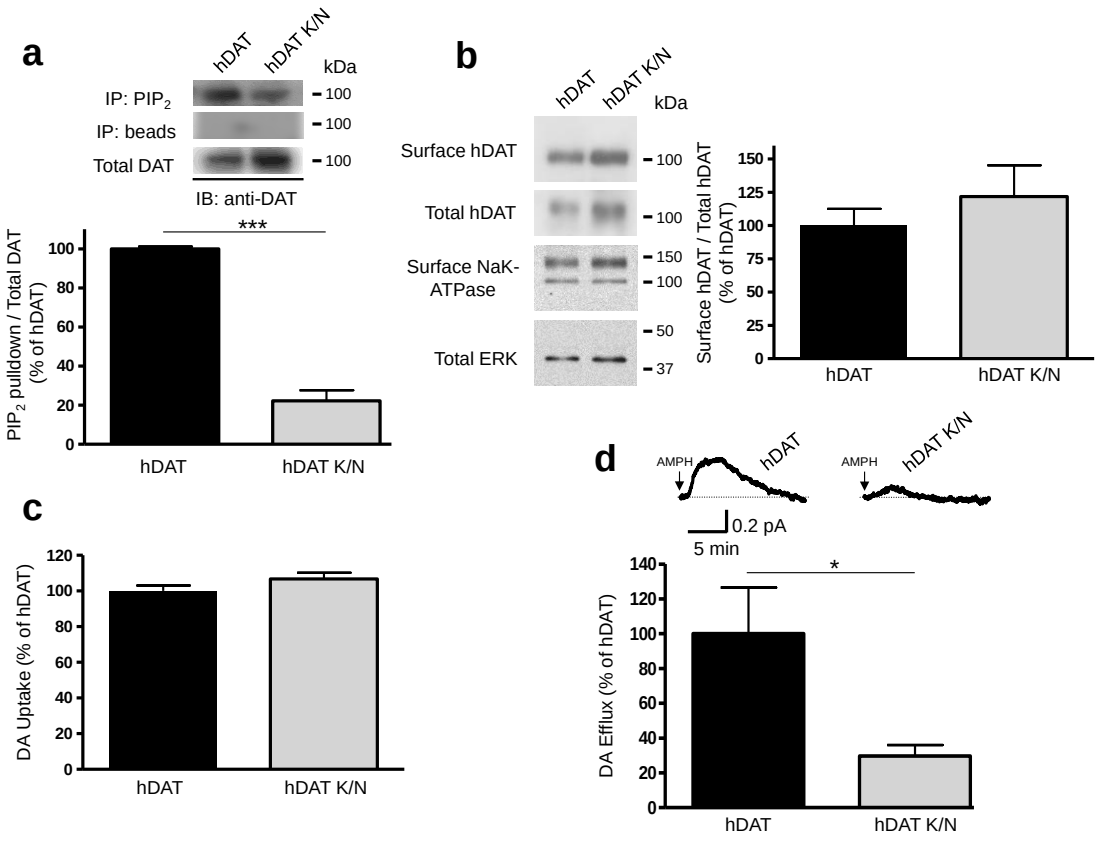

Figure 15. hDAT K/A findings mirrored in hDAT K/N. (a) Top: PIP_2 immunoprecipitates from hDAT and hDAT K/N cells were immunoblotted for DAT (top lane). The beads fraction supports absence of non-specific binding (middle lane). Bottom lane shows total DAT proteins. Bottom: quantitation of PIP_2 pull down band intensities normalized to the respective total DAT and expressed as a percentage hDAT (*** = $p \leq 0.0001$ by Student's t-test; n = 3; mean ± s.e.m.). **(b)** Representative immunoblots for biotinylated (surface) and total protein fractions from hDAT and hDAT K/N cells. Immunoblots for surface NaK-ATPase and total ERK are shown as well. Surface fractions were quantitated, normalized to total DAT, and expressed as a percentage of hDAT ($p \geq 0.41$ by Student's t-test; n = 4-5; mean ± s.e.m.). **(c)** [^{3}H]DA uptake (50 nM) in hDAT and hDAT K/N cells was expressed as a percent of uptake in hDAT cells ($p \geq 0.16$ by Student's t-test; n = 3, in quadruplicate; mean ± s.e.m.). **(d)** Representative AMPH-induced amperometric currents recorded from hDAT and hDAT K/N cells. Arrows indicate application of 10 µM AMPH. Bottom: quantitation of AMPH-induced DA efflux. Data are represented as maximal DA efflux expressed as a percent of the DA efflux recorded in hDAT cells (* = $p \leq 0.02$ by Student's t-test; n = 6-7; mean ± s.e.m.).

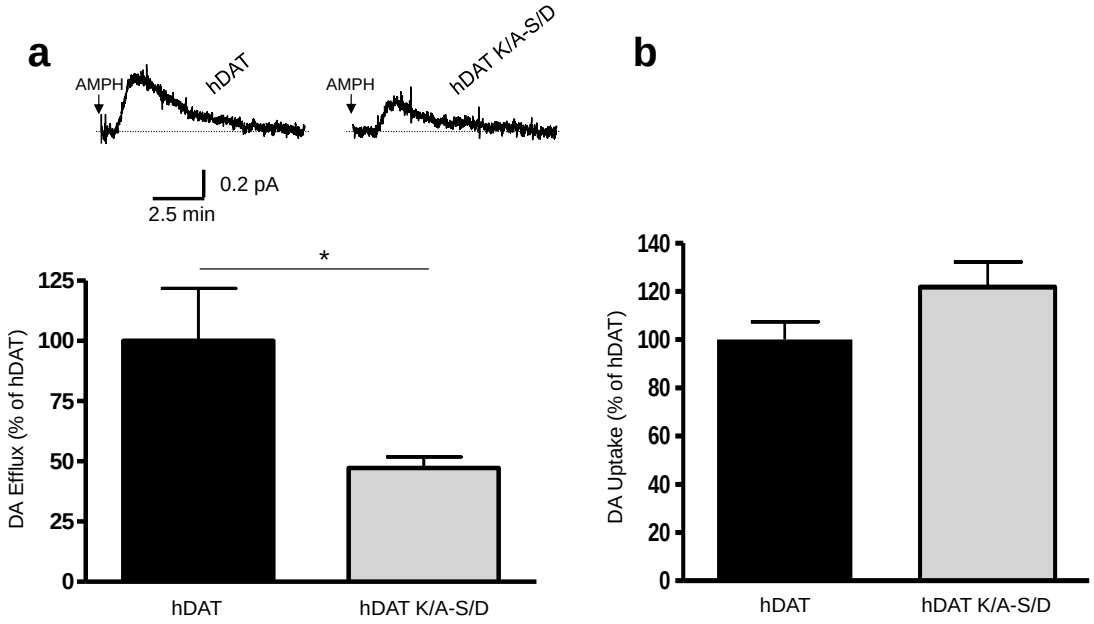

Figure 16. hDAT K/A-S/D displayes reduced DA efflux and normal DA uptake. (a) hDAT K/A-S/D has reduced AMPH-induced DA efflux. Top: representative AMPH-induced amperometric currents recorded from hDAT and hDAT K/A-S/D cells. Arrows indicate application of 10 μM AMPH. Bottom: quantitation of AMPH-induced DA efflux. Data are represented as maximal DA efflux expressed as a percent of DA efflux recorded in hDAT cells (* = $p \leq 0.03$ by Student's t-test; n = 5-6; mean ± s.e.m.). **(b)** hDAT K/A-S/D exhibits normal [^{3}H]DA uptake (50 nM) function. Data expressed as a percent of the uptake measured in hDAT cells ($p \geq 0.2$ by Student's t-test; n = 4-8; mean ± s.e.m.).

discoveries of AMPH actions mechanistically *in vivo*(Hamilton *et al.*, 2013, Pizzo *et al.*, 2013). Thus, *Drosophila* offer a powerful model for elucidating the impact of altered DAT-PIP_2 interactions on locomotion and on the psychomotor stimulant effects of AMPH.

To generate fly lines expressing either hDAT or hDAT K/A selectively in DA neurons, we used the Gal4/UAS system to express a single copy of either hDAT or hDAT K/A in flies with a *Drosophila* DAT (dDAT) null background (dDAT KO; flies are homozygous for the dDAT null allele, DAT^{fmn})(Kume *et al.*, 2005). Using phiC31-based integration, we generated transgenic flies expressing comparable mRNA levels for hDAT or hDAT K/A. Locomotion of flies was quantified by beam crossing detection over a >24 hour period (data binned in 15 minute intervals) including both the light (horizontal white bar) and the dark (horizontal black bar) cycle. While dDAT KO flies were hyperactive(Kume *et al.*, 2005), dDAT KO flies expressing hDAT in DA neurons displayed reduced basal locomotion in comparison to dDAT KO (**Fig. 17a**, compare hDAT to dDAT KO). These data demonstrate the validity of expressing hDAT in *Drosophila* for behavioral studies.

We hypothesized that flies harboring the hDAT K/A would demonstrate comparable locomotion with respect to hDAT expressing flies, since no difference in DA uptake was observed. Figure 17a demonstrates that *Drosophila* expressing hDAT and hDAT K/A displayed comparable basal locomotion, whereas dDAT KO flies exhibited chronically elevated locomotion. Total circadian locomotor activities (24 hour) of hDAT and hDAT K/A flies were not significantly different, while total locomotor activity of dDAT KO flies was significantly higher than hDAT and hDAT K/A (**Fig. 17b**).

Encouraged by the lack of hyperactivity of hDAT K/A flies under basal conditions, we hypothesized that these flies would have blunted AMPH-induced locomotive behaviors resulting

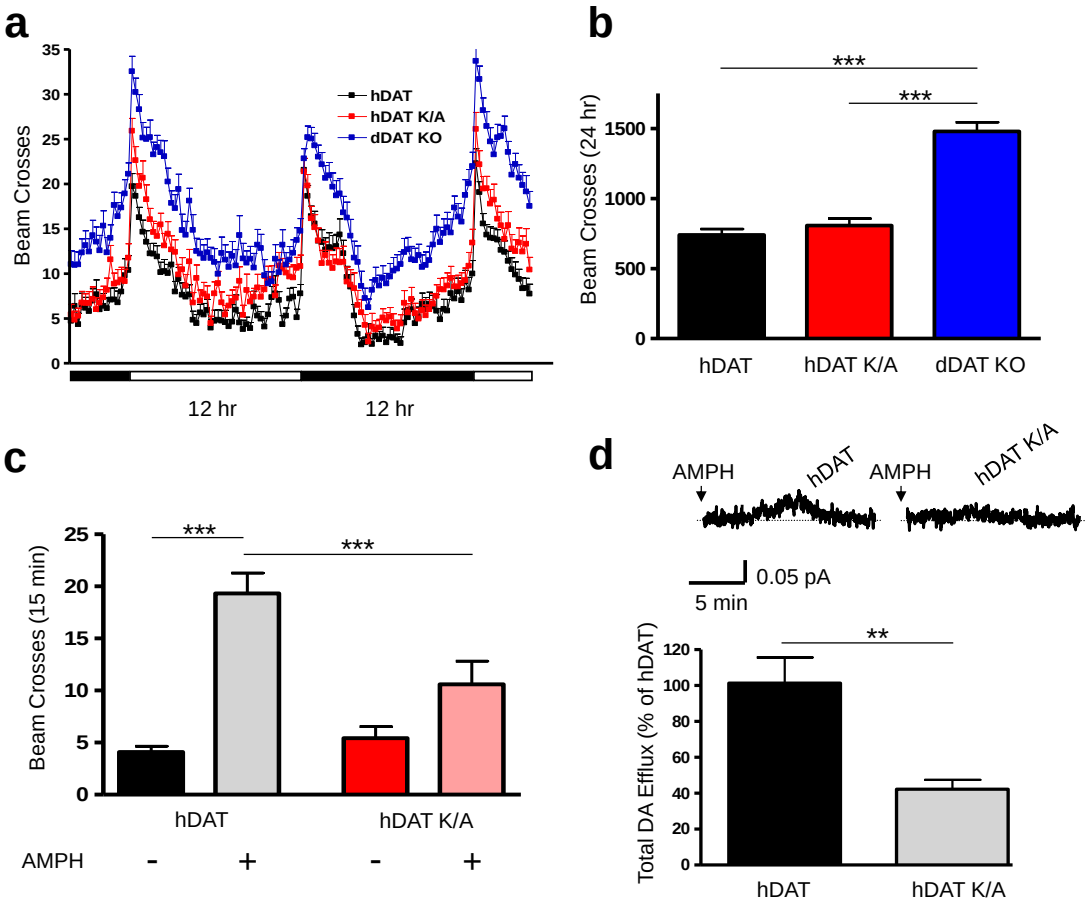

Figure 17. Expression of hDAT K/A in *Drosophila* dopaminergic neurons does not affect circadian locomotor activity yet impairs AMPH-induced locomotion and neuronal DA efflux. hDAT or hDAT K/A was expressed in DA neurons of dDAT KO flies. **(a)** Locomotion was assayed over 32 hours during the light (horizontal white bars) or dark (horizontal black bars) cycle. Flies expressing dDAT KO (blue squares) were hyperactive with respect to flies expressing wild type hDAT (black squares) and flies expressing hDAT K/A (red squares) (beam breaks binned in 15 minute intervals; n = 31-42; mean ± s.e.m.). **(b)** Quantitation of total beam crosses over 24 hours for hDAT, hDAT K/A, and dDAT KO flies (*** = $p \leq 0.001$ by one-way ANOVA followed by Bonferroni post-test; n = 31-42; mean ± s.e.m.). **(c)** AMPH did not cause a significant increase in locomotion in hDAT K/A flies compared to vehicle control ($p \geq 0.05$ by one-way ANOVA followed by Bonferroni post-test; n = 25-49; mean ± s.e.m.). In hDAT flies, AMPH induced a significant increase in locomotion compared to vehicle control (*** = $p \leq 0.001$ by one-way ANOVA followed by Bonferroni post-test; n= 25-60; mean ± s.e.m.). **(d)** hDAT K/A *Drosophila* DA neurons show reduced AMPH-induced DA efflux. Dopaminergic neurons were selected by fluorescence microscopy since the expression of mCherry was driven by TH-GAL4. Top: representative amperometric currents from hDAT and hDAT K/A neurons. Arrows indicate application of 1 μM AMPH. Bottom: quantitation of total AMPH-induced DA efflux. Data represented as cumulative DA efflux expressed as percent of DA efflux from hDAT neurons (** = $p \leq 0.01$ by Student's t-test; n = 4-5; mean ± s.e.m.).

from reduced ability of AMPH to stimulate DA efflux. While AMPH caused a significant increase in locomotion in flies expressing hDAT, this increase was significantly reduced in flies expressing hDAT K/A (**Fig. 17c**). These data demonstrate, for the first time, the behavioral importance of the interaction of PIP_2 with a plasma membrane protein. This discovery is further enhanced by our ability to associate blunted AMPH-induced behaviors with a decreased ability of AMPH to cause DA efflux in isolated DA neurons from flies expressing hDAT K/A. *Ex vivo* cultures of *Drosophila* DA neurons were investigated with amperometry to quantify the magnitude of the AMPH-induced DA efflux in the different fly lines. The DA efflux recorded from hDAT K/A expressing neurons was significantly reduced compared to hDAT expressing neurons (**Fig. 17d**), suggesting that the reduced AMPH-induced locomotion in flies expressing hDAT K/A is due to diminished DA efflux in response to AMPH.

It is possible that this PIP_2 regulation of DA efflux is an evolutionarily conserved mechanism that controls DAT function across phylogeny. To test this possibility, we utilized the APC technique in CHO cells expressing the dDAT (dDAT cells). In dDAT cells, intracellular perfusion of pal-HRQKHFEKRR (3 μM, 10 minutes) was effective in reducing AMPH-induced DA efflux with respect to the efflux obtained with the control peptide pal-HAQKHFEAAA (34.9 ± 12.9% of control peptide; $p \leq 0.01$ by Student's t-test; $n = 3$). These results parallel those obtained in hDAT cells (**Fig. 9**). In this study, we provide the first behavioral evidence for the relevance of the interaction of PIP_2 with a plasma membrane protein, associating AMPH behaviors to altered neuronal DAT function within the same organism.

Discussion

We recently demonstrated that disrupting the localization of DAT in lipid rafts impairs the ability of AMPH to cause both DA efflux (without altering DA uptake)(Cremona *et al.*, 2011), and

associated behaviors(Pizzo *et al.*, 2013). This led us to hypothesize that the molecular underpinnings required for AMPH actions reside in lipid rafts. Raft microdomains are considered scaffolds for PIP_2 signaling, enabling PIP_2 to selectively regulate different cellular processes(Pendleton *et al.*, 2002, van Rheenen *et al.*, 2005). Yet, partitioning of PIP_2 into lipid rafts has been criticized as energetically improbable, since PIP_2 consists of a polyunsaturated acyl side chain (arachidonic acid) that is unlikely to spontaneously partition into cholesterol-rich rafts(McLaughlin and Murray, 2005). Therefore, it is theorized that the partitioning of PIP_2 into rafts is facilitated by interactions with raft-localized proteins(McLaughlin and Murray, 2005). Here we demonstrate that PIP_2 directly interacts with hDAT, a protein that localizes to the rafts(Cremona *et al.*, 2011, Gabriel *et al.*, 2013, Sorkina *et al.*, 2013).

We found that the DAT N-terminus (a domain of functional importance)(Khoshbouei *et al.*, 2004, Fog *et al.*, 2006) is engaged in direct electrostatic interactions with PIP_2, described by both computational and biochemical analysis. We demonstrate that this interaction is direct and distinct from the recently described association of PIP_2 with SERT(Buchmayer *et al.*, 2013). This DAT-PIP_2 interaction, which occurs in brain tissue, involves the two most distal N-terminal Lys (Lys3 and Lys5). These data, combined with the regulatory nature of DAT localization to PIP_2 enriched lipid rafts, led us to hypothesize that PIP_2 participates in coordinating the complex molecular events underlying *specific* DAT activities. This includes AMPH-induced DA efflux. Notably, this interaction does not regulate the physiological function of DAT (DA uptake), DAT surface expression, and AMPH uptake. Other functions of the DAT include AMPH- or DA-stimulated inward currents that represent inward movements of ions associated with the transport of substrate. Therefore, we expected that substrate-induced inward currents would not be affected by disruption of DAT-PIP_2 interaction, in the same way that DA or AMPH uptake is not affected. We show that disrupting DAT-PIP_2 interaction by substitution of Lys3 and Lys5 with Ala did not impair the ability of hDAT to sustain electrical inward currents stimulated by either

DA or AMPH. The regulatory nature of the direct DAT-PIP_2 interaction on DAT-mediated DA efflux is underscored by our results demonstrating that "sequestering" PIP_2, with our palmitoyl-positively charged peptide, or depleting PIP_2, by stimulating PLC activity, results in diminished reverse transport of DA. Consistent with these findings is the notable result that intracellular perfusion of the palmitoyl-positively charged peptide did not impair hDAT-mediated inward currents stimulated by either AMPH or DA relative to control peptide. These data underscore the interaction between DAT and PIP_2 as a key regulator of the specific DAT function of DA efflux.

N-terminal phosphorylation is a requirement for the ability of AMPH to cause a robust DA efflux(Khoshbouei *et al.*, 2004). The results of our specific molecular manipulations support the notion that Lys to Ala substitution did not impair DA efflux by altering primary sequence requirements for phosphorylation of Ser2 and Ser4. Indeed, pseudophosphorylation of these Ser residues in the hDAT K/A background failed to rescue DA efflux. Consistent with this notion, palmitoyl-positively charged peptide (which does not alter the N-terminus primary sequence) disrupts both the direct interaction of the N-terminus with PIP_2 as well as DA efflux. However, the computational modeling reveals the possibility that the strength of the association of Lys3 and Lys5 with PIP_2 regulates the proper conformation of the DAT N-terminus and affects the transporter N-terminus as a whole. Therefore, we cannot exclude the possibility that the observed DAT-PIP_2 association regulates N-terminal phosphorylation of non-adjacent Ser by coordinating suitable conformations. Nevertheless, this possibility does not diminish the importance of the discovery that DAT-interaction with PIP_2 is a key determinant of AMPH-induced DA efflux and behaviors. On the contrary, it highlights an opportunity, in future studies, to understand whether the DAT N-terminal interaction with PIP_2 supports N-terminal phosphorylation and/or the importance of phosphorylation for N-terminal conformations and DAT-PIP_2 association.

The Ser-Lys-Ser-Lys N-terminal sequence of the DAT is conserved across several species, including *Drosophila*, suggesting that the DAT-PIP_2 association is a possible evolutionarily conserved mechanism that regulates specific DAT functions. Our data demonstrate that disruption of the dDAT-PIP_2 interaction impairs DA efflux, which parallels our results in the hDAT. It is tempting to speculate that this mechanism of N-terminal regulation of transporter function through electrostatic interactions with PIP_2 is a potential mode of regulation for other neurotransmitter transporters as well. Examination of sequences of the N-terminal regions of four major neurotransmitter transporters (hDAT, hSERT, hNET, and hVMAT2) reveals that the positively charged residues are not only abundant in this region, but are also often clustered. In the hDAT, we revealed the consequences of this clustering in a structural context, where one of these clusters contains Lys3 and Lys5, which enables this region to attract PIP_2 lipids. Therefore, a mechanism of PIP_2 regulation, similar to the one outlined here for DAT function, may apply to other neurotransmitter transporters with charged clusters in their N-terminal sequences.

Recently we discovered that the AMPH-induced 5-HT efflux mediated by SERT also relies on PIP_2 interactions with positively-charged residues(Buchmayer *et al.*, 2013). However, these residues are not localized to the N-terminus of SERT. These data do not exclude a possible role of SERT N-terminus basic residues in SERT-PIP_2 interaction and AMPH-induced 5-HT efflux. In contrast, in DAT, mutation (to Ala) of the corresponding SERT-PIP_2 binding sites causes substantial trafficking of DAT away from the plasma membrane, disrupting its membrane expression. Thus, this trafficking phenomenon prevents our ability to determine the significance of these residues in the mechanistic aspects of the DAT transport cycle. However, it is clear that they do not functionally replace Lys3 and Lys5 in terms of DA efflux.

Prior to this work, it was unclear whether the association and/or dissociation of plasma membrane proteins with PIP_2 played a role in the regulation of behaviors of complex organisms. Here, we took advantage of an animal model (*Drosophila melanogaster*) to determine the behavioral consequences of disrupting direct interactions of DAT with PIP_2. *Drosophila* expressing hDAT K/A solely in DA neurons did not display altered circadian locomotor activity. This is not surprising, since the cells expressing hDAT K/A have both normal DA uptake and DA affinity. However, hDAT K/A flies exhibit significant reductions in the behavioral psychomotor responses to AMPH. These data convey the significance of the interaction between PIP_2 and plasma membrane proteins (i.e. DAT) in fundamental organismal behaviors, such as locomotion. The discovery of this PIP_2 regulation of the psychomotor actions of AMPH is further enhanced by our ability to record DA efflux (for the first time) directly from DA neurons cultured from the same *Drosophila* lines utilized in our behavioral assays. DA neurons expressing hDAT K/A have a significant reduction in DA efflux with respect to neurons expressing hDAT. This enhances our molecular discoveries outlining the DAT-PIP_2 interaction as required for DA efflux and obligatory in the ability of AMPH to cause psychomotor behaviors. These data promote PIP_2 and its synthetic pathway from its canonical role as a modulator of cell function and metabolism to a new role as a regulatory agent of both elemental behaviors, such as locomotion, and maladaptive behaviors, such as psychostimulant abuse.

Materials and Methods

Cell culture and transfection. The GFP-hDAT-pCIHygro expression vectors containing hDAT, hDAT K/A (Lys3 and Lys5 to Ala), hDAT K/N (Lys3 and Lys5 to Asn), or hDAT K/A-S/D (Lys3 and Lys5 to Ala and Ser2 and Ser4 to Asp) sequence were generated, confirmed and transiently transfected into Chinese hamster ovary (CHO) cells. The *Drosophila* DAT cDNA was generously provided by the laboratory of Dr. Satinder Singh (Yale University). In some

experiments (noted in figure legend), stably transfected hDAT CHO cells were used. These cells were generated as previously described(Bowton *et al.*, 2010). Cells were maintained in a 5% CO_2 incubator at 37°C and maintained in Ham's F-12 medium supplemented with 10% fetal bovine serum (FBS), 1 mM L-glutamine, 100 U/mL penicillin, and 100 µg/mL streptomycin. Stably transfected hDAT CHO cells were kept under selection with 250 µg/mL hygromycin B (Corning Cellgro). Fugene-6 (Roche Molecular Biochemicals) in serum-free media was used to transfect cells using a 6:1 transfection reagent:DNA ratio. Assays were conducted 24-48 hours post transfection.

Drosophila neuron culture. Drosophila neurons were cultured from 1-3 day old males. Brains were dissected in Schneider's medium with 1.5% bovine serum albumen (BSA) and optic lobes were removed. Brains were washed with Schneider's medium and incubated for 40 minutes in collagenase (0.3%) and trypsin (0.125%). They were washed in Schneider's medium supplemented with 10% heat inactivated FBS. Dissociated cells were obtained by brain trituration in medium. Cells from each brain were plated on one poly-D-lysine coated MatTek® dish treated with collagen (type IV). Assays were performed the next day.

Cell imaging. We used the pleckstrin homology (PH) domain from phospholipase C_δ ($PHPLC_\delta$-mRFP) that binds to PIP_2 at the plasma membrane and has been used to monitor pools of PIP_2 at the plasma membrane(Varnai and Balla, 1998). Cells on poly-D-lysine coated MatTek® dishes were co-transfected with GFP-DAT and PHPLCδ-mRFP and, after 48 hours, were deprived of serum overnight. Single confocal image sections were generated by using a LSM 510 inverted confocal microscope (Zeiss) by sequential imaging of live cells.

Co-immunoprecipitations. Cells were grown to confluence in 25 cm^2 culture flasks and serum deprived overnight prior to assay. On the day of the assay, cells were washed three times with

4˚C phosphate-buffered saline (Gibco) containing 1 mM EGTA and 1 mM EDTA and lysed in RIPA buffer (100 mM NaCl, 1.0% IGEPAL CA-630 (NP-40), 0.5% sodium deoxycholate, 0.1% SDS, 50 mM Tris, pH = 8.0, supplemented with a protease inhibitor cocktail (Sigma Aldrich)). Lysates were passed twice through a 27.5 gauge needle and centrifuged at 15,000 x g for 30 minutes. With a portion of the total cell lysate (TCL) collected to run as the totals, 1 mL of the remaining supernatant was incubated at 4°C for 4 hours with Sepharose-G beads (Fisher Scientific), previously washed with 1% BSA in RIPA buffer and preincubated with 2.5 µg PIP_2 antibody (mouse monoclonal, Enzo Life Sciences). For the negative control, TCL supernatant was incubated with BSA-blocked Sepharose-G beads alone. Beads were spun down, washed with cold RIPA buffer, and samples eluted with Laemmli sample buffer at 95˚C for 5 minutes. TCL and eluates were analyzed by SDS-PAGE and immunoblotting (see below for antibody details). Band intensity was quantified using ImageJ software (National Institutes of Health). The association between PIP_2 and hDAT variants was represented as the ratio of eluate:TCL band intensity, normalized to the eluate:TCL ratio observed in hDAT and expressed as a percent. For the mouse DAT-PIP_2 co-immunoprecipitations from striatum, the same protocol was used with the following modifications: striatum was dissected from either wild-type or DAT KO mice, solubilized in RIPA buffer (1:10 weight/volume), homogenized, lysed on ice for 30 minutes and then centrifuged. The remaining protocol was performed as described above. The mice used for these experiments were handled in compliance with IACUC protocols.

Cell surface biotinylation and protein immunoblot. Cells were cultured in 6-well plates. For cell surface biotinylation assays, cells were labeled with sulfo-NHS-SS-biotin (1.0 mg/ml; Pierce) before purification and analysis via SDS-PAGE/immunoblots(Mazei-Robison *et al.*, 2008). hDAT was detected using a rat monoclonal primary antibody to the N-terminus of hDAT (1:1000) (Millipore Bioscience Research Reagents) and a goat-anti-rat-HRP-conjugated secondary antibody (1:5000; Jackson ImmunoResearch).

Gluthathione transferase (GST) fusion proteins. GST and GST fused to the first 64 N-terminal amino acids of hDAT were purified as described previously(Binda *et al.*, 2008) with some modifications. Briefly, GST and the GST fusion proteins were produced in *Escherichia coli* BL21 DE3 LysS. The culture was grown at 30°C, expression induced by the addition of 1 mM isopropylβ-d-1-thiogalactopyranoside at 18°C, and the culture was harvested 8 hours after induction. The frozen pelleted bacteria was thawed in Tris-buffered saline (TBS) containing 10% glycerol and a Bacterial Protease inhibitor cocktail (Roche Diagnostics)(pH 7.4) and treated with 1 mg/mL lysozyme followed by 15 mM CHAPS. It was then sonicated and cleared by centrifugation. The lysate was passed over glutathione Sepharose 4B beads (GE Healthcare) and washed several times with TBS, followed by 10 mM Tris containing 10% glycerol and eluted with TBS containing 10 mM gluthathione. The quality, size, and amount (relative to BSA) of GST fusions were determined by SDS-PAGE and Bio-Safe Coomassie G-250 Stain. The amount was determined by analysis of imaged gels using ImageQuantTL.

Liposome binding. GST and GST fusion proteins where incubated with or without liposomes for 10 minutes at room temperature, centrifuged at 100,000 x g for 20 minutes at 4°C, and analyzed by immunoblot analysis using anti-GST antibodies (The Vanderbilt Antibody and Protein Resource Core). Liposomes were formed by extrusion of synthetic lipids at a final concentration of 1 mM. Liposomes were formed in 10 mM HEPES/TRIS, 100 mM NaCl with 95% phosphatidylcholine (DOPC; Echelon) and 5% PIP_2 (Phosphatidylinositol 4,5-bisphosphate diC16) at a pH of 7.4.

Amperometry and patch clamp electrophysiology. Cells were plated at a density of ~20,000 per 35-mm culture dish. To preload cells with DA, dishes were washed with KRH assay buffer (130 mM NaCl, 1.3 mM KCl, 1.2 mM KH_2PO_4, 10 mM HEPES, and 2.2 mM $CaCl_2$, pH 7.4) containing

10 mM dextrose, 100 µM pargyline, 1 mM tropolone, and 100 µM ascorbic acid, and incubated with 1 µM DA in KRH assay buffer for 20 minutes at 37°C. To preload *Drosophila* neurons, dishes were washed with KRH assay buffer (as above) containing 100 nM raclopride, and incubated with 1 µM DA in KRH assay buffer for 20 minutes at 26°C. All dishes were washed three times with the external bath solution (130 mM NaCl, 10 mM HEPES, 34 mM dextrose, 1.5 mM $CaCl_2$, 0.5 mM $MgSO_4$, 1.3 mM KH_2PO_4, adjusted pH to 7.35, and 300 mOsm).

To deliver DA (2 mM, Sigma Aldrich), PIP_2 inhibitory/control peptides (3 µM pal-HRQKHFEKRR or pal-HAQKHFEAAA), and/or PIP_2 (50 µM, phosphatidylinositol 4,5-bisphosphate diC8, Echelon Biosciences), a programmable puller (model P-2000, Sutter Instruments, Novato CA) was used to fabricate quartz recording pipettes with a resistance of 3-5 MΩ. These pipettes were filled with an internal solution containing: 120 mM KCl, 10 mM HEPES, 0.1 mM $CaCl_2$, 2 mM $MgCl_2$, 1.1 mM EGTA, 30 mM dextrose, pH 7.35, and 275 mOsm. Upon gaining access to the cells, the internal solution was allowed to diffuse into the cell for 10 minutes.

Experiments involving perfusion of AMPH or DA (Fig. 3b and inward current experiments) utilized double-barrel quartz tubing with an inner diameter of 250 µm (Polymicro Technologies, Phoneix AZ) placed ~80 µm from the cell. DAT-mediated inward currents were recorded at -60 mV.

To record DA efflux, a carbon fiber electrode (ProCFE; fiber diameter of 5 µm; obtained from Dagan Corporation) juxtaposed to the plasma membrane and held at +700 mV (a potential greater than the oxidation potential of DA) was used to measure DA flux through oxidation reactions. Amperometric currents in response to the addition of AMPH were recorded using an Axopatch 200B amplifier (Molecular Devices, Union City, CA) with a low-pass Bessel filter set at 1 kHz; traces were digitally filtered offline at 1 Hz using Clampex9 software (Molecular Devices,

Union City, CA). DA efflux was quantified as the peak value of the amperometric current for all experiments except for recordings from *Drosophila* neurons. For *Drosophila* neurons, total DA efflux was quantified as the integral of the trace for a fixed 15 minute window. Dopaminergic neurons were recognized by fluorescence microscopy since the TH-GAL4 drives the expression of mCherry in dopaminergic neurons.

[^{3}H]DA uptake. Cells were plated on poly-D-lysine coated, 24-well plates and grown to ~90% confluence. On the day of the experiment, cells were washed once with 37°C KRH buffer containing 10 mM dextrose, 100 µM pargyline, 1 mM tropolone, and 100 µM ascorbic acid, and equilibrated for 5 minutes at 37°C. Saturation kinetics of DA uptake was determined using a mixture of [^{3}H]DA (PerkinElmer Life Sciences, Waltham, MA) and unlabeled DA diluting to final DA concentrations of 0.01 µM - 10 µM. Uptake was initiated by bath addition of the dilution row mixture. Uptake was terminated after 10 minutes by washing twice in ice-cold KRH buffer. Scintillation fluid (Optiphase HiSafe 3, PerkinElmer Life Sciences) was added to the wells and the plates were counted in a Wallac Tri-Lux β-scintillation counter (Wallac). Nonspecific binding was determined in the presence of 10 µM cocaine. K_m and V_{max} values were derived by fitting Michaelis-Menten kinetics to the background corrected uptake data, using GraphPad Prism 5.0 (GraphPad Software, San Diego, CA). All determinations were performed in triplicates.

Computational Modeling. To evaluate the interactions between PIP_2-enriched membranes and the N-terminal region of the hDAT (residues 1-59), as well as the hDAT K/A and hDAT K/N mutants, molecular models were constructed with the knowledge-based structure-prediction tool Rosetta(Das and Baker, 2008). 1,000 different structures obtained from the structure prediction protocols in Rosetta were filtered through clustering according to a criterion of *maximization of common structure conservation* implemented in the in-house algorithm RMSDTT, which has been introduced into the molecular graphics program, visual molecular dynamics

(VMD)(Humphrey *et al.*, 1996). Clusters with the largest numbers of conformations (usually 2−3 top clusters for each construct) were selected for further refinement with atomistic molecular dynamics (MD) simulations, to find the motifs within each cluster that were most frequently found in the Rosetta prediction. Predicted structures of the hDAT N-terminus, incorporating these most frequent motifs, were then subjected to both unbiased MD and replica exchange MD(Earl and Deem, 2005) simulations to assess the stability of the overall fold of the N-terminus, as well as of the individual structural elements identified with Rosetta.

The top structures that underwent the filtering process, described above, were further examined for suitability in the complete model of the hDAT transmembrane bundle (TMB)(Beuming *et al.*, 2008, Kniazeff *et al.*, 2008, Bisgaard *et al.*, 2011). The structures were embedded into a compositionally-asymmetric lipid membrane model (5:45:50 mixture of PIP_2/POPE (phosphatidylethanolamine) / POPC (phosphatidylcholine) on the intracellular leaflet, and 30:70 mixture of sphingomyelin / POPC on the extracellular leaflet(Kiessling *et al.*, 2009). Docking of the N-terminus (1-59 residues) to the TMB (residues 57-590) was carried out with Modeller(Sali and Blundell, 1993). Specific poses for the N-terminal constructs, relative to the TMB, were selected based on the criterion of positioning the largest positive electrostatic potential isosurfaces (EPIs) towards the membrane surface. As shown before(Khelashvili *et al.*, 2012), such configurations not only result in the strongest electrostatic interactions between the protein and the PIP_2-containing membrane, but also produce the highest levels of concomitant PIP_2 sequestration by the N-terminal peptide. These juxtamembrane poses of the N-terminus served as starting configurations for subsequent studies of the dynamics of PIP_2 lipids near the hDAT N-terminus, as detailed below.

The protocol used to evaluate the interaction of the hDAT N-terminus with PIP_2-containing membranes is based on the application of the self-consistent mean-field model (SCMFM) that

evaluates the steady state distributions of charged lipid species (PIP_2, in this case) under the influence of electrostatic forces from a membrane-adsorbing macromolecule (here, the hDAT N-terminus) and quantifies the corresponding adsorption energies. As described in detail(Khelashvili *et al.*, 2008, Khelashvili *et al.*, 2009, Khelashvili *et al.*, 2012), the SCMFM is a mesoscale approach, based on the non-linear Poisson-Boltzmann (NLPB) theory of electrostatics(Sharp and Honig, 1990) and Cahn-Hilliard dynamics, in which the protein is considered in 3-dimensional full atomistic detail, and the lipid membrane is considered as a 2-dimensional, tensionless, incompressible low-dielectric elastic slab in which the equilibrium distribution of different lipid species around adsorbing protein is obtained by self-consistent minimization. The governing free energy function contains contributions from electrostatic interactions, lipid mixing entropy, and mixing entropy of mobile salt ions in the solution. The SCMFM calculation of the membrane interaction of the hDAT N-terminus constructs (hDAT and the hDAT K/A or hDAT K/N mutants) considered in full atomistic detail (with partial charge and atomic radii taken from the all-atom CHARMM27 force field with CMAP corrections for proteins(Mackerell *et al.*, 2004), was carried out with the N-terminus positioned 2Å away from the lipid surface with average surface charge density of -0.0031*e* (corresponding to a lipid mixture with 5% PIP_2). The NLPB equation was then solved numerically as described(Khelashvili *et al.*, 2008, Khelashvili *et al.*, 2009, Khelashvili *et al.*, 2012), in a 0.1 M ionic solution of monovalent counterions (corresponding to λ=9.65Å Debye length), and using a dielectric constant of 2 for membrane interior and protein, and 80 for the solution.

AMPH Uptake. Plated hDAT, hDAT K/N, and hDAT K/A cells, as well as untransfected cells (to account for non-specific AMPH uptake) were washed with KRH assay buffer and incubated for 5 min at 37 °C with 10 nM AMPH. Cells were washed three times with ice-cold KRH and AMPH was extracted with acidic organic solvent. AMPH was quantified by reversed-phase HPLC using the Waters AccQ·Tag® method which uses pre-column derivatized reagents that help separate

and easily detect fluorescence adducts (Waters Corporation, Milford, MA). AMPH uptake (with non-specific uptake subtracted) was normalized to hDAT levels and expressed as a percent.

Drosophila Genetics, Molecular Biology, and Construction of UAS hDAT. Flies lacking the *Drosophila* dopamine transporter (*DAT*^{fmn})(Kume *et al.*, 2005) and flies harboring TH-Gal4(Friggi-Grelin *et al.*, 2003) were outcrossed to a control line (Bloomington Indiana (BI) 6326) and selected by PCR or by eye color. TH-GAL4 (Bl 8848) and M{vas-int.Dm}ZH-2A, M{3xP3-RFP.attP'} ZH-22A (Bl 24481) were obtained from the BI stock center and outcrossed to flies lacking the *Drosophila* DAT (*DAT*^{fmn}) and carrying the *white* (*w*^{1118}) mutation (BI stock number 6236) for 5–10 generations. Transgenes (hDAT or hDAT K/A) were cloned into pBI-UASC(Wang *et al.*, 2012), and constructs were injected into embryos from M{vas-int.Dm}ZH-2A, M{3xP3-RFP.attP'}ZH-22A (Bl 24481). Initial potential transformants were isolated by selecting for red eyes and lack of GFP signal in the head. Transformants were also verified by RFP fluorescence and outcrossed 5-8 times to *DAT*^{fmn} flies. The presence of *DAT*^{fmn} lesion was verified by PCR. Flies were maintained on a standard cornmeal/molasses/yeast media at 25°C and 65% humidity with a 12 hour/12hour light/dark cycle. Lights came on at 8 AM and off at 8 PM.

Behavioral Analysis. Three-day-old males were collected and placed into tubes with food for three days. After three days locomotion was recorded for 32 hours by beam breaks and analyzed using equipment/software from Trikinetics (www.trikinetics.com). For the AMPH-induced locomotion, males were starved for 6 hours and then fed sucrose (10 mM) containing either AMPH (1 mM) or vehicle.

Statistical Analysis. Compiled data are expressed as normalized mean values ± standard error. For statistical analysis, we used either a Student's t-test or one-way ANOVA depending on the n of the experimental groups. $P < 0.05$ was considered statistically significant.

CHAPTER III

DE NOVO MUTATION IN THE DOPAMINE TRANSPORTER GENE ASSOCIATES DOPAMINE DYSFUNCTION WITH AUTISM SPECTRUM DISORDER[†]

Preface

This chapter explores the effect of an ASD-associated *de novo* variation within the DAT gene on DAT protein function. A complete presentation of these data can be found in Hamilton and Campbell *et al.*(Hamilton *et al.*, 2013).

Genetic factors are commonly implicated as important components of ASD. However, despite the considerable heritability, few genetic risk factors for ASD pathogenesis have been identified. Mounting evidence suggests that *de novo* genetic variation, affecting hundreds of genes across the exome, contributes to the overall genetic risk for ASD. This chapter describes the first ASD-associated *de novo* mutation in the hDAT gene (*SLC6A3*). We show that this *de novo* mutation causes profound functional abnormalities in hDAT function, including an anomalous, persistent, and exaggerated reverse transport of DA (ADE). To test our molecular discoveries mechanistically *in vivo*, we developed a behavioral model in *Drosophila*. Flies expressing the hDAT T356M in DA neurons lacking the dDAT display hyperlocomotion as compared to flies expressing hDAT. These data strongly support the notion that the abnormal function of this

[†] The work presented in this chapter is *in press* as Hamilton PJ[*], Campbell NG[*], Sharma S, Erreger K, Hansen FH, Saunders C, Belovich AN, NIH ARRA Autism Sequencing Consortium, Sahai M, Cook EH, Gether U, Mchaourab HS, Matthies HJG[*], Sutcliffe JS[*], Galli A[*]. (2013). De novo mutation in the dopamine transporter gene associates dopamine dysfunction with autism spectrum disorder. *Molecular Psychiatry* 18(12): 1315–23.

hDAT variant, stemming from this *de novo* mutation, confers anomalous phenotypic behaviors of an intact organism.

In this chapter, a variety of techniques are utilized to define, functionally and structurally, the first ASD-associated *de novo* missense mutation in the hDAT. Our work outlines a potential mechanism by which altered DA homeostasis, due to aberrant hDAT function, plays a role in the etiology of ASD. Collectively, these studies present the first structural and functional analysis of an ASD-identified *de novo* variant and implicate altered regulation of DA homeostasis as a potential liability in ASD risk.

Abstract

De novo genetic variation is an important class of risk factors for autism spectrum disorder (ASD). Recently, whole exome sequencing of ASD families has identified a novel *de novo* missense mutation in the human dopamine (DA) transporter (hDAT) gene, which results in a Thr to Met substitution at site 356 (hDAT T356M). The dopamine transporter (DAT) is a presynaptic membrane protein that regulates dopaminergic tone in the central nervous system by mediating the high-affinity re-uptake of synaptically released DA, making it a crucial regulator of DA homeostasis. Here, we report the first functional, structural, and behavioral characterization of an ASD-associated *de novo* mutation in the hDAT. We demonstrate that the hDAT T356M displays anomalous function, characterized as a persistent reverse transport of DA (substrate efflux). Importantly, in the bacterial homolog leucine transporter, substitution of A289 (the homologous site to T356) with a Met promotes an outward-facing conformation upon substrate binding. In the substrate-bound state, an outward-facing transporter conformation is a required for substrate efflux. In *Drosophila melanogaster*, expression of hDAT T356M in DA neurons lacking *Drosophila* DAT leads to hyperlocomotion, a trait associated with DA dysfunction and

ASD. Taken together, our findings demonstrate that alterations in DA homeostasis, mediated by aberrant DAT function, may confer risk for ASD and related neuropsychiatric conditions.

Introduction

Genetic factors have been implicated as important components in the etiology of autism spectrum disorder (ASD). It is now accepted that rare genetic variation affecting single nucleotides of protein-coding DNA, as well as rare genomic copy number variants (CNVs), are significant ASD risk factors(Sebat *et al.*, 2007, Sanders *et al.*, 2011, Devlin and Scherer, 2012, Sanders *et al.*, 2012). In particular, increasing evidence suggests that *de novo* genetic variation is a risk factor in ASD and other neuropsychiatric diseases(Cook and Scherer, 2008, Pinto *et al.*, 2010, Levy *et al.*, 2011, Sanders *et al.*, 2011, Devlin and Scherer, 2012). Several groups have conducted whole exome sequencing (WES) on ASD families, and collectively, these studies indicate that discrete *de novo* mutation (single nucleotide variation (SNV) or small indels) contribute to the overall genetic risk of ASD(Iossifov *et al.*, 2012, Neale *et al.*, 2012, O'Roak *et al.*, 2012, Sanders *et al.*, 2012). Among these variations is the first ASD-associated, *de novo* mutation found in the human dopamine (DA) transporter (hDAT) gene (*SLC6A3*)(Neale *et al.*, 2012). This mutation results in a Thr to Met substitution at position 356 (hDAT T356M). The consequences of this *de novo* mutation and its impact on DA neurotransmission have yet to be elucidated.

The neurotransmitter DA plays an important role in the central nervous system by regulating a variety of functions, including motor activity, motivation, attention, and reward(Carlsson, 1987, Giros and Caron, 1993, Bjorklund and Dunnett, 2007, Palmiter, 2008). Disrupted DA function is implicated in a number of neuropsychiatric disorders, including bipolar disorder, schizophrenia, attention-deficit hyperactivity disorder (ADHD)(Seeman and Niznik, 1990, Volkow *et al.*, 2007,

Cousins *et al.*, 2009) and, more recently, ASD(Nieminen-von Wendt *et al.*, 2004, Anderson *et al.*, 2008, Nakamura *et al.*, 2010, Tassone *et al.*, 2011). The dopamine transporter (DAT) is a presynaptic membrane protein that regulates DA neurotransmission via the high-affinity reuptake of synaptically released DA(Kristensen *et al.*, 2011). It is the major molecular target of cocaine, amphetamine (AMPH; Adderall™), and methylphenidate (Ritalin™)(Giros *et al.*, 1996, Jones *et al.*, 1998, Khoshbouei *et al.*, 2004, Kahlig *et al.*, 2005, Sulzer *et al.*, 2005). Due to DAT's role in DA neurotransmission, *SLC6A3* variants have been a focus of genetic association studies linking the etiology of brain disorders to dysregulated DA neurotransmission(Kurian *et al.*, 2009, Kurian *et al.*, 2011). Recent studies have identified a rare, inherited, functional missense *SLC6A3* variant, hDAT A559V (rs28364997)(Grunhage *et al.*, 2000, Mazei-Robison *et al.*, 2005), that has been associated with ADHD, which is commonly comorbid in ASD subjects(Roman *et al.*, 2004, Leyfer *et al.*, 2006, de Bruin *et al.*, 2007, Ronald *et al.*, 2008). These studies point to a contribution of DAT genetic variants in complex brain disorders.

While the role of DA in ADHD has been established(Nemoda *et al.*, 2011), DA's role in ASD is poorly understood(Dichter *et al.*, 2012). Many individuals with ASD exhibit co-occurrence of ADHD symptoms (~20-45%)(Goldstein and Schwebach, 2004, Sturm *et al.*, 2004, Yoshida and Uchiyama, 2004, Gadow *et al.*, 2006). The comorbid nature of ADHD with ASD points to dysregulation of common signaling pathways (e.g. DA) as a mechanism underlying these neuropsychiatric disorders(Di Martino *et al.*, 2013).

Here, we characterized the first ASD-identified, *de novo* mutation in hDAT by presenting structural, functional, and behavioral analysis of this *de novo* variant. These results implicate altered DA homeostasis as a potential liability in ASD risk.

Results

T356M *de novo* DAT variant has impaired function

A recent study assessed the role of *de novo* variation in ASD by using WES in 175 ASD parent-child trios(Neale *et al.*, 2012). In this study, a *de novo SLC6A3* variant was identified, resulting in a Thr to Met substitution at site 356(Neale *et al.*, 2012). Given the rarity of non-synonymous *de novo* events, it is not surprising that this mutation was absent in the ~1,000 unrelated ASD cases and controls(Neale *et al.*, 2012) and has not been deposited in 1,000 genomes(Genomes Project *et al.*, 2012), dbSNP (build 137)(Sherry *et al.*, 2001), or the NHLBI Exome Sequencing Project. The subject carried no other coding *de novo* mutations. The T356 is completely conserved across several species (**Fig. 18a**). Importantly, the T356 residue is located in the seventh transmembrane domain of hDAT and resides in a highly conserved region implicated in ion binding(Yamashita *et al.*, 2005). The molecular modeling of hDAT and *in silico* mutagenesis of T356 is shown in figure 18b.

The subject harboring this *de novo* mutation is the elder male child of healthy nonconsanguineous Caucasian parents (proband has a healthy younger sibling). There is no immediate family history of ASD or related psychiatric conditions. The subject has a normal IQ (94) and has no history of seizures or other co-morbidites. By the age of 6 years-old, the proband was diagnosed with ASD (see supplemental material for full clinical reports).

To evaluate whether the T356M variant may be a risk factor in the proband's ASD, we compared the activities of hDAT and hDAT T356M in a heterologous expression system. We examined radioactive [^{3}H]DA uptake and affinity. In hDAT T356M cells, the maximal velocity of DA influx (V_{max}) was significantly reduced, whereas the apparent DA affinity (K_m) of hDAT T356M was not significantly different from that of hDAT (**Fig. 19a**, top). A representative plot of DA uptake kinetics for hDAT and hDAT T356M is shown in figure 19a (bottom). The reduced

a

Human	IVTTSINSLTSFSSGFVVFSFL	368
Gorilla	IVTTSINSLTSFSSGFVVFSFL	368
Dog	VITTSVNSLTSFSSGFVVFSFL	365
Mouse	IITTSINSLTSFSSGFVVFSFL	367
Rat	IITTSINSLTSFSSGFVVFSFL	367
Zebrafish	IITSSINSLTSFFSGFVIFSFL	377
Drosophilia	LLTSFINSATSFIAGFVIFSVL	367
C. elegans	LFTSFINCATSFLSGFVIFSVL	361

b

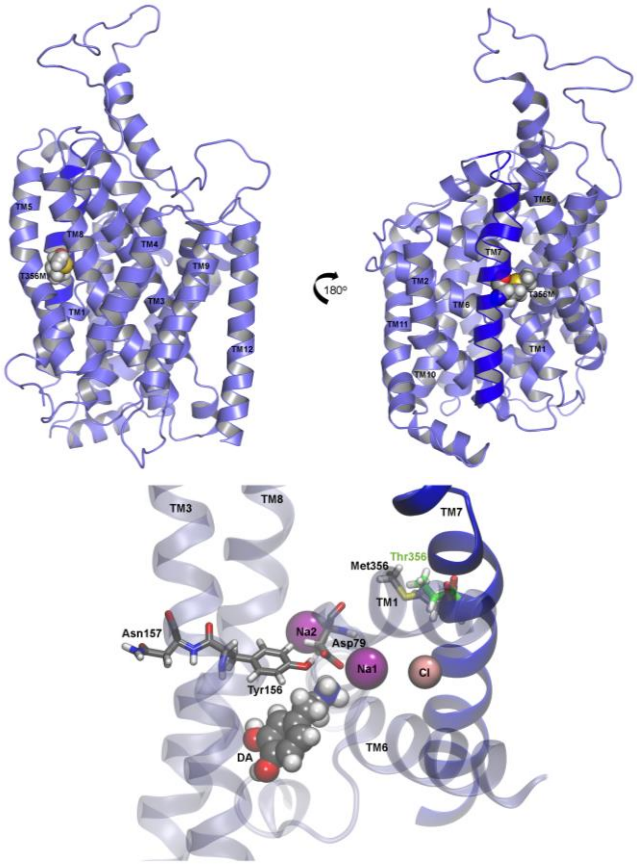

Figure 18. Cross-species conservation and *in silico* mutagenesis of T356. **(a)** Alignment of the DAT amino acid sequence across multiple species. Threonine 356 is represented in red. **(b)** In an equilibrated three-dimensional homology model of hDAT, the T356M mutation is located on transmembrane domain 7 (TM7). Top: Schematic views representing a 180° rotation show T356M with respect to the TM helices. TM7 is shown in dark blue. Bottom: Critical residues that interact with DA are shown, as well as the bound Na^+ and Cl^- ions. The methionine is rendered together at position 356 with the wild type threonine (green).

[^{3}H]DA transport capacity was not associated with a reduction in either total or DAT surface expression (**Fig. 19b**, top), as assessed by measuring changes in DAT proteins in the total and biotinylated fraction, respectively. The total fraction for hDAT and hDAT T356M contained both glycosylated and non-glycosylated forms of the DAT. Surface fractions were quantitated, normalized to total DAT (glycosylated), and expressed as a percent of hDAT (**Fig. 19b**, bottom). Furthermore, normalizing the total DAT fraction (glycosylated) to actin loading control yielded no significant differences between hDAT and hDAT T356M total expression (data are expressed as a percentage of hDAT; hDAT 100 ± 17.6% versus hDAT T356M 96.4 ± 13.7%; $p \geq 0.87$ by Student's t-test; n = 8-11).

hDAT T356M displays ADE

Although hDAT T356M displays similar surface expression to that of hDAT, it demonstrates reduced ability to accumulate intracellular DA. One possibility is that constitutive DA efflux, here referred to as anomalous DA efflux (ADE), contributes to this reduced DA uptake in the hDAT T356M cells. This efflux would impede the intracellular accumulation of DA.

To determine whether hDAT T356M exhibits ADE, cells were whole cell patch clamped and perfused for 10 minutes with an internal solution containing 2 mM DA(Bowton *et al.*, 2010). The electrode, in current clamp configuration, allows the cell to control its membrane voltage. In addition, this technique ensures that cells expressing either hDAT or hDAT T356M were equally loaded with DA. DA efflux was quantified through amperometry(Bowton *et al.*, 2010). We have previously shown that, in the presence of ADE, cocaine decreases the amperometric signal through blockade of DAT(Mazei-Robison *et al.*, 2008). In hDAT cells, amperometric currents were unaffected by application of cocaine (**Fig 20a**, top, hDAT, COC), indicating no ADE. In contrast, amperometric signals from hDAT T356M cells were significantly reduced by the

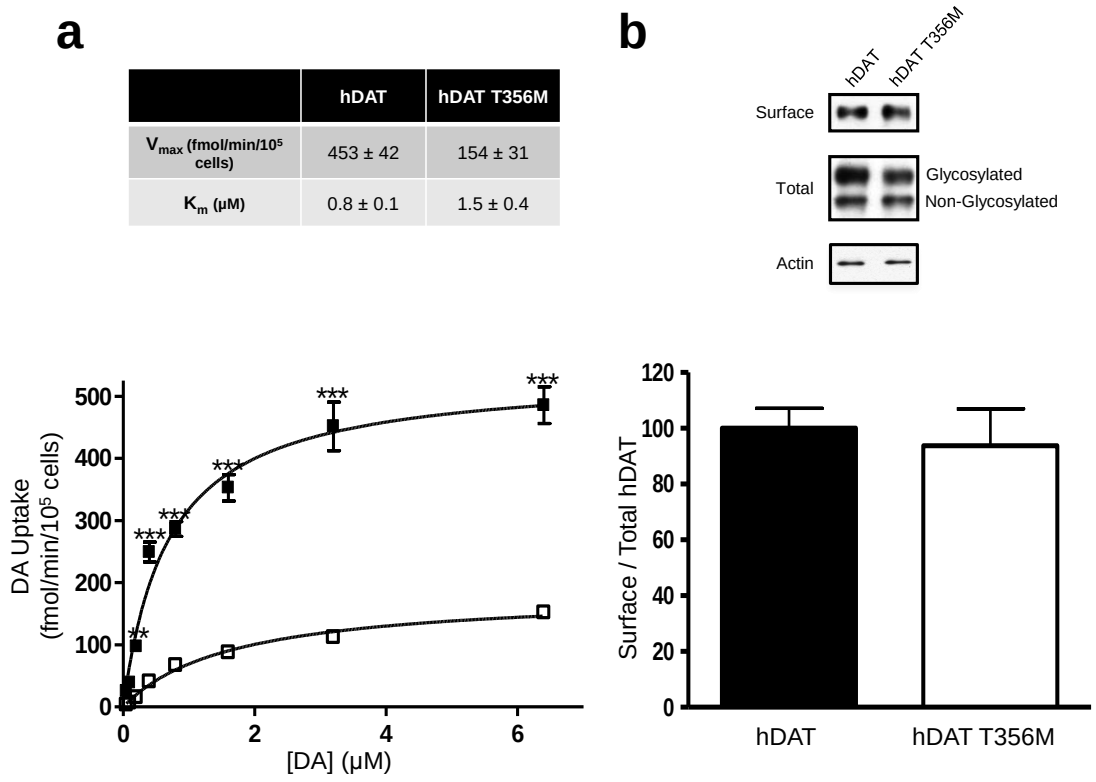

Figure 19. hDAT T356M has impaired function. (a) Top: Kinetic parameters (V_{max} and K_m) for hDAT and hDAT T356M (V_{max}: $p \leq 0.005$; by Student's t-test; n = 3, in triplicate; K_m: $p \geq 0.20$; by Student's t-test; n = 3, in triplicate). Bottom: Representative plot of [^{3}H]DA uptake kinetics in hDAT (filled squares) or hDAT T356M (empty squares) cells (** = $p \leq 0.01$, *** = $p \leq 0.001$; by two-way ANOVA followed by Bonferroni post-test; n = 3, in triplicate). **(b)** Representative immunoblots for biotinylated (surface) and total protein fractions from hDAT and hDAT T356M cells. Surface fractions were quantitated, normalized to total DAT (Glycosylated), and expressed as a percent of hDAT ($p \geq 0.05$; by Student's t-test; n = 8-11).

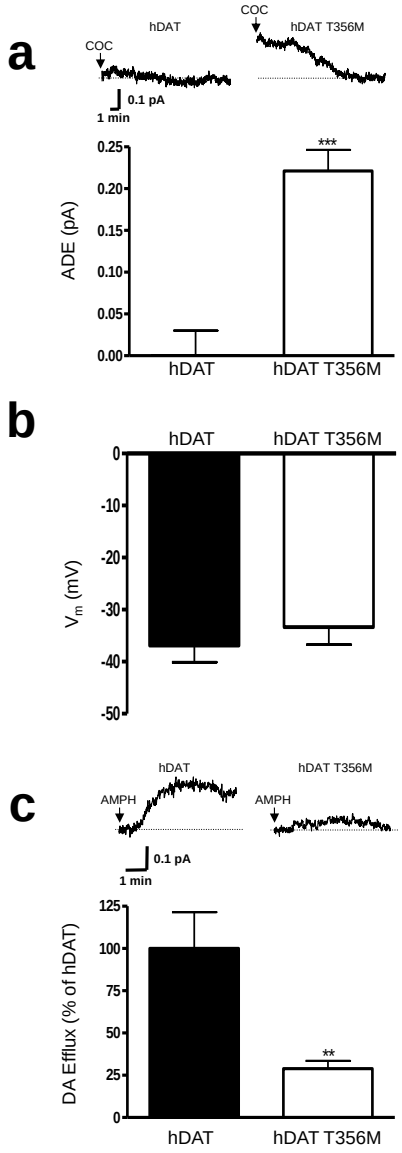

Figure 20. hDAT T356M exhibits robust anomalous DA efflux (ADE). (a) Top: representative amperometric currents recorded from hDAT and hDAT T356M cells. Arrows indicate application of 10 μM cocaine (COC). Bottom: quantitation of the cocaine-induced reduction in the amperometric current (ADE). Data are reported as maximal current (*** = $p \leq 0.001$ by Student's t-test; n = 4-5). **(b)** hDAT T356M cells do not display altered resting membrane potential with respect to hDAT cells ($p \geq 0.05$ by Student's t-test, n = 9-25). **(c)** Representative AMPH-induced amperometric currents recorded from hDAT and hDAT T356M cells. Arrows indicate application of 10 μM AMPH. Bottom: quantitation of AMPH-induced DA efflux. Data are represented as maximal current expressed as percent of the current recorded in hDAT cells (** = $p \leq 0.01$ by Student's t-test; n = 5-7).

application of cocaine (**Fig. 20a**, top, hDAT T356M, COC), revealing ADE. hDAT T356M-expressing cells displayed a significant increase in ADE, compared to hDAT transfected cells (**Fig. 20a**, bottom).

Cell membrane depolarization has been shown to support DA efflux(Khoshbouei *et al.*, 2003). Figure 20b reveals that there is not a significant difference in resting membrane potential (measured in current clamp) between cells expressing hDAT or hDAT T356M. This indicates that differences in the function of hDAT and hDAT T356M are not due to resting membrane potential.

Next, we determined possible changes in the ability of AMPH to cause DA efflux by patch delivering DA into hDAT or hDAT T356M cells while recording DA efflux with amperometry. AMPH dose-response assays (measuring the peak of the amperometric current at different AMPH concentrations) revealed that hDAT T356M and hDAT cells have comparable AMPH EC_{50} (EC_{50}; hDAT: 0.15 ± 0.05 µM; hDAT T356M: 0.16 ± 0.07 µM; n = 4; p ≥ 0.95 by Student's t-test). Then, using a saturating AMPH concentration (10 µM) we determined DA efflux in either hDAT or hDAT T356M cells (**Fig. 20c**, top). AMPH-induced DA efflux was significantly reduced in hDAT T356M cells in comparison to hDAT cells (**Fig. 20c**). These results strongly suggest that ADE does not share common mechanisms with AMPH-induced DA efflux.

In LeuT, substitution of Ala289 with a Met promotes an outward-facing conformation

To investigate the structural consequences of the T356M *de novo* mutation in a DAT homolog with a known crystal structure, we analyzed changes in the conformational cycle of the leucine transporter (LeuT). We substituted A289 (the homologous amino acid to T356) with a Met (LeuT A289M). We measured distances between pairs of spin labels (r (Å)) and the distance

distribution (P(r), the probability of a given distance between the two labels) monitoring the intra- and extracellular gates by double electron electron resonance (DEER)(McHaourab *et al.*, 2011). First, we examined the pair 309/480 (**Fig. 21a**, left) that monitors the relative movement of the extracellular loop 4 (EL4) in LeuT. This loop obstructs the permeation pathway in the Apo conformation(Claxton *et al.*, 2010), as indicated by the close proximity of the pair 309/480 (**Fig. 21a**, middle, Apo black line). Upon Na^+ binding, the distance between EL4 and TM12 increases(Claxton *et al.*, 2010), indicating opening of the extracellular vestibule and enabling substrate access (data not shown)(Claxton *et al.*, 2010). Subsequent Leu binding resets the closed EL4 conformation in the occluded conformation of the transporter (Na^+ and Leu bound in the vestibule) (**Fig. 21a**, right; +Na/L black line). The extracellular Apo state (**Fig. 21a**, middle; Apo; compare red and black lines) as well as Na^+ bound state (data not shown) are similar in LeuT and LeuT A289M. Yet, LeuT A289M with Na^+ and Leu bound in the vestibule has a destabilized bound structure with fluctuations on the extracellular side (**Fig. 21a**, right; +Na/L; compare red and black lines). The probability distribution in the Na/Leu bound state contains distinct populations of conformations that indicate fluctuations of LeuT A289M to a permeation pathway that has increased probability to be open to the outside, relative to LeuT (**Fig. 21a**, right; red line, arrows).

We then examined the pair 7/86 (**Fig. 21b**, left), to determine the distance between the N-terminus and intracellular loop 1 (IL1) and to monitor fluctuation dynamics on the intracellular side(McHaourab *et al.*, 2011). This is necessary to describe changes in the population of transporters with an inward facing conformation(McHaourab *et al.*, 2011). In the LeuT background, distance distributions between spin(McHaourab *et al.*, 2012) or fluorescent probes(Zhao *et al.*, 2011) in the Apo state are bimodal, reflecting the equilibrium of this intracellular gate between closed and open conformations (**Fig. 21b**, middle; Apo; black lines). Introduction of the A289M leads to a shift in the equilibrium to favor the closed conformation

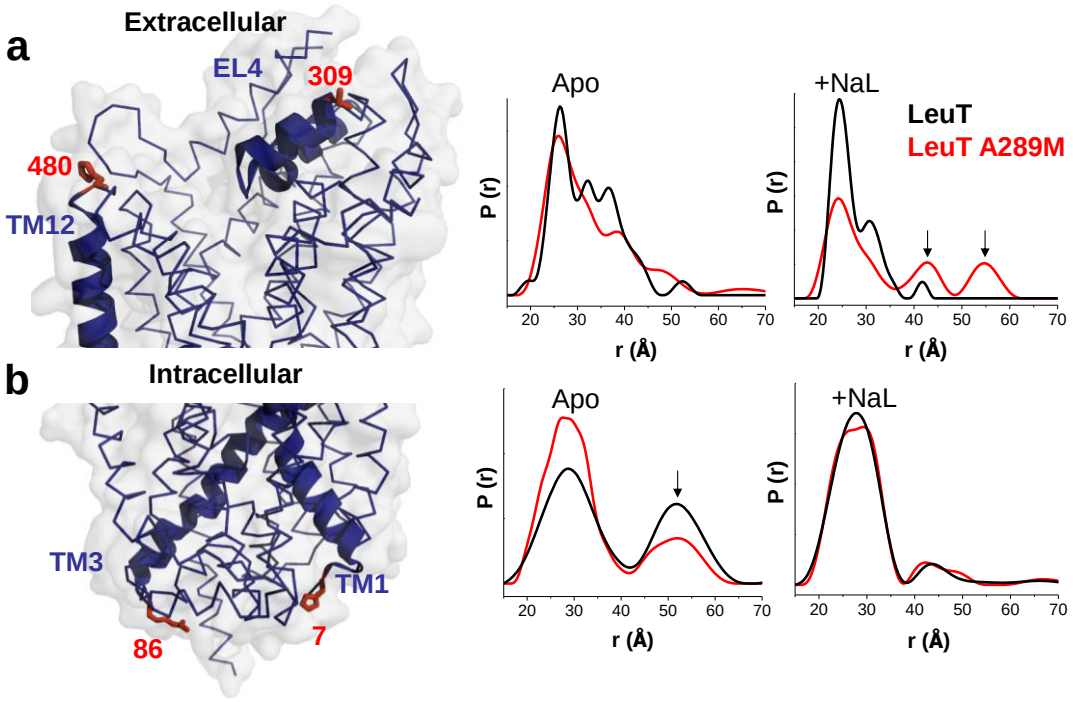

Figure 21. In the leucine transporter (LeuT), substitution of Ala289 with a Met supports an outward-open facing conformation. Distance distributions of extracellular and intracellular spin labeled Cys pairs in LeuT reveal changes in the conformational equilibrium caused by mutating Ala289 to a Met. **(a)** Left: extracellular reporter pairs (309-480) tagged on three-dimensional structure of LeuT. Right: distance of the extracellular reporter pair for LeuT (black) and A289M (red), in the Apo conformation (Apo) and in the presence of Na+ and Leu (+NaL). **(b)** Left: intracellular reporter pairs (7-86) tagged on the three-dimensional structure of LeuT. Right: distance of the intracellular reporter pair for LeuT (black) and A289M (red), in the Apo conformation (Apo) and in the presence of Na+ and Leu (+NaL). The LeuT structure was obtained from PDB 2A65. The structures were generated using PyMOL.

side (**Fig. 21b**, middle; Apo; compare red and black lines, arrow). Na^+ binding does not alter the equilibrium between the two conformations (data not shown), while Na^+ and Leu binding resets this shift to LeuT-like conformations (**Fig. 21b**, middle; +Na/L; compare red and black lines).

Our results demonstrate that, because of the A289M, the presence of substrate and Na^+ fails to completely close the extracellular pathway as in LeuT, inducing fluctuations on the extracellular side. These fluctuations to an open-to-the-outside permeation pathway persist, possibly enabling substrate release. This is in contrast to LeuT, where substrate binding closes the extracellular permeation pathway.

Drosophila expressing hDAT T356M in DA neurons are hyperactive

Locomotion is an elemental behavior regulated across species, including *Drosophila melanogaster*, by DA(Pendleton *et al.*, 2002, Wicker-Thomas and Hamann, 2008, Pizzo *et al.*, 2013). Thus, locomotion in flies offers a powerful model for elucidating the behavioral impact of ADE associated with hDAT T356M.

We expressed hDAT or hDAT T356M in flies homozygous for the *Drosophila* DAT null allele, DAT^{fmn} (dDAT KO)(Kume *et al.*, 2005), by using the Gal4/UAS system to express a single copy of hDAT or hDAT T356M in a $dDAT^{fmn}$ mutant background, selectively in DA neurons(Matthies and Broadie, 2003). To generate the transgenic flies, we used phiC31 based integration, which leads to the expression of comparable levels of mRNA for the relevant transgenes (hDAT or hDAT T356M). Locomotion was quantitated by beam crossing detection over a >24 hour period (data binned in 15 minute intervals) during both the light (horizontal white bar) and dark (horizontal black bar) cycle. While dDAT KO are hyperactive(Kume *et al.*, 2005), flies expressing

hDAT in DA neurons have reduced locomotion as compared to dDAT KO, demonstrating the behavioral significance of our approach (**Fig. 22a**, compare hDAT to dDAT KO).

We hypothesized that flies harboring the hDAT T356M would be hyperactive with respect to hDAT expressing flies due to an increase in extracellular DA promoted by ADE. This is shown in figure 22a. Figure 22b shows total (24 hour) locomotor activity in the different fly lines. Total activity (24 hours) of hDAT T356M and dDAT KO flies is significantly higher than hDAT flies (**Fig. 22b**).

hDAT T356M cells display compromised AMPH-induced DA efflux (**Fig. 20c**). This suggests a reduced ability of AMPH to increase locomotion in flies expressing hDAT T356M. Changes in locomotion were determined upon AMPH or vehicle exposure (15 minutes) and calculated as beam crosses. We observed no significant increase in locomotion in hDAT T356M flies when exposed to AMPH as compared to vehicle control (hDAT T356M (vehicle) 9.7 ± 0.7 beam breaks versus hDAT T356M (AMPH) 12.7 ± 1.6 beam breaks; $n = 24$; $p \geq 0.05$). This is in contrast to flies expressing hDAT, where AMPH induced a significant increase in locomotion (hDAT (vehicle) 6.2 ± 0.9 beam breaks versus hDAT (AMPH) 18.2 ± 1.0 beam breaks; $n = 24$; $p \leq 0.001$). Moreover, in the dDAT KO flies, similar to the hDAT T356M flies, AMPH failed to induce a significant increase in locomotion (data not shown).

Discussion

Alterations in DA tone underlie multiple neuropsychiatric disorders, including bipolar disorder, schizophrenia, and ADHD(Seeman and Niznik, 1990, Volkow *et al.*, 2007, Cousins *et al.*, 2009). With respect to ADHD, altered DA signaling, including changes in DAT function, may contribute

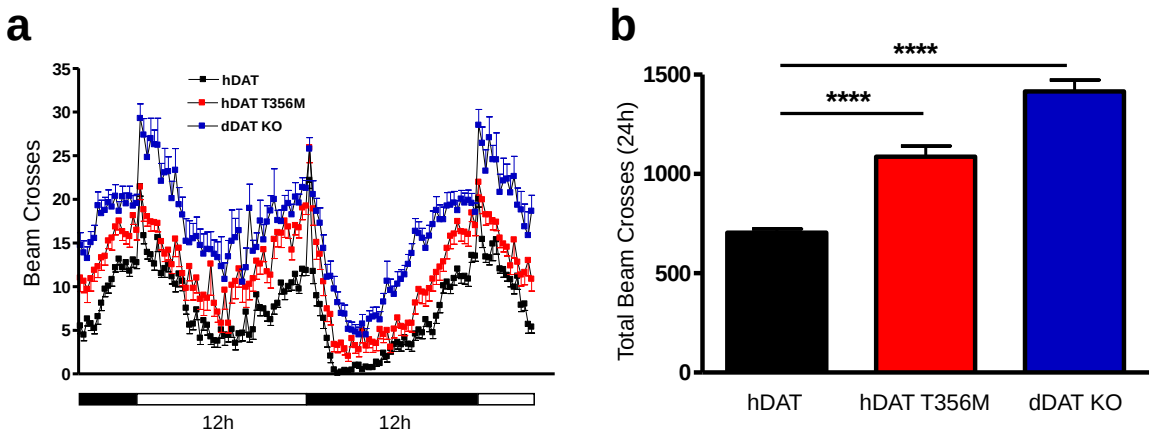

Figure 22. Expression of hDAT T356M in *Drosophila* leads to hyperactivity. hDAT or hDAT T356M was expressed in DA neurons of dDAT KO flies. **(a)** Locomotor activity was assayed over 32 hours during the light (horizontal white bars) or dark (horizontal black bars) cycle. Flies expressing hDAT T356M (red squares), as well as dDAT KO flies (blue squares), were hyperactive throughout the 32 hour period with respect to flies expressing wild type hDAT (black squares) (n = 32; beam breaks binned in 15 minute intervals). **(b)** Quantitation of total beam crosses over 24 hours for hDAT, hDAT T356M, and dDAT KO flies (**** = $p \leq 0.0001$; n = 32).

to the cognitive and hyperactive traits of the disorder(Mazei-Robison *et al.*, 2008, Bowton *et al.*, 2010). ASD, like ADHD, is phenotypically and etiologically complex. However, there is mounting evidence that risk for ASD resides, at least in part, in dopaminergic factors. Variants in DA receptor (DRD) sub-type genes, including *DRD1, DRD3,* and *DRD4*, have been associated with increased risk for ASD(Hettinger *et al.*, 2008) as well as with specific phenotypic behavior within ASD. These include repetitive or stereotyped behaviors(de Krom *et al.*, 2009, Gadow *et al.*, 2010, Staal *et al.*, 2012), oppositional defiant disorder, and separation anxiety disorder(Gadow *et al.*, 2010). Male children carrying four tandem repeats in the promoter region of the *MAOA* gene (the gene product responsible for degrading amine neurotransmitters, including DA) showed elevated risk for developing ASD(Tassone *et al.*, 2011). It must be noted that none of these genes are significant in genome-wide association studies of ASD. However, in positron emission tomography (PET) studies in adults with ASD, DAT binding was significantly elevated in the orbitofrontal cortex(Nakamura *et al.*, 2010).

Genes harboring *de novo* events are highly significant for understanding the etiology of ASD(Neale *et al.*, 2012). This is not surprising since rate of reproduction is typically low in individuals with autism. Consequently, genetic variants would be subject to negative selection(Devlin and Scherer, 2012). This suggests that the biological networks identified from these *de novo* events, and the broader pathways they function within, are candidate risk factors for ASD. In this study, we examine the functional, structural, and behavioral consequences of the first identified *de novo* hDAT missense variant associated with ASD.

Our amperometric recordings demonstrate that the *de novo* hDAT T356M mutation confers cocaine sensitive ADE. We also show that ADE does not share common mechanisms with AMPH-induced DA efflux since hDAT T356M has an impaired AMPH response. It is intriguing to speculate that anomalous transporter-mediated neurotransmitter efflux may be an

unappreciated source of risk for mental illness, especially in disorders associated with altered DA signaling. It is possible that ADE, driven by DAT variants or variants in other genes in the DAT regulatory network (such as DRD subtypes), could impact risk for ASD. A similar point for ADE has been argued previously, in the context of ADHD, for the hDAT variant A559V, in its functional identification(Mazei-Robison *et al.*, 2008) and original characterization(Bowton *et al.*, 2010).

The question remains as to how the hDAT T356M *de novo* mutation perturbs transporter structure to trigger ADE. Since the crystal structure of hDAT is unavailable, we analyzed changes in the conformational cycle of the hDAT bacterial homolog, LeuT. In LeuT A289M, we measured the distances between pairs of spin labels monitoring the intra- and extracellular gates by DEER. The spin labels monitoring the extracellular gate clearly show that in LeuT A289M, in contrast to LeuT, the presence of Na^+ and leucine promotes a permeation pathway unoccluded to the outside. In terms of transporter function, it is difficult to draw parallels between hDAT T356M and LeuT A289M. Nevertheless, it is compelling to speculate that the mechanism by which the substrate promotes an outward open conformation in LeuT A289M, could also support the ability of hDAT T356M to promote ADE when cytoplasmic DA is available. This would suggest that the mechanism of ADE for hDAT T356M is distinct from that of hDAT A559V, which is a result of a tonic activation of DRD2 and the downstream kinase CaMKII(Bowton *et al.*, 2010). Thus, there may be multiple mechanistic routes to promote hDAT-mediated ADE, and yet ADE might support the comorbid nature of ASD with ADHD.

In an *in vivo* context, hDAT T356M may alter extracellular DA levels and, as a consequence, increase locomotion(Kume *et al.*, 2005). We selectively expressed hDAT T356M specifically in DA neurons of dDAT KO flies. *Drosophila* expressing hDAT T356M exhibited prominent hyperactivity as compared to *Drosophila* expressing hDAT. In addition, AMPH has an impaired

ability to increase locomotion in hDAT T356M and dDAT KO flies. This might stem from the decreased ability of AMPH to cause DA efflux in hDAT T356M cells.

Here, we report novel and profound functional abnormalities associated with the hDAT *de novo* mutation T356M, resulting in enhancement of non-vesicular, DAT-dependent DA release, referred to as ADE. Our data raise the possibility that ADE could impact the risk for ASD.

Materials and Methods

Subjects and clinical assessment. Subjects from this family correspond to the proband, unaffected sibling, and both parents (AC04-0029-01, AC04-0029-02, AC04-0029-03, AC04-0029-04), who were recruited by the Boston-based Autism Consortium(Wolfson, 2007). Clinical assessment followed standard research criteria for ASD diagnosis. The proband was classified as having a comparatively "narrow" diagnosis (as opposed to a "broader ASD") based on diagnostic algorithms from the Autism Diagnostic Interview Revised (ADI-R)(Lord *et al.*, 1994) using criteria described by Risi *et al.*(Risi *et al.*, 2006), and classification resulting from the diagnostic algorithm of the Autism Diagnostic Observational Session (ADOS)(Lord *et al.*, 2000). Proband IQ was assessed at age 5 years, 9 months using the Wechsler Preschool and Primary Scale of Intelligence (WPPSI; Wechsler, D. (1967)). The Social Responsiveness Scale (SRS; Western Psychological Services) was performed on both parents to index the presence and severity of broader autism phenotype traits, followed by medical and family history provided by the biological mother.

SLC6A3 T356M de novo discovery. Methodological details and validation of the *de novo* mutation are published(Neale *et al.*, 2012). Briefly, DNA derived from whole blood of both parents and the probands was subjected to whole exome sequence analysis. The T356M

variant, identified as a heterozygote in the proband and absent in both parents, was experimentally validated and confirmed to be a *de novo* mutation that does not appear in the unaffected sibling.

Cell culture and transfection. The GFP-hDAT-pCIHygro expression vectors containing either hDAT or hDAT T356M sequence were generated, confirmed and transiently transfected into Chinese hamster ovary cells using FuGENE-6 (Promega). Assays were conducted 24-48 hours post transfection.

Amperometry and patch clamp electrophysiology. hDAT and hDAT T356M cells were plated at a density of ~30,000 per 35-mm culture dish and experiments conducted as previously described(Mazei-Robison *et al.*, 2008, Bowton *et al.*, 2010).

[^{3}H]DA uptake. hDAT and hDAT T356M cells were seeded (50,000 cells/well) into polyornithine coated, 24-well plates, 48 hours before assaying. Uptake kinetic assays were performed as described in the supplementary information of Rickhag *et al*.(Rickhag *et al.*, 2013) and in Rasmussen *et al.*(Rasmussen *et al.*, 2009).

AMPH uptake. Plated hDAT and hDAT T356M cells were washed with KRH buffer and incubated for 5 min at 37°C with 10 nM AMPH. Cells were washed three times with ice-cold KRH. AMPH was quantified using a HPLC system previously described(Siuta *et al.*, 2010).

Cell surface biotinylation and western blot. For cell surface biotinylation assays and Western blots, hDAT and hDAT T356M cells were cultured in 6-well plates and experiments conducted as in Mazei-Robinson *et al*.(Mazei-Robison *et al.*, 2008).

Homology Modeling of hDAT and construction of the T356M simulation system. As the template, the homology model uses the known crystal structure for the cognate and homologous structure of the recent outward-open crystal structure of LeuT(Krishnamurthy and Gouaux, 2012). The substrate DA, two Na^+ ions and a Cl^- ion were positioned as described in Shan *et al*.(Shan *et al.*, 2011). To model the mutant hDAT construct with T356M, the mutation was introduced using the free energy perturbation (FEP) method(Guptaroy *et al.*, 2009).

Double Electron Electron Resonance. Cysteine residues were introduced using site directed mutagenesis into LeuT and LeuT A289M constructs(Claxton *et al.*, 2010). Experiments were conducted as in Claxton *et al.*(Claxton *et al.*, 2010). Apo refers to ion Na^+ and leucine-free transporter while the +NaL state was obtained by addition of 200 mM NaCl and 4-fold molar excess of Leu relative to LeuT. Double Electron Electron Resonance (DEER)(Jeschke and Polyhach, 2007) was performed at 83K on a Bruker 580 pulsed EPR spectrometer operating at Q-band frequency using a standard 4-pulse sequence(Zou and McHaourab, 2010). DEER echo decays were analyzed to obtain distance distributions(Jeschke *et al.*, 2002).

Drosophila Genetics. Drosophila homozygotes for the DAT null allele DAT^{fmn} (dDAT KO)(Kume *et al.*, 2005) and flies harboring TH-Gal4(Friggi-Grelin *et al.*, 2003) were outcrossed to a control line (Bloomington Indiana (BI) 6326) and selected by PCR or eye color. TH-GAL4 (Bl 8848) and M{vas-int.Dm}ZH-2A, M{3xP3-RFP.attP'} ZH-22A (Bl 24481) were obtained from the BI stock center and outcrossed to dDAT KO flies carrying the *white* (w^{1118}) mutation (BI stock number 6236) for 5–10 generations. Transgenes (hDAT or hDAT T356M) were cloned into pBI-UASC(Wang *et al.*, 2012) and constructs were injected into embryos from M{vas-int.Dm}ZH-2A, M{3xP3-RFP.attP'}ZH-22A (Bl 24481). Initial potential transformants were isolated and selected.

Behavioral Analysis. Three-day-old males were collected and placed into tubes with food for 72 hours. Locomotion was recorded by beam breaks and analyzed using equipment/software from Trikinetics (www.trikinetics.com). For the AMPH-induced locomotion, males were starved for six hours and then fed sucrose (5 mM) containing either AMPH (10 mM) or vehicle. Data were analyzed by One-way ANOVA followed by a Newman-Keuls Multiple Comparison Post-test.

Clinical Information

Proband (male) is the eldest of two children and heterozygous for the mutation described herein.

Patient ID: AC04-0029-01 (proband)

Event: *SLC6A3 de novo* missense (T356M) mutation

At the time of testing, patient was a 66-69-month-old non-Hispanic male Caucasian diagnosed with autism (on both ADOS and ADIR). Maternal interview on pregnancy provided the following details: Mother experienced anemia during pregnancy (gestational age = 39 weeks). Labor was induced (use of Pitocin) because of failure to progress (Note: no C-section was done). Child was born 8 lbs 6 oz (134 ounces), with no other delivery issues.

Subset and composite scores on the Wechsler Preschool and Primary Scale of Intelligence (WPPSI) indicate normal intelligence. Full Scale IQ was Average (94), and the subsets of Verbal-IQ and Performance-IQ was scored as Average (101) and Low Average (86) respectively, indicating normal intelligence.

ADIR revealed deficits across all four subsets: (1) Reciprocal Social Interaction (score=13; cutoff=10); (2) Abnormalities in Communication (score=13; cutoff=8); (3) Restricted, Repetitive

and Stereotyped Patterns of Behavior (score=4; cutoff=3); (4) Development Evident at or before 36 Months (score=1; cutoff=1).

Patient experienced a delay in speech requiring therapy. No history of seizures, gastrointestinal conditions, sleep deficits, and no diet restrictions. Currently taking multivitamins, with no use of other medications (besides amoxicillin, Tylenol, and Benadryl).

No family history for psychiatric illness requiring hospitalization. Known history of Asperger's Disorder (Mother's cousin's son), and depression (Father's paternal uncle).

Patient ID: AC04-0029-02 (father)

Father is an adult non-Hispanic Caucasian male. Age at conception of proband is 36. Slightly above normative range of intelligence (IQ=118; Wechsler Adult Intelligence Scale). No presence of broader autism phenotype, and no psychiatric medication use current or past. No co-morbid diagnoses. He holds a postgraduate degree and reports an annual household income of $81-101k.

Patient ID: AC04-0029-03 (mother)

Mother is an adult non-Hispanic Caucasian female. Age at conception of proband is 32. Above normative range of intelligence (IQ=131; Wechsler Adult Intelligence Scale); no presence of broader autism phenotype, and no psychiatric medication use current or past. No co-morbid diagnoses. She holds a postgraduate degree and reports an annual household income of $81-101k. No medication use reported for mother before, during, or after pregnancy except for epidural during labor.

Patient ID: AC04-0029-04 (sibling)

Sibling is a non-Hispanic Caucasian 3 year old (37 months) of unspecified sex. Normative intelligence (IQ=118; WPPSI). No behavioral problems reported. No medication use endorsed for current or past. No comorbid diagnoses.

CHAPTER IV

ZN^{2+} REVERSES FUNCTIONAL DEFECITS IN A DE NOVO DOPAMINE TRANSPORTER VARIANT ASSOCIATED WITH AUTISM SPECTRUM DISORDER‡

Preface

This chapter explores the role of Zn^{2+} exposure in ameliorating the deficits observed in the hDAT T356M. The work presented in this chapter is currently submitted to *Molecular Autism*.

Chapter III outlined the recently characterized and novel ASD-associated *de novo* missense mutation in *SLC6A3* (hDAT T356M). This hDAT variant exhibits significantly decreased DA uptake, as well as reduced reverse transport of DA. These dysfunctional transport properties are hypothesized to contribute to DA dysfunction in ASD. Previous biophysical studies have shown that binding of Zn^{2+} to an endogenous hDAT binding site can regulate hDAT functions and conformations (**Fig. 4**).

In this chapter, we report that in the hDAT T356M variant, Zn^{2+} enhances both DA uptake (forward transport) and DA efflux (reverse transport). Engaging a Zn^{2+} activated switch in the conformation of the hDAT transporter reverses, at least partially, the functional deficits of ASD-associated hDAT T356M variant. Our work suggests that the molecular mechanism targeted by

‡ The work presented in this chapter is *submitted* as Peter J. Hamilton*, Aparna Shekar*, Andrea N. Belovich, Nicole Bibus Christianson, Nicholas G. Campbell, James S. Sutcliffe, Aurelio Galli, Heinrich J.G. Matthies*, Kevin Erreger*. (2014). Zn^{2+} reverses functional deficits in a de novo dopamine transporter variant associated with autism spectrum disorder. *Molecular Autism*.

Zn^{2+} to restore partial function in hDAT T356M is a novel therapeutic target to rescue functional deficits in hDAT variants associated with ASD.

Abstract

Alterations in dopamine (DA) homeostasis may represent a complication associated with autism spectrum disorder (ASD) and related neuropsychiatric conditions. Rare variants of the human dopamine transporter (hDAT) gene (*SLC6A3*) have been associated with a range of neuropsychiatric disorders, including ASD. Our laboratory recently characterized a novel ASD-associated de novo missense mutation in *SLC6A3* (hDAT T356M). This hDAT variant exhibits significantly decreased DA uptake, as well as reduced reverse transport of DA. These dysfunctional transport properties may contribute to DA dysfunction in ASD. Previous biophysical studies have shown that binding of Zn^{2+} to an endogenous hDAT binding site can regulate hDAT functions and conformations. Here we report that in the hDAT T356M variant, Zn^{2+} enhances both DA uptake (forward transport) and DA efflux (reverse transport). Our work suggests that the molecular mechanism targeted by Zn^{2+} to restore partial function in hDAT T356M as a novel therapeutic target to rescue functional deficits in hDAT variants associated with ASD.

Introduction

The dopamine (DA) transporter (DAT) tunes DA neurotransmission by active re-uptake of DA from the synapse(Kristensen *et al.*, 2011). Rare variants in the human DAT (hDAT) (including the first identified *de novo* mutation in the DAT gene) have been demonstrated to disrupt DA neurotransmission, contributing to the etiology of a number of neuropsychiatric disorders, including schizophrenia, bipolar disorder, attention deficit hyperactivity disorder (ADHD)(Seeman and Niznik, 1990, Volkow *et al.*, 2007, Cousins *et al.*, 2009), and autism

spectrum disorder (ASD)(Anderson *et al.*, 2008, Gadow *et al.*, 2008, Hamilton *et al.*, 2013, Bowton *et al.*, 2014). Extracellular zinc (Zn^{2+}) inhibits DAT-mediated DA uptake(Norregaard *et al.*, 1998). Three amino acid side chains have been identified in DAT which co-ordinate zinc: H193 in extracellular loop 2 (EL2), H375 in the first helical part of extracellular loop 4 (EL4A) and E396 in the second helix of extracellular loop 4 (EL4B)(Norregaard *et al.*, 1998, Loland *et al.*, 1999)(**Fig. 4**). Structural data from the DAT-homolog LeuT in the inward- and outward-facing conformation suggests that the relative orientation of H375 and E396 shifts during the transport cycle(Krishnamurthy and Gouaux, 2012). Binding of Zn^{2+} to the coordinating residues in the DAT (H193, H375 and E396) alters the conformational equilibrium between the inward- and outward-facing state of the DAT(Loland *et al.*, 2002, Stockner *et al.*, 2013). However, mutation of an intracellular tyrosine to alanine (Y335A) converts the inhibitory Zn^{2+} switch into an activating Zn^{2+} switch, whereby Zn^{2+} rescues functions of the mutant transporter(Loland *et al.*, 2002, Kahlig *et al.*, 2006).

Our laboratory has recently characterized the first *de novo* mutation in the hDAT reported in a patient diagnosed with ASD, which results in a Thr to Met substitution at site 356 (hDAT T356M). hDAT T356M displays decreased both forward and reverse-transport function compared with wild-type hDAT(Hamilton *et al.*, 2013). The reduced transport capacity of the mutant was not associated with a reduction in hDAT surface expression. Amphetamine (AMPH) is a psychostimulant that targets the hDAT causing reverse transport of DA (DA efflux)(Sulzer *et al.*, 2005). hDAT T356M exhibits impaired AMPH-induced DA efflux. Here we show that the presence of Zn^{2+} partially rescues both the DA uptake and the AMPH-induced DA efflux impairments of hDAT T356M. Rescue of hDAT function by Zn^{2+} might reveal new molecular mechanism for pharmacological interventions in patients with ASD.

Results

Zn^{2+} enhances [^{3}H]DA uptake in hDAT T356M

CHO cells were transiently transfected with either wild-type hDAT or hDAT T356M. Cells were incubated with 50 nM [^{3}H]DA at 37°C for 5 min in the presence of varying concentrations of Zn^{2+}. Consistent with previous reports(Norregaard *et al.*, 1998, Loland *et al.*, 1999), Zn^{2+} decreases the DA uptake rate for wild-type hDAT (**Fig. 23a**, filled squares). In contrast, for hDAT T356M cells, Zn^{2+} increases DA uptake, partially reversing the functional deficit of this variant (**Fig. 23a**, open circles).

Zn^{2+} enhances AMPH-induced DA efflux in hDAT T356M

To specifically measure reverse transport, DA was loaded into the cytoplasm of hDAT T356M cells by a whole-cell patch clamp pipette held in current-clamp mode. This configuration supplies intracellular DA directly to the cell independent of forward transport by hDAT and allows the cell to control its membrane voltage. The whole-cell patch pipette was filled with an internal solution containing 2 mM DA as described previously(Hamilton *et al.*, 2013). DA efflux in response to 10 µM AMPH was measured by amperometry with a carbon fiber electrode(Hamilton *et al.*, 2013). Zn^{2+} increases AMPH-induced DA efflux in hDAT T356M compared to absence of Zn^{2+} (**Fig. 23b**), indicating an enhancement of reverse transport DA in the presence of Zn^{2+}. Representative amperometric traces are shown in figure 23b (top). The peak of DA efflux normalized to vehicle control is shown in figure 23b (bottom).

Discussion

Here we explore the potential for Zn^{2+} in rescuing the biophysical abnormalities in the hDAT variant T356M that we recently reported in Hamilton *et al.* 2013(Hamilton *et al.*, 2013). These functional deficits in hDAT T356M may contribute to the dysfunction in DA neurotransmission associated with ASD. Zn^{2+} was previously shown to partially restore DA uptake function in DAT

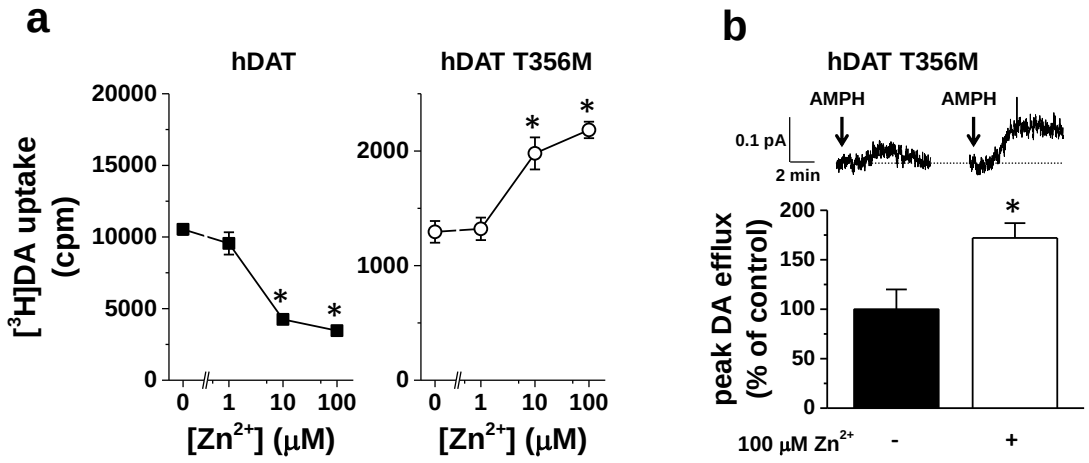

Figure 23. Zn^{2+} partially reverses the hDAT T356M deficits in [^{3}H]DA uptake and AMPH-induced efflux. (a) [^{3}H]DA uptake counts (cpm) are plotted for hDAT and hDAT T356M over a range of Zn^{2+} concentrations. While Zn^{2+} inhibits hDAT [^{3}H]DA uptake, Zn^{2+} instead increases hDAT T356M [^{3}H]DA uptake (* = $p < 0.05$ by one-way ANOVA followed by Dunnett's test compared to 0 Zn^{2+} control; n = 4). **(b)** Top: representative AMPH-induced amperometric currents (reflecting DA efflux) are displayed in the presence or absence of 100 μM Zn^{2+}. Arrows indicate application of 10 μM AMPH. Bottom: maximal DA efflux amperometric current recorded in the presence of Zn^{2+} normalized to maximal current recorded in the presence of vehicle. (* = $p < 0.05$ by Student's t-test; n = 5).

mutant Y335A, which exhibits low uptake under basal conditions(Kahlig *et al.*, 2006). Here, we demonstrate that Zn^{2+} reverses deficits in both forward and reverse transport in the T356M variant. This is a novel and intriguing finding in terms of ameliorating irregularities in DAT function in a *de novo* ASD-associated mutation.

Clinical data has previously established that mean serum Zn^{2+} levels are significantly lower in children diagnosed with ASD compared to unaffected children, and that there exist disturbances in Zn^{2+} metabolism in patients diagnosed with ASD(Jackson and Garrod, 1978, Faber *et al.*, 2009)(Li *et al.*, 2014). Whether or not Zn^{2+} regulation of hDAT may be directly relevant for the etiology of ASD is presently unknown. However, our work suggests that the molecular mechanism engaged by Zn^{2+} to partially restore function in hDAT T356M may be a novel therapeutic target to rescue, at least in part, functional deficits in hDAT variants associated with ASD.

CHAPTER V

AUTISM ASSOCIATED VARIANTS REVEAL SYNTAXIN 1 PHOSPHORYLATION AND THE DOPAMINE TRANSPORTER AS REGULATORS OF DOPAMINE NEUROTRANSMISSION AND BEHAVIORS[§]

Preface

This chapter explores the role of ASD-associated variations in the DAT and DAT-interacting proteins and how these variations can affect the DAT function and related behaviors. The work presented in this chapter is currently in preparation to be submitted to *Lancet Psychiatry*.

As introduced in chapter I, STX1 is a protein expressed in the CNS that participates in synaptic vesicle fusion. STX1 has been observed to regulate SLC6 transporter function, including the DAT. In this chapter, we characterize two separate variations identified in an ASD population. One variation is present in the STX1A gene and one variation is in the hDAT gene. The functional consequences of these variations converge to disrupt the molecular mechanisms that regulate reverse transport of DA, resulting in DA dysfunction and associated behavioral abnormalities. We observe that the STX1 variant is hypo-phosphorylated at a key regulatory residue, resulting in a reduction in the capacity of the DAT to reverse transport DA. In parallel, we observe that the hDAT variant has reduced interactions with STX1, which also results in a reduction in the capacity of the DAT to transport DA in reverse.

[§] The work presented in this chapter is in preparation to be *submitted* as Etienne Cartier[*], Peter J. Hamilton[*], Andrea Belovich, Aparna Shekar, Nicholas Campbell, Christine Saunders, Ulrik Gether, Jeremy Veenstra-Vanderweele, Jim S. Sutcliffe, Paula G. Ulery-Reynolds, Kevin Erreger[#], Heinrich J.G. Matthies[#], and Aurelio Galli[#]. (2014) Autism associated variants reveal syntaxin 1 phosphorylation and the dopamine transporter as regulators of dopamine neurotransmission and behaviors. *Lancet Psychiatry*

This chapter reveals STX1 phosphorylation at Ser14, mediated by the activity of casein kinase 2 (CK2), as a novel regulator of DAT reverse transport. In *Drosophila melanogaster*, we evaluated the behavioral significance of our molecular discoveries by exploring their relevance in AMPH-induced behaviors. We report that hindering STX1 phosphorylation at Ser14 or obstructing the STX1/DAT interaction in the dopaminergic neurons of these flies reduces the psychomotor effects of AMPH exposure.

This study presented within this chapter has broad implications, including: 1) presenting the first amperometric recording of DAT-mediated reverse transport of DA at the level of a synaptic bouton; 2) defining phosphorylation of STX1 at Ser14 as a posttranslational modification that dictates specific aspects of DAT transport cycle *via* its direct STX1/DAT interactions; 3) further implicating alterations in DA neurotransmission, induced by rare variations in DA-related genes, in the pathogenesis of ASD.

Abstract

Syntaxin 1 (STX1) is a plasma membrane protein that coordinates synaptic vesicle fusion. STX1 also regulates the function of neurotransmitter transporters, including the dopamine (DA) transporter (DAT). The DAT is a presynaptic membrane protein that controls DA homeostasis through the high-affinity re-uptake of synaptically released DA. Here, we characterize two independent autism-associated mutations in the genes that encode STX1 and the DAT. We demonstrate that each variant dramatically alters DAT function. We identify molecular mechanisms that converge to inhibit reverse transport of DA and DA-associated behaviors. These mechanisms include decreased phosphorylation of STX1 at Ser14 mediated by casein kinase 2 as well as a reduction in STX1/DAT interaction. These findings implicate alterations in

DA homeostasis, promoted by aberrant STX1/DAT interactions and STX1 phosphorylation, in the pathogenesis of autism.

Introduction

Release of neurotransmitter by synaptic vesicle fusion requires the concerted action of the soluble *N*-ethylmaleimide-sensitive factor attachment protein receptor (SNARE) complex, which includes the plasma membrane protein syntaxin 1 (STX1)(Sudhof and Rothman, 2009). Aside from being a member of the SNARE complex, STX1 plays a pivotal role in regulating the functions of neurotransmitter:sodium symporters (NSS)(Quick, 2006), including the serotonin transporter (SERT)(Quick, 2002, Quick, 2003), the norepinephrine transporter (NET)(Binda *et al.*, 2006, Dipace *et al.*, 2007, Sung and Blakely, 2007), the γ-aminobutyric acid transporter (GAT)(Wang *et al.*, 2003, Fan *et al.*, 2006), and the dopamine (DA) transporter (DAT)(Lee *et al.*, 2004, Binda *et al.*, 2008, Cervinski *et al.*, 2010). The DAT regulates DA neurotransmission *via* high-affinity reuptake of synaptically released DA(Kristensen *et al.*, 2011). Therefore, at the dopaminergic synapse, the actions of STX1 may converge on DAT to regulate DA clearance and, as a consequence, DA neurotransmission and associated behaviors.

Single nucleotide polymorphisms (SNPs) in genes encoding STX1 have been associated with high functioning autism (HFA)(Nakamura *et al.*, 2008, Nakamura *et al.*, 2011) and Asperger syndrome(Durdiakova *et al.*, 2014). *STX1A* mRNA expression is reduced in the anterior cingulate gyrus in the post-mortem brain tissue of autism spectrum disorder (ASD) individuals(Nakamura *et al.*, 2011) and increased in lymphoctyes of people with HFA(Nakamura *et al.*, 2008). These data suggest that altered STX1 expression and function may be important in the pathogenesis of ASD. Parallel to the involvement of STX1 in ASD, variations in genes encoding DA receptors(Reiersen and Todorov, 2011, Hettinger *et al.*, 2012, Qian *et al.*, 2013),

enzymes involved both in DA synthesis and catabolism(Yoo *et al.*, 2013, Nguyen *et al.*, 2014), and the DAT(Hamilton *et al.*, 2013, Bowton *et al.*, 2014) have been associated with ASD. These data point to DA dysfunction as an emerging and under-appreciated risk in ASD. Here, we examine the impact of two separate rare, inherited, ASD-identified missense variants. One in the gene that encodes STX1 (*STX1A*; resulting in an Arg to Gln substitution at site 26) and another in the gene that encodes DAT (*SLC6A3*; resulting in an Arg to Trp substitution at site 51). Both these variations disrupt the molecular mechanisms that regulate reverse transport of DA, resulting in DA dysfunction and associated behavioral abnormalities.

ASD is defined by impairments in social communication, including deficits in social interaction, nonverbal communication, and establishing relationships, as well as the presence of restricted and repetitive behaviors and interests, with repetitive behaviors being among the first signs of ASD. Recently, it has been reported that in childhood, the abnormal increase in the growth rate of striatal structures in individuals with ASD correlates with the severity of the repetitive behaviors(Langen *et al.*, 2014). Consistent with the involvement of striatal dysfunction in ASD, there is evidence that individuals with ASD display neural dysfunction in response to reward(Damiano *et al.*, 2012, Dichter *et al.*, 2012) that stems from striatal hypofunction(Kohls *et al.*, 2013, Kohls *et al.*, 2014) and disproportionate impairment in social reward(Lin *et al.*, 2012). The striatum, a brain structure rich in dopaminergic innervation, expresses high levels of DAT. Several genes within the DA network are required for the development of the striatum(Novak *et al.*, 2013), play a fundamental role in reward, and are suggested as important in the etiology of ASD, including the human DAT (hDAT)(Hamilton *et al.*, 2013, Bowton *et al.*, 2014) and STX1(Binda *et al.*, 2008).

In this study, we identify novel molecular events involved in the STX1 regulation of DAT. We show that ASD-associated variation in both the DAT and STX1 genes impair the molecular

events leading to disruption in reverse transport of DA which manifests in specific behavioral abnormalities. Our results outline a coordinated molecular network, including STX1 and DAT, in which dysfunction induced by SNPs is associated with the pathogenesis of ASD and possibly other related neuropsychiatric conditions. Considering that DAT and STX1 directly associate, a disruption of the coordinated interaction of DAT and STX1 caused by SNPs could lead to DA dysfunction as a complication of ASD.

Results

Autism-associated hDAT and STX1 variants alter DA transport

Exome capture and sequencing analysis has identified two families harboring separate rare and inherited SNPs. One family was found to be harboring a SNP in the gene that encodes hDAT (*SLC6A3*; resulting in an Arg to Trp substitution at site 51; hDAT R/W) (**Fig. 24a**, left panel). The other family was revealed to be harboring a SNP in the gene that encodes STX1A (*STX1A*; resulting in an Arg to Gln substitution at site 26; STX1 R/Q) (**Fig. 24a**, right panel). Both of these SNPs were identified in ASD samples (n = 1722), absent in a control comparison cohort (n = 1463), and not deposited in the NHLBI Exome Sequencing Project (URL: http://evs.gs.washington.edu/EVS/) [3 (November, 2014) accessed], thus we are classifying these variations as ASD-specific. All ASD cases were ascertained using the Autism Diagnostic Interview-Revised (ADIR), the Autism Diagnostic Observation Schedule-Generic (ADOS), and the DSM-IV diagnosis of pervasive developmental disorder(Neale *et al.*, 2012, Lim *et al.*, 2013)(Liu *et al.*, 2013). The hDAT Arg51 is located at the N-terminus in a region highly conserved across multiple species (**Fig. 24b**). STX1A Arg26 is located at the N-terminus and is also conserved across several species as well other STX1 isoforms, including STX1B (**Fig. 24c**). The two redundant neuronal STX1 isoforms (STX1A and STX1B) are 84% identical(Teng *et al.*, 2001).

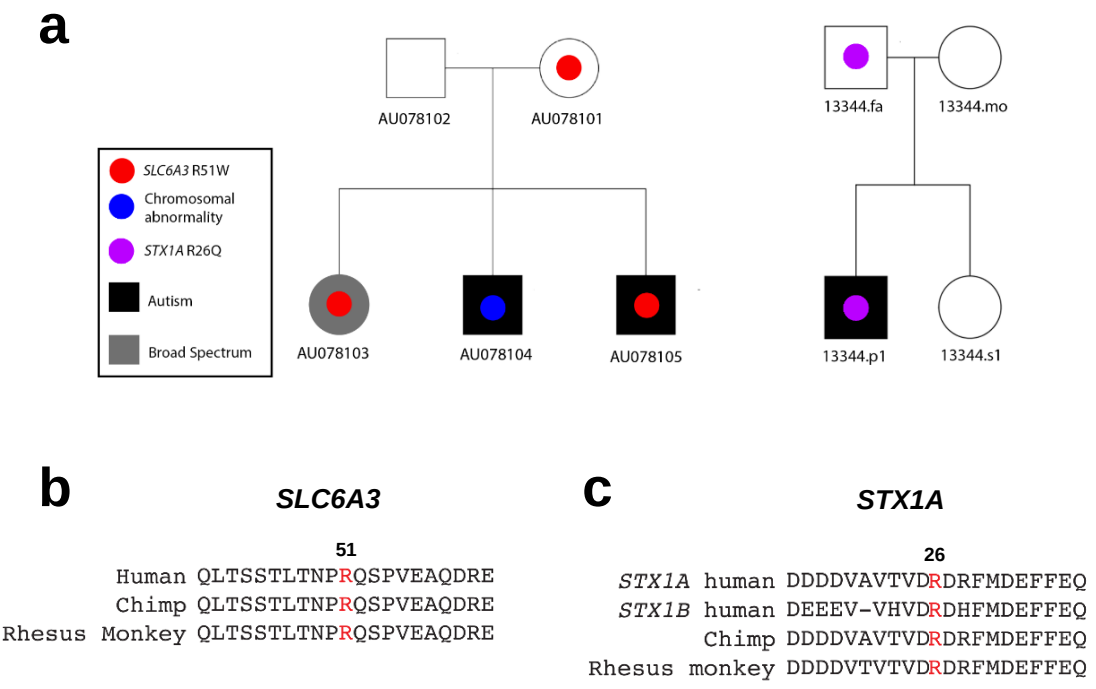

Figure 24. Pedigree and cross-species conservation of hDAT R/W and STX1 R/Q. (a) Variant inheritance is shown for the families harboring the hDAT R/W and the STX1 R/Q genotypes. Filled symbols indicate individuals with an ASD diagnosis, while open symbols reflect individuals without an ASD diagnosis. **(b)** Alignment of the DAT amino acid sequence across multiple species. Arginine 51 is represented in red. **(c)** Alignment of the STX1 amino acid sequence across isoforms and multiple species. Arginine 25 is represented in red.

Both isoforms are present in DA neurons and striatal DA terminals(Ruiz-Montasell *et al.*, 1996) and colocalize with DAT (**Fig. 25**). In this study we utilize STX1B, here simply referred as STX1.

To evaluate whether the STX1 R/Q variant is a potential risk factor for DA dysfunction in ASD, we determined the impact of this variant on a STX1 regulatory site (Ser14) involved in neuropsychiatric disorders(Castillo *et al.*) and hDAT function. hDAT cells (see Methods) expressing STX1 R/Q show reduced STX1 phosphorylation at Ser14, a key STX1 regulatory site (**Fig. 26a**). A documented function of STX1 is to regulate the DAT-mediated reverse transport of DA in response to AMPH(Binda *et al.*, 2008). Therefore, we used AMPH as a tool to probe whether STX1 R/Q has an altered ability to regulate DA efflux. We probed DA efflux with amperometry in hDAT cells expressing STX1 R/Q. The amperometric electrode, a carbon fiber electrode juxtaposed to the cell membrane, measures DA efflux by oxidation/reduction reactions, with DA efflux represented as a positive current. hDAT cells expressing STX1 R/Q display a significantly reduced AMPH-induced DA efflux as compared to hDAT cells expressing STX1 (**Fig. 26b**). It is important to point out that in hDAT cells expressing STX1 R/Q, the V_{max} of DA uptake was significantly increased, whereas the K_m of DA was not significantly different from that of hDAT cells expressing STX1 (**Fig. 26c**, top). A representative plot of DA uptake kinetics is shown in figure 26c (bottom). These data indicate that the STX1 R/Q variant asymmetrically regulates hDAT function by selectively impairing DA efflux.

In order to determine whether ASD-associated variants in genes involved in DA neurotransmission can disrupt DAT function by similar mechanisms, we explored changes in hDAT function in cells expressing hDAT R/W. The AMPH-induced reverse transport of DA was reduced in hDAT R/W cells with respect to hDAT cells (**Fig. 27a**). These data parallel the reduction in DA efflux observed in hDAT cells expressing the STX1 R/Q variant (**Fig. 26b**). This reduction in AMPH-induced DA efflux in the hDAT R/W is not mirrored by a significant reduction

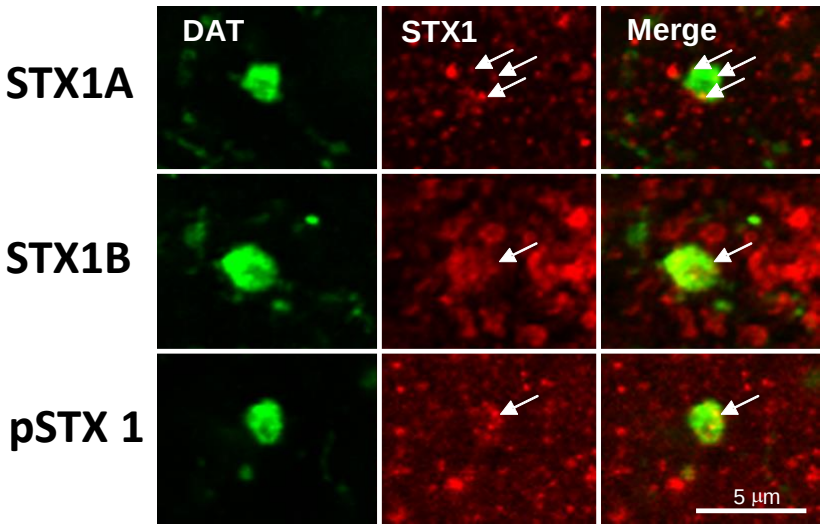

Figure 25. STX1A and STX1B colocalize with the DAT. In mouse striatal slices, DAT (green) co-localizes with STX1A, STX1B, and pSTX1 (red).

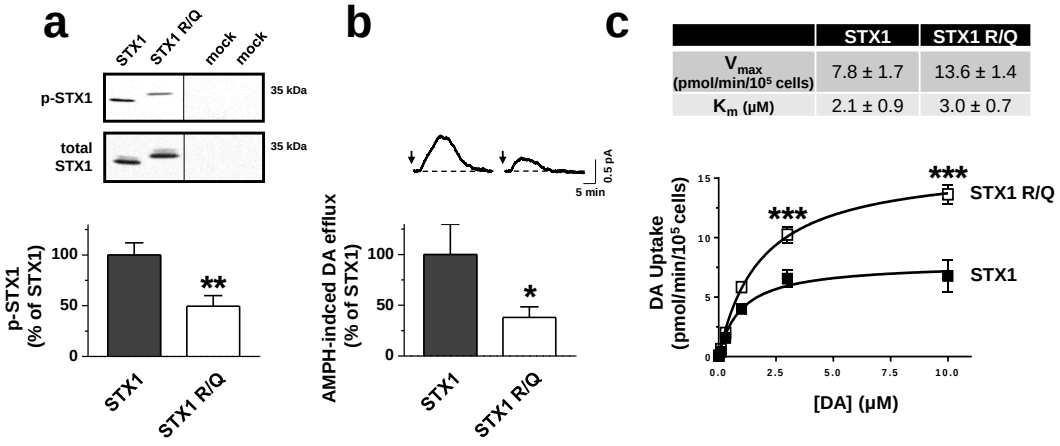

Figure 26. STX1 R to Q missense mutation decreases STX1 phosphorylation and reverse transport of DA without decreasing DA uptake. (a) Top: stably transfected hDAT cells expressing either STX1 or STX1 R/Q were immunoblotted with a phospho-specific antibody directed against STX1 at Ser14 (top lane). The mock transfection of GFP alone (mock) supports absence of non-specific binding. Bottom lane shows total STX1 proteins. Bottom: quantitation of band intensities of phospho-STX1 (p-STX1) normalized to the respective total STX1 and expressed as a percentage STX1 (** = $p < 0.01$ by Student's t-test; n = 5, in triplicate). **(b)** Top: representative AMPH-induced DA efflux recorded from stably transfected hDAT cells expressing either STX1 or STX1 R/Q. Arrows indicate application of 10 μM AMPH. Bottom: quantitation of AMPH-induced DA efflux. Data are represented as maximal current expressed as percent of the current recorded in hDAT cells expressing STX1 (* = $p < 0.05$ by Student's t-test; n = 7). **(c)** STX1 R/Q promotes DAT-mediated DA uptake. Top: kinetic parameters (V_{max} and K_m) for stably transfected hDAT cells expressing either STX1 or STX1 R/Q (V_{max}: $p < 0.05$ by Student's t-test; n = 3, in triplicate; K_m: $p > 0.46$ by Student's t-test; n = 3, in triplicate). Bottom: representative plot of [^{3}H]DA uptake kinetics in stably transfected hDAT cells expressing STX1 (filled squares) and STX1 R/Q (empty squares) cells (*** = $p < 0.001$, by two-way ANOVA followed by Bonferroni post-test; in triplicate).

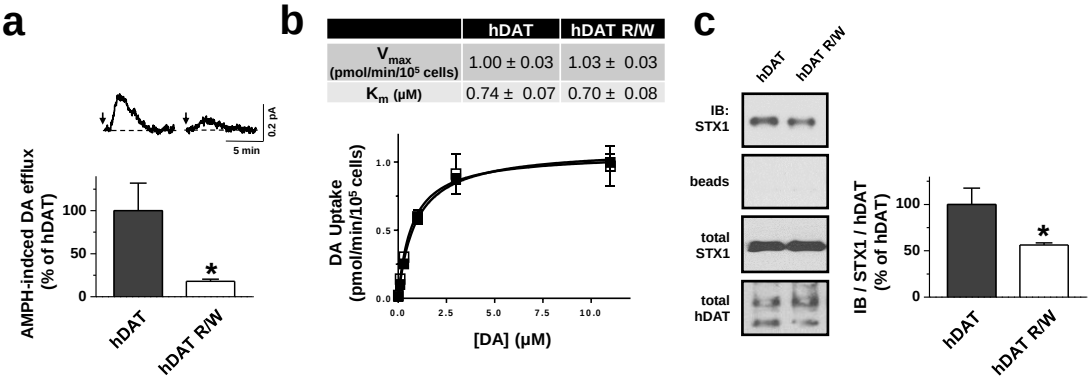

Figure 27. hDAT R to W missense mutation has decreased STX1 association, reduced reverse transport of DA, but normal DA uptake. (a) Top: representative AMPH-induced DA efflux recorded from hDAT or hDAT R/W cells expressing STX1. Arrows indicate application of 10 μM AMPH. Bottom: quantitation of AMPH-induced DA efflux. Data are represented as maximal current expressed as percent of the current recorded in hDAT cells (* = $p < 0.05$ by Student's t-test; n = 5). **(b)** hDAT R/W exhibits normal DA uptake function. Top: kinetic parameters (V_{max} and K_m) for hDAT and hDAT R/W (V_{max}: $p > 0.92$ by Student's t-test; n = 3, in triplicate; K_m: $p > 0.62$ by Student's t-test; n = 3, in triplicate). Bottom: representative plot of [^{3}H]DA uptake kinetics in hDAT (filled squares) and hDAT R/W (empty squares) cells ($p > 0.05$, by two-way ANOVA followed by Bonferroni post-test; in triplicate). The difference in V_{max} between figure 2C is primarily due to a difference in the expression of hDAT in the cell lines. **(c)** Top: hDAT immunoprecipitates from either hDAT or hDAT R/W cells expressing STX1 were immunoblotted for STX1 (top lane). The beads fraction supports the absence of non-specific binding. Third lane shows an immunoblot for total STX1 proteins. Bottom lane shows an immunoblot for total hDAT proteins. Bottom: quantitation of hDAT pulldown band intensities normalized to the respective total STX1 and total hDAT; expressed as a percentage hDAT cells (* = $p < 0.05$ by Student's t-test; n = 5).

in DA uptake or DA apparent affinity (**Fig. 27b**), indicating the hDAT R/W variant also asymmetrically regulates hDAT function by selectively impairing DA efflux.

Previously, we determined that reverse transport of DA induced by AMPH is tightly regulated by the interaction of STX1 at the DAT N-terminus(Binda *et al.*, 2008). Therefore, we explored whether the reduced reverse transport of DA in hDAT R/W cells stemmed from a decreased association of STX1 to hDAT R/W. We immunoprecipitated hDAT and immunoblotted the immunoprecipitates for STX1 (**Fig. 27c**). The amount of STX1 recovered in the DAT immunoprecipitates was reduced in the hDAT R/W cells compared to the hDAT cells (**Fig. 27c**, IB: STX1). In the absence of antibody against DAT, no signal was detected for STX1 in the immunoprecipitates (**Fig. 27c**, beads). The total STX1 and hDAT in the hDAT R/W cells was not decreased with respect to hDAT cells (**Fig. 27c**, total STX1 and total hDAT). These data demonstrate that the hDAT R/W variant has a reduced STX1/DAT interaction. Quantitation of multiple experiments is shown in the bar graph of figure 27c. These data highlight that the ASD-associated hDAT and STX1 variants both impair reverse transport of DA without inhibiting DAT-mediated DA uptake functions. Yet, it is unknown whether these variants converge on a common molecular mechanism to impair reverse transport of DA.

STX1 phosphorylation regulates STX1/DAT interaction

STX1 is phosphorylated at Ser14 by the kinase CK2(Hirling and Scheller, 1996, Foletti *et al.*, 2000), a posttranslational modification involved in the functional regulation of STX1(Rickman and Duncan, Dubois *et al.*, 2002, Khelashvili *et al.*, 2012). Figure 26a shows that the STX1 R/Q variant promotes a reduction in STX1 phosphorylation at Ser14. Therefore, we sought to determine the functional consequences of impaired Ser14 phosphorylation. First, we demonstrated that the highly selective ATP/GTP-competitive inhibitor of CK2, 4,5,6,7-

tetrabromobenzotriazole (TBB, 10 μM), effectively reduces p-STX1 in hDAT cells. p-STX1 levels were determined either under TBB treatment or control conditions with a phospho-specific antibody that recognizes phosphorylation of Ser14(Castillo *et al.*) (**Fig. 28a**). TBB significantly decreases basal levels of p-STX1, demonstrating that CK2 regulates the phosphorylation state of STX1 at Ser14.

Next, we investigated whether STX1 phosphorylation at Ser14 regulates the association of STX1 with the DAT. hDAT cells were treated with either TBB (10 μM for 20 minutes) or vehicle control, and the cell lysates were immunoprecipitated for DAT and subsequently immunoblotted for STX1. Inhibition of STX1 phosphorylation with TBB reduces STX1/DAT association (**Fig. 28b**), demonstrating that phosphorylation promotes the STX1/DAT interaction. TBB (10 μM for 20 minutes) did not change the level of DAT available at the cell surface (hDAT surface expression for TBB exposure was 89.0 ± 12.9 % of vehicle control; $p > 0.40$ by Student's t-test; $n = 4$), indicating that the reduced STX1/DAT interaction following CK2 inhibition is not due to DAT trafficking away from the plasma membrane. Collectively, these results are consistent with a coordinated signaling complex whereby phosphorylation of STX1 at Ser14 promotes its association to DAT.

STX1 can be phosphorylated at residues other than Ser14. For example, casein kinase 1 can promote STX1 phosphorylation at Thr21(Dubois *et al.*, 2002). Therefore, we validated whether the level of phosphorylation of Ser14 alone supports STX1/DAT interactions. We generated STX1 constructs that either prevent Ser14 phosphorylation, by mutating Ser14 to Ala (STX1 S14A), or mimic Ser14 phosphorylation, by mutating Ser14 to Asp (STX1 S14D). We performed immunoprecipitation experiments in hDAT cells transfected with the different STX1 constructs. We observed that the STX1/DAT association is blunted in hDAT cells expressing STX1 S14A as compared to hDAT cells expressing STX1 (**Fig. 28c**). Furthermore, the pseudo-phosphorylated

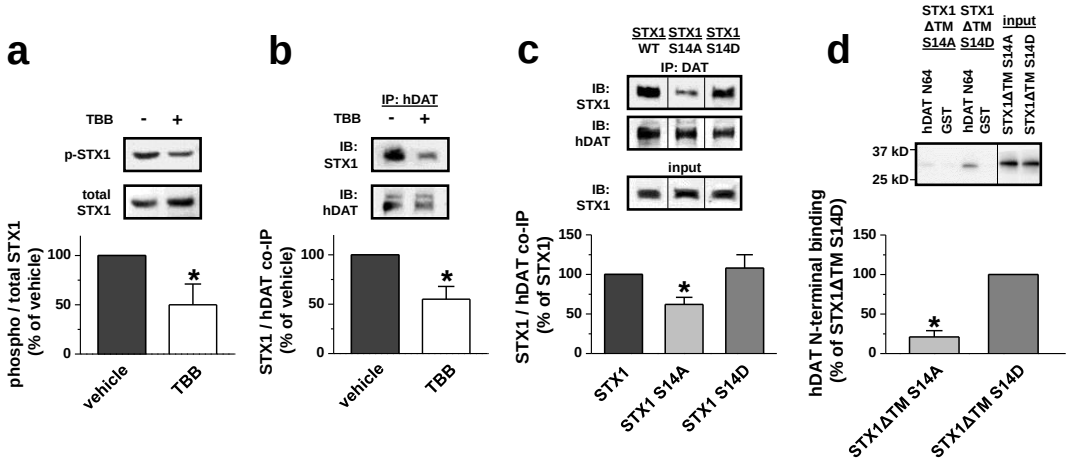

Figure 28. CK2-mediated phosphorylation of STX1 at S14 promotes STX1/DAT interaction. (a) Stably transfected hDAT cells transfected with STX1 were treated with either vehicle or 10 µM TBB for 20 minutes. STX1 proteins were immunoblotted for p-STX1 (with a phospho-specific antibody directed against Ser14) and STX1. p-STX1 band densities were normalized to the corresponding total STX1 band densities and expressed as a percentage of vehicle control. CK2 inhibition with TBB significantly decreased the levels of p-STX1 (* = $p < 0.05$ by Student's t-test; n = 4). **(b)** Stably transfected hDAT cells transfected with STX1 were treated with either vehicle or 10 µM TBB for 20 minutes. hDAT proteins were immunoprecipitated and immunoblotted for STX1 and DAT. STX1 band densities were normalized to DAT and expressed as a percentage of vehicle control. CK2 inhibition significantly decreased STX1/DAT interaction (* = $p < 0.05$ by Student's t-test; n = 4). **(c)** Stably transfected hDAT cells were transfected with either STX1, STX1 S14A, or STX1 S14D. hDAT immunoprecipitates were immunoblotted for either STX1 (top band) or hDAT (middle band). Input (bottom band) serves as loading control. All STX1 isoform band densities were normalized to hDAT and expressed as a percentage of STX1. STX1 S14A displays a significantly decreased association with DAT (* = $p < 0.05$ by one-way ANOVA followed by Newman-Keuls Multiple Comparison Test; n = 6). **(d)** Purified STX1ΔTM peptides (S14A or S14D) were incubated with a GST fusion protein of the first 64 amino acids of the hDAT N-terminus (N64) or with GST alone. The samples were then immunoblotted for STX1. STX1 band densities were expressed as a percentage of STX1ΔTM S14D. STX1ΔTM S14A displays reduced binding to the hDAT N-terminus (* = $p < 0.05$ by Student's t-test; n = 5).

STX1 S14D exhibits increased interaction with hDAT with respect to STX1 S14A. Thus, phosphorylation of STX1 at Ser14 supports STX1/DAT association. Plasma membrane levels of hDAT, as measured by biotinylation, were not altered by the expression of either STX1 S14A or STX1 S14D when compared to STX1 (STX1 S14A: hDAT surface expression was 101 ± 39% and STX1 S14D: hDAT surface expression was 88 ± 16% relative to hDAT cells expressing STX1; $p > 0.89$ by one-way ANOVA; $n = 5\text{-}6$).

To determine whether Ser14 phosphorylation regulates the direct association between STX1 and DAT, we used an *in vitro* GST pull-down assay as described in Binda *et al*.(Binda *et al.*, 2008), which previously demonstrated that the hDAT N-terminus directly interacts with STX1(Binda *et al.*, 2008). Therefore, in this study, we used a GST hDAT N-terminal fusion protein (hDAT N64, see Methods) to pull down recombinant soluble constructs of STX1 lacking the transmembrane domain (STX1ΔTM) with Ser14 mutated to Ala (STX1ΔTM S14A) or Asp (STX1ΔTM S14D) (**Fig. 28d**). hDAT N64 robustly pulled down STX1ΔTM S14D. However, hDAT N64 pull down of STX1ΔTM S14A was dramatically blunted. GST alone did not pull down either STX1ΔTM construct. Quantitative analysis of band densities in figure 28d demonstrates that the STX1ΔTM S14A peptide exhibits a significantly reduced direct association with the DAT N-terminus relative to the STX1ΔTM S14D peptide. Input bands show that the STX1ΔTM constructs were of expected size and exhibited minimal degradation. These data further support the notion that STX1 phosphorylation at Ser14 is a key regulator of the dynamic, direct interaction between STX1 and DAT.

STX1 phosphorylation supports reverse transport of DA

Figure 26b shows that the STX1 R/Q variant promotes a reduction in DA efflux. Therefore, it is possible that the CK2-mediated phosphorylation of STX1 at Ser14 support reverse transport of

DA. We first determined whether AMPH causes an increase in STX1 phosphorylation. To test this, p-STX1 levels were measured in hDAT cells transfected with STX1 and treated either with vehicle, AMPH, or AMPH in the presence of TBB (**Fig. 29a**). AMPH treatment increased the level of p-STX1 with respect to vehicle control. Pre-treatment of cells with TBB (10 μM for 20 minutes) prevented the AMPH-induced phosphorylation of STX1 at Ser14, demonstrating that AMPH induces phosphorylation of STX1 in a CK2-dependent manner. Quantitation of the band density of p-STX1, normalized to total STX1 and expressed as a percent of control is shown in figure 29a (bottom).

These findings implicate CK2 and phosphorylation of STX1 at Ser14 as possible novel molecular mediators of reverse transport of DA. Thus, we investigated the role of CK2 function and STX1 phosphorylation at Ser14 in AMPH-induced DA efflux. DA efflux was quantified by amperometry in hDAT cells expressing STX1 under control conditions or pharmacological inhibition of CK2 with TBB (10 μM for 20 minutes). TBB reduced AMPH-induced DA efflux as compared to vehicle control treated cells (**Fig. 29b**). These data support our hypothesis that STX1 phosphorylation at Ser14 regulates reverse transport of DA. To further test this hypothesis, we determined if the ability of TBB to regulate DA efflux is altered by preventing or mimicking phosphorylation of STX1. We expressed STX1 S14A or STX1 S14D constructs in hDAT cells and measured AMPH-induced DA efflux in the presence or absence of TBB. In hDAT cells expressing STX1 S14A, AMPH-induced DA efflux was not sensitive to pharmacological inhibition of CK2, and the absolute DA efflux in vehicle control was comparable to TBB treated hDAT cells expressing STX1 (**Fig. 29c**, compare to **Fig. 29b** TBB treated). Further, in hDAT cells expressing STX1 S14D, AMPH-induced DA efflux was also not sensitive to TBB. However, the absolute DA efflux in the presence of TBB was comparable to vehicle treated hDAT cells expressing STX1 (**Fig. 29d**, compare to **Fig. 29b** vehicle treated). These results demonstrate that preventing STX1 phosphorylation (STX1 S14A) parallels

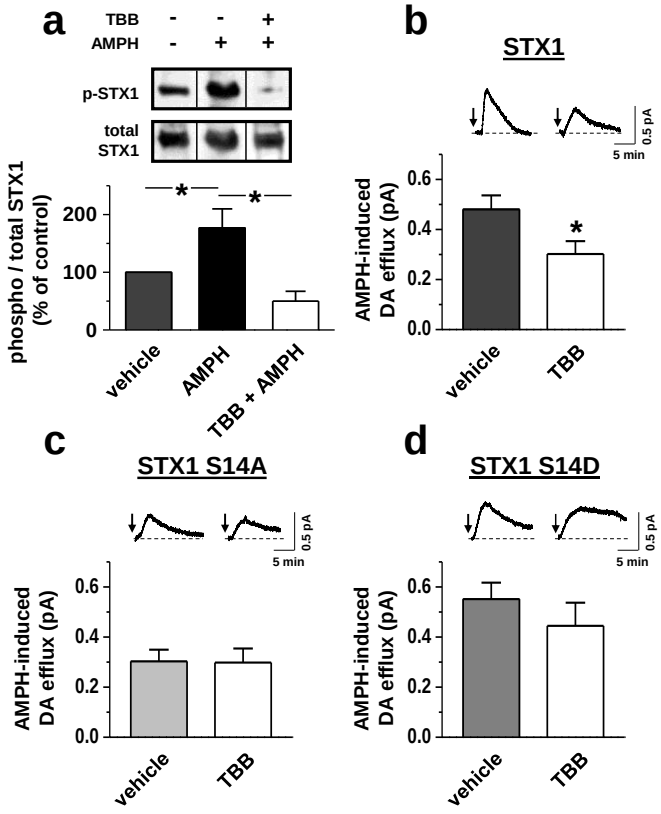

Figure 29. STX1 phosphorylation promotes reverse transport of DA. (a) Top: stably transfected hDAT cells expressing STX1 were treated with either vehicle or 10 µM TBB for 20 minutes. This was followed by an additional treatment with vehicle or 10 µM AMPH for 15 minutes. STX1 immunoprecipitates were immunoblotted for either p-STX1 (Ser14) or STX1. Bottom: the immunoprecipitated band densities were quantified, normalized to the corresponding density of total precipitated STX1, and expressed as a percentage of vehicle control (* = $p < 0.05$ by one-way ANOVA followed by Newman-Keuls Multiple Comparison Test; n = 3). **(b)** Representative AMPH-induced DA efflux recorded from stably transfected hDAT cells expressing STX1 treated with either vehicle or 10 µM TBB for 20 minutes just before the amperometric recordings. Arrows indicate application of 10 µM AMPH. Bottom: quantitation of AMPH-induced DA efflux. Data are represented as maximal oxidative current (* = $p < 0.05$ by Student's t-test; n = 5). **(c)** Representative AMPH-induced amperometric currents recorded from stably transfected hDAT cells expressing STX1 S14A treated with either vehicle or 10 µM TBB for 20 minutes. Arrows indicate application of 10 µM AMPH. Bottom: quantitation of maximal oxidative current ($p > 0.05$ by Student's t-test; n = 4-7). **(d)** Representative AMPH-induced amperometric currents recorded from stably transfected hDAT cells expressing STX1 S14D treated with either vehicle or 10 µM TBB for 20 minutes. Arrows indicate application of 10 µM AMPH. Bottom: quantitation of AMPH-induced DA efflux. Data are represented as maximal oxidative current ($p > 0.05$ by Student's t-test; n = 6).

pharmacological inhibition of CK2, and mimicking STX1 phosphorylation (STX1 S14D) obscures the ability of TBB to inhibit DA efflux. It also points to the phosphorylation state of STX1 at Ser14 as a determining factor in the magnitude of reverse transport of DA, further supporting our hypothesis that the STX1 R/Q variation alters DA neurotransmission *via* reduced phosphorylation.

The data described thus far provide clear mechanistic evidence that CK2-mediated phosphorylation of STX1 promotes STX1/DAT interaction and reverse transport of DA, in a controlled and well-defined heterologous expression system. Use of this expression system yields feasibility for mechanistic insights in a timely fashion(Hamilton *et al.*, 2013, Hamilton *et al.*, 2014). However, it is important to translate these discoveries to neuronal release sites, the site of DAT actions. Cultured catecholamine neurons from the superior cervical ganglion (SCG) have large presynaptic boutons that are amenable to imaging approaches, allowing us to determine whether AMPH drives STX1 phosphorylation at these release sites. SCG neurons natively express the NET, which has 66% amino acid sequence homology with the DAT, as well as the accompanying catecholamine presynaptic machinery(Matthies *et al.*, 2009). We and others have shown that NET is a useful marker of catecholaminergic presynaptic terminals in cultured SCG neurons(Matthies *et al.*, 2009). Here, we utilized confocal imaging of SCG presynaptic boutons coupled with immunofluorescence to reveal the presence of endogenous p-STX1, closely localized to the NET (**Fig. 30a**). Consistent with our findings in hDAT cells, AMPH treatment (10 µM for 20 minutes) enhances STX1 phosphorylation at Ser14 in SCG presynaptic terminals (**Fig. 30b**). SCG cultured neurons also express endogenous CK2α, the catalytic domain of CK2 required for the phosphorylation of STX1 at Ser14 (**Fig. 30c**). Lastly and notably, in mouse striatal slices, a brain region enriched in DA projections, there is a similar profile of endogenous STX1 and p-STX1 expression compared to cultured SCG neurons (**Fig. 30c**). These data demonstrate that AMPH stimulates phosphorylation of endogenous STX1 at

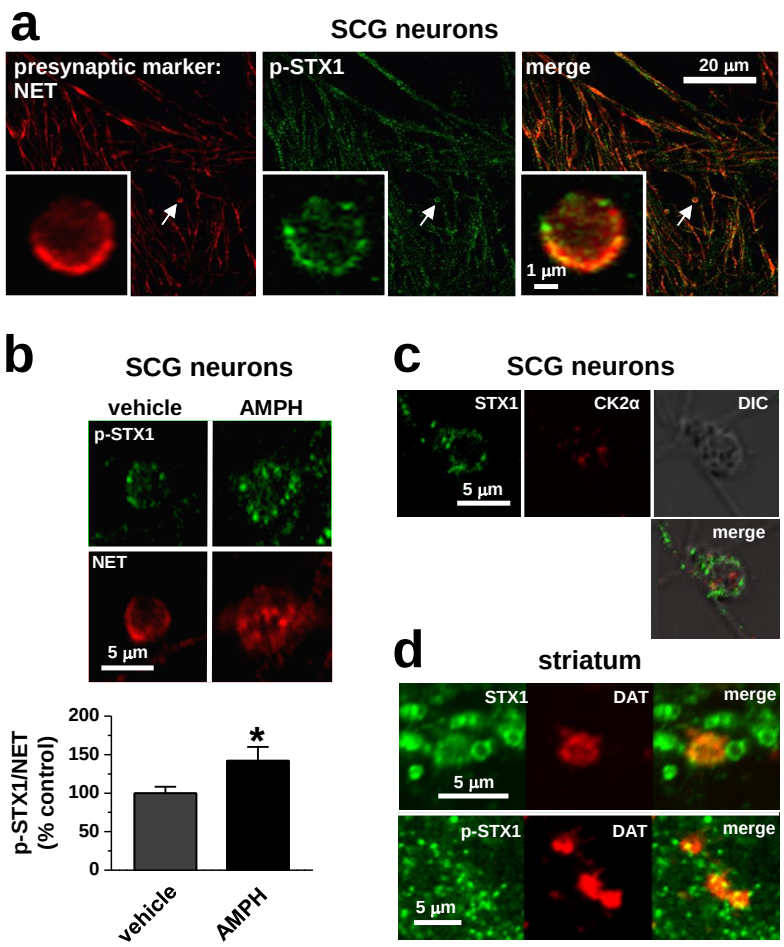

Figure 30. AMPH treatment increases p-STX1 levels in boutons. (a) Mouse superior cervical ganglion (SCG) neurons were fixed and p-STX1 (green) was visualized by immunoflourescence. The norepinephrine transporter (NET, red) was used as a marker of presynaptic boutons. The merge shows that p-STX1 is present in presynaptic boutons of cultured catecholamine neurons. *Inset*: Confocal sections of a single presynaptic bouton (arrow). **(b)** Top: SCG neurons were treated with either vehicle or 10 µM AMPH for 20 minutes. Cells were fixed and immunostained for p-STX1 (green) and for the NET (red). AMPH increases the intensity of p-STX1 in presynaptic boutons. Bottom: p-STX1 levels were quantified by the ratio of p-STX1 pixel intensity normalized to NET pixel intensity. AMPH significantly increases the intensity of p-STX1 in presynaptic boutons (* = $p < 0.05$ by Student's t-test; n = 5-6). **(c)** In SCG neurons cultured from NET KO mice, p-Stx1 colocalizes with CK2. **(d)** In mouse striatal slices, DAT co-localizes with STX1 and p-STX1.

neuronal release sites, presenting SCG neurons as a biologically relevant preparation in which to observe the functional role of STX1 in reverse transport of DA.

STX1 phosphorylation regulates reverse transport of DA at neuronal release sites

Next, we explored the role of STX1 phosphorylation in DAT-mediated reverse transport of DA at the level of the SCG presynaptic boutons. Since SCG neurons do not natively express DAT, we used neurons cultured from NET knockout mice transiently transfected with hDAT labeled with a GFP tag (**Fig. 31a**, inset). GFP fluorescence was used to identify neurons positive for hDAT expression. AMPH-induced DA efflux was recorded with amperometry from individual synaptic boutons (**Fig. 31a**). This DA efflux was cocaine sensitive, indicating its DAT dependence (data not shown). TBB (10 μM for 20 minutes) reduced AMPH-induced DA release as compared to vehicle control (**Fig. 31a**). These data demonstrate, for the first time at the level of a single bouton, that CK2 function and STX1 phosphorylation are critical mediators of AMPH-induced DAT-mediated DA release.

We then determined the importance of STX1 for reverse transport of DA in *ex vivo* preparations. In mouse striatal slices, pre-incubation in botulinum toxin serotype C (BoNT/C, 100 nM for 60 minutes), a protein known to cleave STX1(Schiavo *et al.*, 1995), inhibits AMPH-induced DA efflux as measured by high speed chronoamperometry (**Fig. 31b**). Importantly, this BoNT/C pre-incubation paradigm was not effective in significantly altering DA uptake (**Fig. 31c**). These data demonstrate the pivotal role of STX1 in supporting DA efflux without altering forward transport of DA in neuronal tissues.

STX1 phosphorylation and STX1/DAT association regulates dopaminergic behaviors

For a complete understanding of how ASD-associated variants affect DA neurotransmission, it

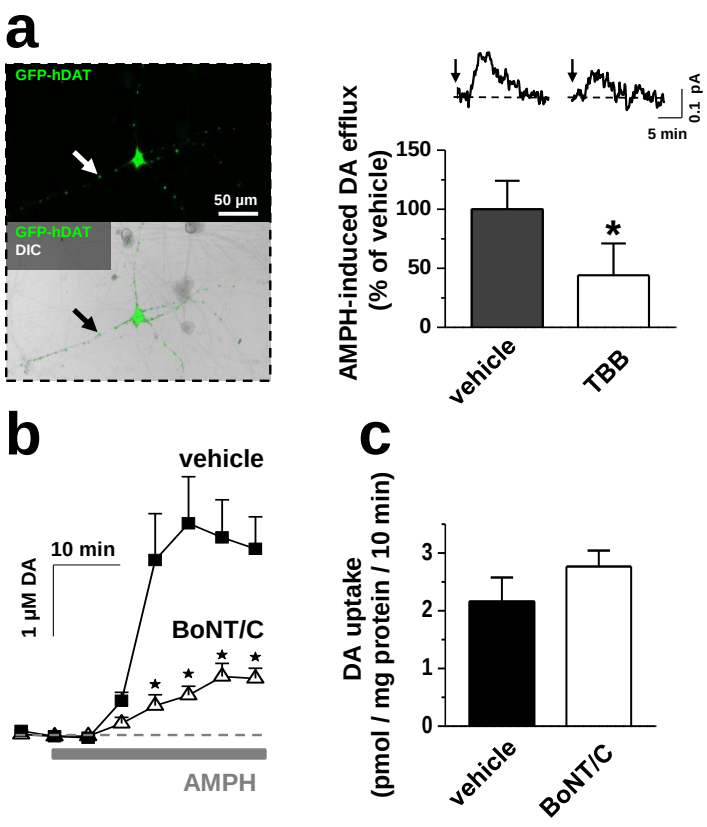

Figure 31. Inhibition of either STX1 phosphorylation or cleavage of STX1 inhibits DA efflux but not uptake. (a) Inset: Image of a single GFP-hDAT transfected SCG neuron; arrows indicate the site of amperometric recording (i.e. the presynaptic bouton). Top: representative AMPH-induced amperometric currents recorded from a single presynaptic bouton of SCG neurons expressing GFP-hDAT after treatment with either vehicle or 10 µM TBB for 20 minutes. Bottom: quantitation of the maximal oxidative current normalized to vehicle treatment (* = $p < 0.05$ by Student t-test; n = 5). **(b)** AMPH (10 µM)-induced DA efflux recorded in mouse striatal slices preincubated (1 hr) either with vehicle or BoNT/C (100 nM) (* = $p < 0.05$ by two-way ANOVA; n = 6). **(c)** [^{3}H]DA uptake measure in striatal slices receiving identical treatment as in panel (c) ($p > 0.05$ by Student's t-test; n = 4).

is imperative to translate our molecular discoveries *in vivo*. *Drosophila melanogaster* offer a powerful genetic model for elucidating the importance of targeted molecular manipulations. In adult *Drosophila* males, we developed locomotor assays for an *in vivo* mechanistic examination of DAT-mediated reverse transport of DA and how ASD variants affect this transport process. First, we explored how impairments in STX1 phosphorylation, which affects STX1/DAT associations, regulate DA associated behaviors. In *Drosophila*, locomotion requires functional DA neurotransmission(Pendleton *et al.*, 2002, Wicker-Thomas and Hamann, 2008, Hamilton *et al.*, 2013, Pizzo *et al.*, 2013, Hamilton *et al.*, 2014). To probe for changes in locomotion, we developed a behavioral assay in which adult males were fed a sucrose solution containing either AMPH (1 mM) or vehicle. We observed that AMPH significantly stimulated locomotion in wild-type (WT) *Drosophila* (**Fig. 32a**). However, AMPH did not significantly increase locomotion in flies lacking dDAT (DAT KO)(Kume *et al.*, 2005), indicating that AMPH-induced locomotion is a DAT-dependent behavior (**Fig. 32a**). These data strongly support this assay as a model in which functional DAT is critical for AMPH-induced behavior.

CK2 function promotes STX1 phosphorylation at Ser14, STX1/DAT interaction, and reverse transport of DA. Thus, to probe the behavioral significance of impaired STX1 phosphorylation at Ser14 and STX1/DAT interaction, we evaluated whether inhibited CK2 function alters AMPH-induced locomotion. We expressed a dominant negative form of CK2 (CK2DN) in flies by using the Gal4/UAS system to express a single copy CK2DN in a WT background, selectively in DA neurons(Friggi-Grelin *et al.*, 2003, Matthies and Broadie, 2003). We compared the AMPH-induced behavioral responses of flies expressing CK2DN to WT flies. AMPH did not significantly increase locomotor activity in flies expressing dominant negative CK2 mutant (**Fig. 32b**). Furthermore, vehicle treatment did not modify locomotion of flies expressing CK2DN with respect to WT flies, suggesting that extracellular DA level did not change under basal conditions. Consistent with this, CK2 inhibition by TBB treatment (10 μM for 15 minutes) did not

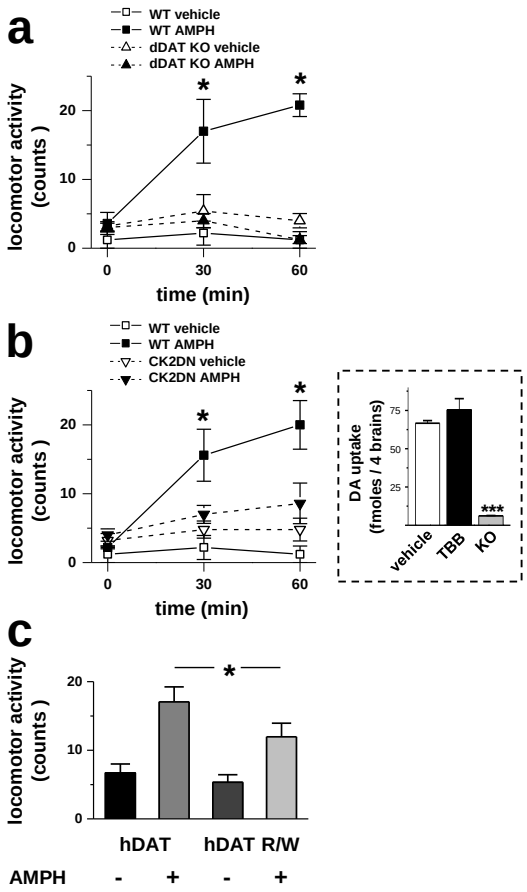

Figure 32. AMPH induced behavior in *Drosophila* is regulated by STX1 phosphorylation in DA neurons. (a) DAT knockout (KO) flies demonstrate that AMPH-induced locomotor behavior is DAT-dependent. Locomotor activity in response to vehicle (open symbols) or (1mM) AMPH (filled symbols) in either wild-type (WT) (squares) or in DAT KO flies (triangles). WT flies exhibit a significant AMPH-induced increase in locomotion while DAT KO flies do not exhibit this significant increase (* = $p < 0.05$ for vehicle vs AMPH, two-way ANOVA followed by Bonferroni post-test; n = 5). **(b)** *Drosophila* were generated expressing a dominant-negative (DN) version of CK2α expressed specifically in dopaminergic neurons. Locomotor activity in response to vehicle (open symbols) or AMPH (filled symbols) in either wild-type (WT) (squares) or in CK2 dominant negative flies (CK2DN) (triangles). WT flies exhibit a significant increase in AMPH-induced locomotion while CK2DN flies do not (* = $p < 0.05$ for vehicle vs AMPH, two-way ANOVA followed by Bonferroni post-test; n = 5). (inset) DA uptake in intact fly brains in the presence of 10 μM TBB or vehicle. The absence of uptake in the dDAT KO fly brains shows the dependence of DA uptake on the dDAT (*** = $p < 0.0001$ by one-way ANOVA followed by Newman-Keuls Multiple Comparison Test; n = 3). **(c)** hDAT R/W expressing flies have blunted locomotor responses to AMPH. Changes in locomotion were determined upon AMPH or vehicle exposure over 30 minutes and calculated as beam crosses. AMPH (1 mM) caused a significant increase in locomotion in both hDAT flies ($p < 0.001$ by one-way ANOVA followed by Newman-Keuls Multiple Comparison Test; n = 24) and hDAT R/W flies ($p < 0.05$ by one-way ANOVA followed by Newman-Keuls Multiple Comparison Test; n = 24). However, in hDAT R/W flies, AMPH exposure led to a less hyperactivity than in hDAT flies (* = $p < 0.05$ by one-way ANOVA followed by Newman-Keuls Multiple Comparison Test; n = 24).

alter DA uptake in intact *Drosophila* brains (**Fig. 32b**, inset). Importantly, brains obtained from dDAT KO fly shows robustly reduced DA uptake, demonstrating the DAT dependence of DA uptake in our newly developed uptake assay. Collectively, these data point to CK2 activity, STX1 phosphorylation at Ser14, and STX1/DAT association as critical mediators of reverse transport of DA and associated behaviors.

Next, we explored how the ASD-associated hDAT R/W variant which impairs STX1/DAT association affects DA-dependent behaviors in our *Drosophila* model system. We expressed hDAT or hDAT R/W in DA neurons of dDAT KO flies as described above. We fed male *Drosophila* a sucrose solution containing either AMPH (1 mM) or vehicle and quantified locomotion in 30 minute intervals. AMPH exposure induced an increase in locomotion in both the hDAT and hDAT R/W expressing flies (**Fig. 32c**). However, AMPH exposure led to significantly reduced locomotion in hDAT R/W expressing flies as compared to hDAT expressing flies (**Fig. 32c**, compare hDAT +AMPH versus hDAT R/W +AMPH). These data are consistent with the reduced ability of AMPH to cause DA efflux in hDAT R/W expressing cells. Also, it is important to note that basal locomotion of flies expressing hDAT R/W did not significantly differ from that of hDAT expressing flies.

Discussion

Alterations in DA neurotransmission are thought to underlie several neuropsychiatric disorders, including bipolar disorder, schizophrenia, attention deficit hyperactivity disorder (ADHD), and ASD(Seeman and Niznik, 1990, Volkow *et al.*, 2007, Cousins *et al.*, 2009)(Volkow *et al.*, 2007, Nguyen *et al.*, 2014). Defining the disruptions in signaling molecules and mechanisms that underlie impairments in DA neurotransmission may help in understanding the etiology of these DA-associated disorders. Recently, we demonstrated that an ASD-associated hDAT *de novo*

variant displays dramatically altered DAT function, including constitutive reverse transport of DA, which leads to hyperlocomotion(Hamilton *et al.*, 2013). Thus, we hypothesized that novel DAT variation (or variation in the genes known to regulate the DAT) that affects DA neurotransmission might contribute to the pathology and/or complications of ASD. Here, we identify and describe two novel gene variants from two separate ASD families. One variation is located in *STX1A* (resulting in a missense mutation in STX1; an Arg to Gln substitution at site 26) and the other variation is located in *SLC6A3* (resulting in a missense mutation in hDAT; an Arg to Trp substitution at site 51). These variations are in separate gene products, yet converge mechanistically to disrupt DAT function and associated behaviors, with distinct mechanisms regulating either STX1 phosphorylation or STX1/DAT interaction.

We found that the STX1 R/Q variant has decreased phosphorylation of Ser14, a key residue involved in the functional regulation of STX1(Rickman and Duncan, Dubois *et al.*, 2002, Khelashvili *et al.*, 2012). This hypo-phosphorylated STX1 acts to inhibit DAT-mediated reverse transport of DA without inhibiting DA uptake function. In hDAT cells expressing STX1 R/Q, we observe a significantly increased V_{max} of DA uptake. This ability of STX1 R/Q to alter DAT-mediated uptake is not surprising since STX1 has been observed to decrease DAT uptake activity(Cervinski *et al.*, 2010). In parallel experiments in mouse striatal slices, cleaving STX1 with BoNT/C promotes a decrease in reverse transport of DA with a trend towards increased DA uptake. These data suggest that STX1 function asymmetrically regulates reverse transport of DA and DA uptake. Importantly, STX1 R/Q displays reduced level of CK2-mediated phosphorylation of Ser14. Therefore, to define how hypo-phosphorylation of STX1 R/Q impairs DA reverse transport, we studied the regulatory effects of CK2 function on DA efflux.

The expression of CK2, as well as the phosphorylation state of STX1 at Ser14, has been shown to be decreased in the post-mortem brain tissue of subjects with schizophrenia(Castillo *et al.*,

Aksenova *et al.*, 1991). CK2 phosphorylates STX1 at Ser14 to regulate STX1 function and protein interactions(Rickman and Duncan, Hirling and Scheller, 1996, Foletti *et al.*, 2000, Dubois *et al.*, 2002). Here, we discovered that CK2-mediated phosphorylation of STX1 at Ser14 increases the direct association between STX1 and the hDAT N-terminus to potentiate reverse transport of DA. Thus, we present CK2 as a key player involved in DA efflux and implicate its function in ASD. To have a more complete understanding of how ASD-associated variants within the DA network alter behaviors, we translated our molecular discoveries to an *in vivo* context. We selectively expressed CK2DN specifically in DA neurons of WT flies. *Drosophila* expressing CKDN exhibited a robust reduction in AMPH-induced hyperlocomotion as compared to WT flies. These data underscore the importance of CK2 function and STX1 phosphorylation in regulating behaviors sustained by reverse transport of DA. Interestingly, inhibiting CK2 function did not regulate basal locomotion or DA uptake in intact *Drosophila* brains.

Parallel to STX1 R/Q, we found that the hDAT R/W variant displays inhibited reverse transport of DA without impairments in uptake function. Thus, we strove to determine whether these ASD-associated variants disrupt the molecular mechanisms that converge in regulating reverse transport of DA, resulting in DA dysfunction and associated behavioral abnormalities. It is important to note that CK2 function, in addition to phosphorylating STX1 at Ser14, also promotes STX1/DAT interactions. Here, we show that hDAT R/W has reduced association with STX1, resulting in altered DA-related behaviors. Indeed, *Drosophila* expressing hDAT R/W selectively in DA neurons demonstrate reduced sensitivity to the psychomotor effects of AMPH, as observed in a significantly lower AMPH-induced locomotion when compared to hDAT expressing flies. Interestingly, basal locomotion remained unaltered in hDAT R/W flies, indicating normal DAT-mediated uptake function as supported by our uptake data. These data suggest that the phosphorylation state of STX1 at Ser14 and STX1/DAT interaction asymmetrically regulate reverse transport of DA over DAT-mediated uptake functions.

It is widely accepted that DAT primarily regulates synaptic DA concentration *via* DA re-uptake(Kristensen *et al.*, 2011). Mounting evidence also demonstrates that reverse transport of DA and associated behaviors can be promoted by changes in the association between DAT and STX1(Binda *et al.*, 2008), as well as by signaling molecules such as CaMKII, which drive DAT N-terminus phosphorylation(Fog *et al.*, 2006, Pizzo *et al.*, 2013, Pizzo *et al.*, 2014). Therefore, it has been suggested that reverse transport of DA might participate in shaping DA neurotransmission(Leviel, 2011). Here, we used AMPH as a tool to induce the molecular events that are required for reverse transport of DA to determine whether ASD-associated variants disrupt these events. In both *in vitro* and *ex vivo* preparations, CK2 function is the key molecular event that promotes phosphorylation of STX1 at Ser14 and STX1/DAT interaction to cause reverse transport of DA. We bring the study of CK2 function and its relationship to DA efflux for the first time at the level of a single active site, the SCG bouton.

Several ASD-associated variants have now been found to impact DAT-mediated DA efflux, including the STX1 R26Q and DAT R51W variants reported here, each of which interferes with STX1 phosphorylation the STX1/DAT interaction and thereby ablates AMPH-induced efflux. Interestingly, two other variants were previously found to cause dysregulated, anomalous DAT efflux, including a *de novo* DAT T356M variant and the recurrent DAT A559V variant seen in two boys with ASD, as well as in individuals with bipolar disorder and ADHD. These seemingly contradictory findings align with other examples of neurodevelopmental risk emerging from genetic variants causing opposite effects on gene expression or signaling cascades (Weiss *et al.*, 2008, Sanders *et al.*, 2011)(Cook *et al.*, 1997, Auerbach *et al.*, 2011)(Van Esch *et al.*, 2005). The physiological importance of DA efflux has only recently emerged and remains incompletely understood. These convergent data from ASD variants direct our attention to neurodevelopment, when DAT blockade or receptor stimulation at different time periods leads to

long-lasting changes in brain function(Stanwood and Levitt, 2007), as well as adult social behavior, including pair-bonding(Hostetler *et al.*, 2011) and aggression(Yu *et al.*, 2014). Understanding the impact of these variants on AMPH sensitivity may also shape the use of psychostimulants in children with ASD, since psychostimulant medications including AMPH (Adderall™) are frequently prescribed as a pharmocotherapy to treatment frequently co-occurring hyperactivity and inattention in ASD(Mahajan *et al.*, 2012). This altered sensitivity to AMPH observed in the ASD-associated variants may help to interpret changes in the efficacy of these psychostimulant-based therapies for ASD.

Materials and Methods

Subjects and clinical assessment. Subjects from this family correspond to the proband, unaffected sibling, and both parents (AC04-0029-01, AC04-0029-02, AC04-0029-03, AC04-0029-04), who were recruited by the Boston-based Autism Consortium(Wolfson, 2007). Clinical assessment followed standard research criteria for ASD diagnosis. The proband was classified as having a comparatively “narrow” diagnosis (as opposed to a “broader ASD”) based on diagnostic algorithms from the Autism Diagnostic Interview Revised (ADI-R)(Lord *et al.*, 1994) using criteria described by Risi *et al.*(Risi *et al.*, 2006), and classification resulting from the diagnostic algorithm of the Autism Diagnostic Observational Session (ADOS)(Lord *et al.*, 2000). Proband IQ was assessed at age 5 years, 9 months using the Wechsler Preschool and Primary Scale of Intelligence (WPPSI; Wechsler, D. (1967)). The Social Responsiveness Scale (SRS; Western Psychological Services) was performed on both parents to index the presence and severity of broader autism phenotype traits, followed by medical and family history provided by the biological mother.

SLC6A3 R/W and STX1A R/Q discovery. Methodological details and validation of the *de novo* mutation are published(Neale *et al.*, 2012). Briefly, DNA derived from whole blood of both parents and the probands was subjected to whole exome sequence analysis. The T356M variant, identified as a heterozygote in the proband and absent in both parents, was experimentally validated and confirmed to be a *de novo* mutation that does not appear in the unaffected sibling.

Cell culture and transfection. STX1 constructs in the pcDNA3.1(-) expression vector and the GFP-hDAT-pCIHygro expression vectors containing hDAT or hDAT R/W (Arg51 to Trp) sequence were generated, confirmed and transiently transfected into Chinese hamster ovary (CHO) cells. In some experiments (noted in figure legend), stably transfected hDAT CHO cells were used. These cells were generated as described in Bowton *et al*.(Bowton *et al.*, 2010). Cells were maintained in a 5% CO_2 incubator at 37°C and maintained in Ham's F-12 medium supplemented with 10% fetal bovine serum (FBS), 1 mM l-glutamine, 100 U/mL penicillin, and 100 µg/mL streptomycin. Stably transfected hDAT CHO cells were kept under selection with 250 µg/mL hygromycin B (Corning Cellgro). Fugene-6 (Roche Molecular Biochemicals) in serum-free media was used to transfect cells using a 6:1 transfection reagent:DNA ratio. Assays were conducted 24-48 hours post transfection.

Superior Cervical Ganglion neuron culture and transfection. SCG neurons were cultured from 1-3 day old male mouse pups. SCGs were dissected in complete Ultraculture medium (Lonza) supplemented with 20 ng/mL nerve growth factor (NGF). SCGs were washed with PBS and incubated for 20 minutes in collagenase (3%) and trypsin (2.5%) at 37°C. They were washed in complete Ultraculture medium with NGF. Dissociated cells were obtained by SCG trituration in medium. Cells plated on poly-D-lysine coated MatTek® dish treated with collagen (type IV). 24

hours post-plating, the media was replaced with Ultraculture medium with NGF and 10 µM 5-fluoro-2-deoxyuridine (FDU). SCGs were transfected via intranuclear microinjection of DNA.

Cell surface biotinylation and protein immunoblot. Cells were cultured in 6-well plates. For cell surface biotinylation assays, cells were labeled with sulfo-NHS-SS-biotin (1.0 mg/ml; Pierce) before purification and analysis via SDS-PAGE/immunoblots(Mazei-Robison *et al.*, 2008). hDAT was detected using a rat monoclonal primary antibody to the N-terminus of hDAT (1:1000) (Millipore Bioscience Research Reagents, catalog number MAB369) and a goat-anti-rat-HRP-conjugated secondary antibody (1:5000) (Jackson ImmunoResearch, catalog number sc-2006). The phosphorylation level of STX1 at Ser14 was detected using a rabbit polyclonal antibodies to phospho-S14 either from Castillo *et al.*(Castillo *et al.*) or with a commercially available antibody (1:2500) (abcam, catalog number ab63571) and a goat-anti-rabbit-HRP-conjugated secondary antibody (1:5000) (Jackson ImmunoResearch, catalog number sc-3837). Total STX1 was detected using a mouse monoclonal antibody (1:5000) (Sigma, catalog number S 0664) and a goat-anti-mouse-HRP-conjugated secondary antibody (1:5000) (Jackson ImmunoResearch, catalog number sc-2005).

Immunostaining. SCG neurons (at least 14 days in culture) were serum starved for one hour in DMEM:F12 and treated with vehicle or AMPH for 20 minutes. Neurons were subsequently fixed with PBS plus Ca^{2+}/Mg^{2+} and 4% paraformaldehyde, washed three times with PBS plus Ca^{2+}/Mg^{2+}, permeabilized, and blocked with PBS with 4% bovine serum albumin (BSA)/0.15% Tween 20, and immunostained with the appropriate antibody dissolved in PBS plus 4% BSA and 0.05% Tween 20. NET was detected using a mouse monoclonal antibody (1:5000) (Mab technologies; NET05-2) and pSTX1 with an affinity purified rabbit polyclonal (1:1000), anti pSTX at Ser14(Castillo *et al.*). Primary antibodies were visualized with the appropriate covalently Alexa-labeled secondary antibody from Invitrogen.

Mouse brain slices were prepared as outlined in *High Speed Chronoamperometry* method section, except recovery was in aCSF was for one hour at 37°C. Slices were fixed, permeabilized, washed, and blocked as outlined above. DAT was visualized using rat monoclonal against DAT and STX1A and STX1B were detected using rabbit polyclonal antiserum from SYSY catalogs # 110 302 STX1A and 110 402 STX1B respectively. pSTX at Ser14 was detected using an affinity purified rabbit polyclonal(1:1000)(Castillo *et al.*). Primary antibodies were visualized with the appropriate covalently Alexa-labeled secondary antibody from Invitrogen.

Immunofluorescence was imaged by capturing Z-series using a Zeiss using a •63x / 1.40 Plan-APOCHROMAT oil lens (Vanderbilt University Medical Center Cell Imaging Shared Resource). All images shown are always from single confocal sections, and image processing was performed using ImageJ and Adobe Photoshop.

Co-immunoprecipitations. Cells were grown to confluence in 25 cm^2 culture flasks and serum deprived for one hour prior to assay. Cells were washed three times with 4˚C phosphate-buffered saline (Gibco) containing 1 mM EGTA and 1 mM EDTA, and then lysed in RIPA buffer (100 mM NaCl, 1.0% IGEPAL CA-630 (NP-40), 0.5% sodium deoxycholate, 0.1% SDS, 50 mM Tris, pH = 7.4, supplemented with a protease inhibitor cocktail (Sigma)). Lysates were passed twice through a 27.5 gauge needle, and centrifuged at 15,000 x g for 30 minutes. With a portion of the total cell lysate (TCL) collected to run as the totals, 1 mL of the remaining supernatant was incubated at 4°C for 4 hours with Sepharose-G beads (Fisher Scientific), previously washed with 1% BSA in RIPA buffer, and then preincubated with 2.5 µg DAT antibody (rat monoclonal, #MAB369, Millipore). For the control, supernatant was incubated with BSA-blocked Sepharose-G beads alone (no DAT antibody). After the 4 hour incubation, beads were spun

down, washed with cold RIPA buffer, and eluted with Laemmli sample buffer at 37˚C for 30 minutes. TCL and bead eluates were analyzed by SDS-PAGE (10%) and immunoblotted for total STX1 and DAT. Band intensity was quantified using ImageJ software (National Institutes of Health).

Expression and purification of STX1. The cDNAs encoding STX, STX S14D and STX S14A lacking the transmembrane domain (STX ΔTM, STX1ΔTM S14A and STX1ΔTM S14D) were inserted into the bacterial expression vector pGEX, thereby adding an N-terminal GST-tag followed by a thrombin cleavage site. The resulting fusion proteins were produced in *Escherichia coli* BL21 DE3 LysS. The culture was grown at 30°C to OD 0.8 and expression was induced with 1 mM isopropylβ-d-1-thiogalactopyranoside at 30°C, and the culture was harvested 4 hours after induction. The frozen pelleted bacteria was lyzed in buffer (PBS, 0,1% TX-100, 20µg/mL DNAse I, 1mM DTT, mix protease inhibitor (GE Healthcare). The lysate was cleared by centrifugation followed by incubation with 100 µl glutathione sepharose beads (GE Healthcare, Uppsala, Sweden) at 4°C for 1½ h. The beads were pelleted at 3000 rpm for 5 min. and washed 3 times in buffer (PBS, 0,1% TX-100, 1 mM DTT) before elution by cleavage with 1µl thrombin (GE Healthcare, Uppsala, Sweden) O/N at 4°C. PMSF (1 mM) was added and the beads were filtered through a P200 tip. The concentration of the purified STX1B was measured by BCA assay (Thermo Fisher Scientific, Waltham, MA).

GST pull-down assay. A DAT GST fusion protein containing the 64 N-terminal residues of the transporter (GST hDAT 1-64) was expressed and bound to glutathione sepharose beads as described (Binda *et al.*, 2008). For the pull-down, 20 µl beads with either GST or GST hDAT 1-64 bound were incubated with 2 µg of purified STX ΔTM, STX1ΔTM S14A or STX1ΔTM S14D in 500 µl buffer (PBS, 0.1% TX-100, 0.1% BSA) for 30 minutes at 4°C and washed 3 times in buffer without BSA. Bound protein was eluted by incubation of beads for 1 hour at RT with 1 µl

thrombin in 15 µl buffer (PBS, 0.1% TX-100) followed by addition of SDS loading buffer + 100mM DTT and incubation for 25 min. at 70°C. Each sample was split in two and loaded on two different Any-kD precast gels (BioRad, Hercules, CA). One gel was used as a Coomassie loading control and the other was transfered to a PDVF membrane and immunoblotted with primary mouse STX antibody (Sigma Aldrich. St. Louis, MO) 1:1000 and anti-mouse HRP-conjugated secondary antibody (Thermo Fisher Scientific, Waltham, MA) 1:5000.

Amperometry. Cells were plated at a density of ~20,000 per 35-mm culture dish. To load cells with DA, dishes were washed with KRH assay buffer (130 mM NaCl, 1.3 mM KCl, 1.2 mM KH_2PO_4, 10 mM HEPES, and 2.2 mM $CaCl_2$, pH 7.4) containing 10 mM dextrose, 100 µM pargyline, 1 mM tropolone, and 100 µM ascorbic acid, and incubated with 1 µM DA in KRH assay buffer for 20 min at 37°C. To preload SCG neurons, dishes were washed with KRH assay buffer (as above) containing 100 nM raclopride. Dishes were washed three times with the external bath solution (130 mM NaCl, 10 mM HEPES, 34 mM dextrose, 1.5 mM $CaCl_2$, 0.5 mM $MgSO_4$, 1.3 mM KH_2PO_4, adjusted pH to 7.35, and 300 mOsm). A carbon fiber electrode (ProCFE; fiber diameter of 5 µm; obtained from Dagan Corporation) juxtaposed to the plasma membrane and held at +700 mV (a potential greater than the oxidation potential of DA) was used to measure DA flux through oxidation reactions. Amperometric currents in response to the addition of 10 µM AMPH were recorded using an Axopatch 200B amplifier (Molecular Devices, Union City, CA) with a low-pass Bessel filter set at 1 kHz; traces were digitally filtered offline at 1 Hz using Clampex9 software (Molecular Devices, Union City, CA). DA efflux was quantified as the peak value of the amperometric current for all experiments except for recordings from SCG neurons. For SCG neurons, total DA efflux was quantified as the integral of the trace for a fixed 15 minute window.

High Speed Chronoamperometry. Striatal hemislices (300 µm) from 6-10 week old C57Bl6 mice were prepared with a vibratome (Leica VT1000S) in an ice cold oxygenated (95% O2 / 5% CO2) sucrose cutting solution consisting of (in mM): 210 sucrose, 20 NaCl, 2.5 KCl, 1 $MgCl_2$, 1.2 NaH_2PO_4, 10 glucose, 26 $NaHCO_3$. Slices were then transferred to oxygenated artificial cerebrospinal fluid (aCSF) at 28°C for a minimum of 1 hour. The aCSF consisted of (in mM): 125 NaCl, 2.5 KCl, 1 $MgCl_2$, 2 $CaCl_2$, 1.2 NaH_2PO_4, 10 glucose, 26 $NaHCO_3$, 0.25 ascorbic acid. Striatal slices were treated at 37°C for 1 hour with either 100 nM BONT/C or vehicle control. Dopamine concentration was measured by chronoamperometry in striatal slices as previously described(Hoffman and Gerhardt, 1999, Gerhardt and Hoffman, 2001). Briefly, carbon fiber electrodes (100 µm length × 30 µm O.D.) coated with nafion for dopamine selectivity were lowered into the desired recording site or sites so that the tip of the recording electrode was positioned at a depth of 75-100 µm. The voltage was stepped from 0 mV to 550 mV for 100 ms and then back to 0 mV and the charging current of the carbon fiber electrode was allowed to decay for 20 ms before the signals were integrated. Data were collected at a frequency of 1 Hz with an Axopatch 200B amplifier. The integrated charge was converted to dopamine concentration based on in vitro calibration with dopamine.

[^{3}H]DA uptake. For DA uptake in a heterologous expression system: cells were plated on poly-D-lysine coated, 24-well plates and grown to ~90% confluence. On the day of the experiment, cells were washed with 37°C KRH buffer containing 10 mM dextrose, 100 µM pargyline, 1 mM tropolone, and 100 µM ascorbic acid, and equilibrated for 5 minutes at 37°C. Saturation kinetics of DA uptake was determined using a mixture of [^{3}H]DA (PerkinElmer Life Sciences, Waltham, MA) and unlabeled DA (Sigma Aldrich) diluting to final DA concentrations of 0.05 µM - 10 µM. Uptake was initiated by bath addition of the dilution row mixture. Uptake was terminated after 10 minutes by washing twice in ice-cold KRH buffer. Scintillation fluid (Optiphase HiSafe 3, PerkinElmer Life Sciences) was added to the wells and the plates were counted in a Wallac Tri-

Lux β-scintillation counter (Wallac). Nonspecific binding was determined in the presence of 10 µM cocaine. K_m and V_{max} values were derived by fitting Michaelis-Menten kinetics to the background corrected uptake data, using GraphPad Prism 5.0 (GraphPad Software, San Diego, CA). All determinations were performed in triplicates.

For DA uptake in striatal slices*:* striatal hemislices (prepared as previously mentioned) were treated at 37°C for 1 hour with either 100 nM BONT/C or vehicle control. Slices were then exposed to 50 nM [^{3}H]DA for 10 minutes. DAT-specific DA uptake was determined by subtracting the non-specific signal in the presence of 3 µM GBR12909. At the end of the [^{3}H]DA treatment, the slices were washed with cold aCSF and the striatum dissected. Tissue samples were then homogenized in 200 µL of lysis buffer consisting of 150 mM NaCl, 25 mM HEPES, 2 mM sodium orthovanadate, 2 mM sodium fluoride, 1% Triton-100. The homogenate was centrifuged at 13,000g 4°C for 30 minutes and the supernatant added to 500 µL of buffer 150 mM NaCl, 25 mM HEPES, 2 mM sodium orthovanadate, 2 mM sodium fluoride, 0.1% Triton-100. The protein concentration of each sample was measured and 500 µL of each sample was added to scintillation vials to count [^{3}H]DA. Counts were expressed as a ratio to protein content and normalized to the mean value for the control condition within each experiment.

For DA uptake in dissected Drosophila brains: 2-5 day old males were collected, anesthetized with CO_2, and brains were dissected in Schneider's medium (GIBCO) with 1.5% BSA. The retina were removed, and four brains per condition were pooled in Millipore Millicell inserts in 24 well plates. Brains were washed with Schneider's medium, then washed in a standard fly saline solution (HL3)(Feng *et al.*, 2004) plus 1.5% BSA and 10 mM $MgSO_4$. For 15 minutes at room temperature, brains were exposed to 200 nM [^{3}H]DA in HL3 plus 1.5% BSA and 115 uM ascorbic acid. Brains were then washed six times with 1.4 mL HL3 plus 1.5% BSA at 4°C.

Brains were placed into scintillation vials in 100 uL 0.1% SDS. Scintillation fluid was added to count [^{3}H]DA.

Drosophila Genetics, Molecular Biology, and Construction of UAS hDAT. Flies lacking the *Drosophila* dopamine transporter (*DAT^{fmn}*)(Kume *et al.*, 2005) and flies harboring TH-Gal4(Friggi-Grelin *et al.*, 2003) were outcrossed to a control line (Bloomington Indiana (BI) 6326) and selected by PCR or by eye color. TH-GAL4 (Bl 8848) and M{vas-int.Dm}ZH-2A, M{3xP3-RFP.attP'} ZH-22A (Bl 24481) were obtained from the BI stock center and outcrossed to flies lacking the *Drosophila* DAT (*DAT^{fmn}*) and carrying the *white* (*w^{1118}*) mutation (BI stock number 6236) for 5–10 generations. Transgenes (hDAT or hDAT R/W) were cloned into pBI-UASC(Wang *et al.*, 2012), and constructs were injected into embryos from M{vas-int.Dm}ZH-2A, M{3xP3-RFP.attP'}ZH-22A (Bl 24481). Initial potential transformants were isolated by selecting for red eyes and lack of GFP signal in the head. Transformants were also verified by RFP fluorescence and outcrossed 5-8 times to *DAT^{fmn}* flies. The presence of *DAT^{fmn}* lesion was verified by PCR. Flies were maintained on a standard cornmeal/molasses/yeast media at 25°C and 65% humidity with a 12 hour/12hour light/dark cycle. Lights came on at 8 AM and off at 8 PM.

Behavioral Analysis. Three day old males were collected and placed into tubes with food for three days. After three days locomotion was recorded for 32 hours by beam breaks and analyzed using equipment/software from Trikinetics (www.trikinetics.com). For the AMPH-induced locomotion, males were starved for 6 hours and then fed sucrose (10 mM) containing either AMPH (1 mM) or vehicle.

Statistical Analysis. Compiled data are typically expressed as normalized mean ± s.e.m. For statistical analysis, we used either a Student's t-test or one-way ANOVA depending on the n of the experimental groups. $P < 0.05$ was considered statistically significant.

CHAPTER VI

FUTURE DIRECTIONS

The results presented herein outline multiple molecular and structural regulators of the reversal of DAT function. Identifying and understanding these regulatory events is a vital research priority, and may lead to valuable pharmacotherapies for treating psychostimulant abuse, ASD, and related neuropsychiatric disorders. Each chapter presents a different mechanism of DAT molecular regulation, yet it is possible that some of these regulators converge mechanistically to fine-tune DAT functions. In this chapter, I will describe potential future mechanistic experiments to determine the role of N-terminal phosphorylation and how this posttranslational modification transmits the actions of AMPH. I will focus this discussion particularly in the context of the research outlined in chapter II.

Chapter II identified the N-terminus of the hDAT as a structural domain that directly interacts with PIP_2. I propose that this interaction may be an anchor for the N-terminus of the hDAT, targeting its localization to the plasma membrane and regulating its conformations. This may preferentially prime the hDAT for forward transport function. Experiments targeted at observing the consequences of the steric constraint of the N-terminus to the plasma membrane may help clarify how the mobility of the N-terminus regulates the transporter cycle (experiments could include probing for changes in the voltage dependence of DA efflux and/or hDAT affinity for substrates). It has been stated that the N-terminus of DAT is a “lever” required for the actions of AMPH(Sucic *et al.*); therefore, I hypothesize that irreversibly anchoring the N-terminus of the hDAT to the plasma membrane would selectively impair the ability of AMPH to cause DA efflux,

without altering hDAT-mediated DA uptake. These experiments would help clarify the role of hDAT N-terminal mobility in AMPH actions.

Our lab and others have demonstrated that that phosphorylation of five key Ser residues on the hDAT N-terminus is an event required for AMPH to induce DA efflux(Khoshbouei *et al.*, 2004, Fog *et al.*, 2006). I predict that hDAT-PIP_2 interactions are required for the phosphorylation of these N-terminal residues by presenting the hDAT N-terminus at a membrane localization or conformation conducive to phosphorylation by kinases such as PKC and CaMKII. Thus, I hypothesize that PIP_2 depletion or interfering with the hDAT-PIP_2 interaction would block hDAT N-terminal phosphorylation and the subsequent DA efflux. Consistently, I anticipate hDAT mutants with reduced PIP_2 interactions (e.g. hDAT K/N or hDAT K/A) would be resistant to the ability of AMPH to cause N-terminal phosphorylation. This would explain the observed reduction in DA efflux presented in chapter II.

It is possible that AMPH-induced phosphorylation uncouples the hDAT N-terminus from PIP_2, to support DA efflux. Therefore, I further predict that there is a series of molecular events required for the reversal of hDAT function, and that hDAT N-terminal phosphorylation would circumvent the requirements for hDAT to interact with PIP_2 to support DA efflux. One experiment that may elucidate this series of events would involve the use of an hDAT construct with all five distal Ser residues mutated to Asp, to mimic phosphorylation at these residues (hDAT S/D). Expressing the hDAT S/D in heterologous cells and introducing the PIP_2-inhibitory peptide through the whole-cell pipette in the APC setup while recording the magnitude of the AMPH-induced DA efflux (similar to the setup in **Fig. 9**) would allow me to clarify the role of hDAT N-terminal phosphorylation and PIP_2 interaction in the AMPH-induced reverse transport of DA. I predict that the cells expressing hDAT S/D would be impervious to a decrease reverse transport of DA induced by interfering with hDAT-PIP_2 membrane interactions with the PIP_2-inhibitory peptide.

The hDAT S/D would not depend on PIP_2 interactions to induce reverse transport of DA because transporter is already pseudo-phosphorylated. Therefore, it would not require PIP_2 interactions to promote hDAT N-terminal phosphorylation. This would indicate that PIP_2 interactions with the hDAT N-terminus are a necessary precursor for phosphorylation of key Ser residues, and would shed light onto the temporal sequence of events that are required for AMPH to induce a reversal in hDAT function.

The work outlined in this thesis advances the understanding of the molecular mechanisms involved in AMPH actions. This understanding may allow for the development of small molecules that selectively inhibit AMPH's ability to induce DA efflux without affecting the physiological function of DAT uptake. At first glance, it might seem reasonable to inhibit the kinases involved in hDAT N-terminal phosphorylation, in order to reduce the efficacy of AMPH actions at the hDAT. This is a complex solution since these kinases (e.g. PKC and CaMKII) are ubiquitous in the CNS and involved in many processes. Alternatively, specifically inhibiting the hDAT-PIP_2 interaction may prove to be a more targeted and effective strategy for reducing AMPH-induced DA efflux while leaving DA uptake intact. This may prove to be effective treatment for AMPH abuse, where there currently is none.

REFERENCES

Ahmed, I., L. I. Cosen-Binker, Y. M. Leung, H. Y. Gaisano and N. E. Diamant (2007). "Modulation of the K(v)4.3 channel by syntaxin 1A." Biochem Biophys Res Commun **358**(3): 789-795.

Aksenova, M. V., G. S. Burbaeva, K. V. Kandror, D. V. Kapkov and A. S. Stepanov (1991). "The decreased level of casein kinase 2 in brain cortex of schizophrenic and Alzheimer's disease patients." FEBS Lett **279**(1): 55-57.

Anderson, B. M., N. Schnetz-Boutaud, J. Bartlett, H. H. Wright, R. K. Abramson, M. L. Cuccaro, J. R. Gilbert, M. A. Pericak-Vance and J. L. Haines (2008). "Examination of association to autism of common genetic variationin genes related to dopamine." Autism Res **1**(6): 364-369.

Auerbach, B. D., E. K. Osterweil and M. F. Bear (2011). "Mutations causing syndromic autism define an axis of synaptic pathophysiology." Nature **480**(7375): 63-68.

Bailey, A., A. Le Couteur, I. Gottesman, P. Bolton, E. Simonoff, E. Yuzda and M. Rutter (1995). "Autism as a strongly genetic disorder: evidence from a British twin study." Psychol Med **25**(1): 63-77.

Baio, Jon (2012). "Prevalence of autism spectrum disorders--Autism and Developmental Disabilities Monitoring Network, 14 sites, United States, 2008." MMWR Surveill Summ **61**(3): 1-19.

Balla, T., Z. Szentpetery and Y. J. Kim (2009). "Phosphoinositide signaling: new tools and insights." Physiology (Bethesda) **24**: 231-244.

Beitz, J. M. (2014). "Parkinson's disease: a review." Front Biosci (Schol Ed) **6**: 65-74.

Ben-Aissa, K., G. Patino-Lopez, N. V. Belkina, O. Maniti, T. Rosales, J. J. Hao, M. J. Kruhlak, J. R. Knutson, C. Picart and S. Shaw (2012). "Activation of moesin, a protein that links actin cytoskeleton to the plasma membrane, occurs by phosphatidylinositol 4,5-bisphosphate (PIP2) binding sequentially to two sites and releasing an autoinhibitory linker." J Biol Chem **287**(20): 16311-16323.

Beuming, T., J. Kniazeff, M. L. Bergmann, L. Shi, L. Gracia, K. Raniszewska, A. H. Newman, J. A. Javitch, H. Weinstein, U. Gether and C. J. Loland (2008). "The binding sites for cocaine and dopamine in the dopamine transporter overlap." Nat Neurosci **11**(7): 780-789.

Binda, F., C. Dipace, E. Bowton, S. D. Robertson, B. J. Lute, J. U. Fog, M. Zhang, N. Sen, R. J. Colbran, M. E. Gnegy, U. Gether, J. A. Javitch, K. Erreger and A. Galli (2008). "Syntaxin 1A interaction with the dopamine transporter promotes amphetamine-induced dopamine efflux." Mol Pharmacol **74**(4): 1101-1108.

Binda, F., B. J. Lute, C. Dipace, R. D. Blakely and A. Galli (2006). "The N-terminus of the norepinephrine transporter regulates the magnitude and selectivity of the transporter-associated leak current." Neuropharmacology **50**(3): 354-361.

Bisgaard, H., M. A. Larsen, S. Mazier, T. Beuming, A. H. Newman, H. Weinstein, L. Shi, C. J. Loland and U. Gether (2011). "The binding sites for benztropines and dopamine in the dopamine transporter overlap." Neuropharmacology **60**(1): 182-190.

Bjorklund, A. and S. B. Dunnett (2007). "Fifty years of dopamine research." Trends Neurosci **30**(5): 185-187.

Blakely, R. D., H. E. Berson, R. T. Fremeau, Jr., M. G. Caron, M. M. Peek, H. K. Prince and C. C. Bradley (1991). "Cloning and expression of a functional serotonin transporter from rat brain." Nature **354**(6348): 66-70.

Bowton, E., C. Saunders, K. Erreger, D. Sakrikar, H. J. Matthies, N. Sen, T. Jessen, R. J. Colbran, M. G. Caron, J. A. Javitch, R. D. Blakely and A. Galli (2010). "Dysregulation of dopamine transporters via dopamine D2 autoreceptors triggers anomalous dopamine efflux associated with attention-deficit hyperactivity disorder." J Neurosci **30**(17): 6048-6057.

Bowton, E., C. Saunders, I. A. Reddy, N. G. Campbell, P. J. Hamilton, L. K. Henry, H. Coon, D. Sakrikar, J. M. Veenstra-VanderWeele, R. D. Blakely, J. Sutcliffe, H. J. Matthies, K. Erreger and A. Galli (2014). "SLC6A3 coding variant Ala559Val found in two autism probands alters dopamine transporter function and trafficking." Transl Psychiatry **4**: e464.

Buchmayer, F., K. Schicker, T. Steinkellner, P. Geier, G. Stubiger, P. J. Hamilton, A. Jurik, T. Stockner, J. W. Yang, T. Montgomery, M. Holy, T. Hofmaier, O. Kudlacek, H. J. Matthies, G. F. Ecker, V. Bochkov, A. Galli, S. Boehm and H. H. Sitte (2013).

"Amphetamine actions at the serotonin transporter rely on the availability of phosphatidylinositol-4,5-bisphosphate." Proc Natl Acad Sci U S A **110**(28): 11642-11647.

Carlsson, A. (1987). "Perspectives on the discovery of central monoaminergic neurotransmission." Annu Rev Neurosci **10**: 19-40.

Castillo, M. A., S. Ghose, C. A. Tamminga and P. G. Ulery-Reynolds "Deficits in syntaxin 1 phosphorylation in schizophrenia prefrontal cortex." Biol Psychiatry **67**(3): 208-216.

Cervinski, M. A., J. D. Foster and R. A. Vaughan (2005). "Psychoactive substrates stimulate dopamine transporter phosphorylation and down regulation by cocaine sensitive and protein kinase C dependent mechanisms." J Biol Chem.

Cervinski, M. A., J. D. Foster and R. A. Vaughan (2010). "Syntaxin 1A regulates dopamine transporter activity, phosphorylation and surface expression." Neuroscience **170**(2): 408-416.

Chen, R., C. A. Furman and M. E. Gnegy (2010). "Dopamine transporter trafficking: rapid response on demand." Future Neurol **5**(1): 123.

Claxton, D. P., M. Quick, L. Shi, F. D. de Carvalho, H. Weinstein, J. A. Javitch and H. S. McHaourab (2010). "Ion/substrate-dependent conformational dynamics of a bacterial homolog of neurotransmitter:sodium symporters." Nat Struct Mol Biol **17**(7): 822-829.

Cook, E. H., Jr., V. Lindgren, B. L. Leventhal, R. Courchesne, A. Lincoln, C. Shulman, C. Lord and E. Courchesne (1997). "Autism or atypical autism in maternally but not paternally derived proximal 15q duplication." Am J Hum Genet **60**(4): 928-934.

Cook, E. H., Jr. and S. W. Scherer (2008). "Copy-number variations associated with neuropsychiatric conditions." Nature **455**(7215): 919-923.

Cousins, D. A., K. Butts and A. H. Young (2009). "The role of dopamine in bipolar disorder." Bipolar Disord **11**(8): 787-806.

Cowell, R. M., L. Kantor, G. H. Hewlett, K. A. Frey and M. E. Gnegy (2000). "Dopamine transporter antagonists block phorbol ester-induced dopamine release and dopamine transporter phosphorylation in striatal synaptosomes." Eur J Pharmacol **389**(1): 59-65.

Crawley, J. N. (2012). "Translational animal models of autism and neurodevelopmental disorders." Dialogues Clin Neurosci **14**(3): 293-305.

Cremona, M. L., H. J. Matthies, K. Pau, E. Bowton, N. Speed, B. J. Lute, M. Anderson, N. Sen, S. D. Robertson, R. A. Vaughan, J. E. Rothman, A. Galli, J. A. Javitch and A. Yamamoto "Flotillin-1 is essential for PKC-triggered endocytosis and membrane microdomain localization of DAT." Nat Neurosci **14**(4): 469-477.

Cremona, M. L., H. J. Matthies, K. Pau, E. Bowton, N. Speed, B. J. Lute, M. Anderson, N. Sen, S. D. Robertson, R. A. Vaughan, J. E. Rothman, A. Galli, J. A. Javitch and A. Yamamoto (2011). "Flotillin-1 is essential for PKC-triggered endocytosis and membrane microdomain localization of DAT." Nat Neurosci **14**(4): 469-477.

Czech, M. P. (2000). "PIP2 and PIP3: complex roles at the cell surface." Cell **100**(6): 603-606.

Damiano, C. R., J. Aloi, M. Treadway, J. W. Bodfish and G. S. Dichter (2012). "Adults with autism spectrum disorders exhibit decreased sensitivity to reward parameters when making effort-based decisions." J Neurodev Disord **4**(1): 13.

Das, R. and D. Baker (2008). "Macromolecular modeling with rosetta." Annu Rev Biochem **77**: 363-382.

de Bruin, E. I., P. F. de Nijs, F. Verheij, C. A. Hartman and R. F. Ferdinand (2007). "Multiple complex developmental disorder delineated from PDD-NOS." J Autism Dev Disord **37**(6): 1181-1191.

de Krom, M., W. G. Staal, R. A. Ophoff, J. Hendriks, J. Buitelaar, B. Franke, M. V. de Jonge, P. Bolton, D. Collier, S. Curran, H. van Engeland and J. M. van Ree (2009). "A common variant in DRD3 receptor is associated with autism spectrum disorder." Biol Psychiatry **65**(7): 625-630.

Devlin, B. and S. W. Scherer (2012). "Genetic architecture in autism spectrum disorder." Curr Opin Genet Dev **22**(3): 229-237.

Di Martino, A., X. N. Zuo, C. Kelly, R. Grzadzinski, M. Mennes, A. Schvarcz, J. Rodman, C. Lord, F. X. Castellanos and M. P. Milham (2013). "Shared and distinct intrinsic functional network centrality in autism and attention-deficit/hyperactivity disorder." Biol Psychiatry **74**(8): 623-632.

Dichter, G. S., C. A. Damiano and J. A. Allen (2012). "Reward circuitry dysfunction in psychiatric and neurodevelopmental disorders and genetic syndromes: animal models and clinical findings." J Neurodev Disord **4**(1): 19.

Dichter, G. S., J. A. Richey, A. M. Rittenberg, A. Sabatino and J. W. Bodfish (2012). "Reward circuitry function in autism during face anticipation and outcomes." J Autism Dev Disord **42**(2): 147-160.

Dipace, C., U. Sung, F. Binda, R. D. Blakely and A. Galli (2007). "Amphetamine induces a calcium/calmodulin-dependent protein kinase II-dependent reduction in norepinephrine transporter surface expression linked to changes in syntaxin 1A/transporter complexes." Mol Pharmacol **71**(1): 230-239.

Dreher, J. C., P. Kohn, B. Kolachana, D. R. Weinberger and K. F. Berman (2009). "Variation in dopamine genes influences responsivity of the human reward system." Proc Natl Acad Sci U S A **106**(2): 617-622.

Dubois, T., P. Kerai, M. Learmonth, A. Cronshaw and A. Aitken (2002). "Identification of syntaxin-1A sites of phosphorylation by casein kinase I and casein kinase II." Eur J Biochem **269**(3): 909-914.

Durdiakova, J., V. Warrier, S. Banerjee-Basu, S. Baron-Cohen and B. Chakrabarti (2014). "STX1A and Asperger syndrome: a replication study." Mol Autism **5**(1): 14.

Earl, D. J. and M. W. Deem (2005). "Parallel tempering: theory, applications, and new perspectives." Phys Chem Chem Phys **7**(23): 3910-3916.

Enter, D., L. S. Colzato and K. Roelofs (2012). "Dopamine transporter polymorphisms affect social approach-avoidance tendencies." Genes Brain Behav **11**(6): 671-676.

Faber, S., G. M. Zinn, J. C. Kern, 2nd and H. M. Kingston (2009). "The plasma zinc/serum copper ratio as a biomarker in children with autism spectrum disorders." Biomarkers **14**(3): 171-180.

Fan, H. P., F. J. Fan, L. Bao and G. Pei (2006). "SNAP-25/syntaxin 1A complex functionally modulates neurotransmitter gamma-aminobutyric acid reuptake." J Biol Chem **281**(38): 28174-28184.

Faraone, S. V. and M. T. Tsuang (2003). "Heterogeneity and the genetics of bipolar disorder." Am J Med Genet C Semin Med Genet **123C**(1): 1-9.

Feng, Y., A. Ueda and C. F. Wu (2004). "A modified minimal hemolymph-like solution, HL3.1, for physiological recordings at the neuromuscular junctions of normal and mutant Drosophila larvae." J Neurogenet **18**(2): 377-402.

Fischer, J. F. and A. K. Cho (1979). "Chemical release of dopamine from striatal homogenates: evidence for an exchange diffusion model." J Pharmacol Exp Ther **208**(2): 203-209.

Fitzgerald, P. and T. G. Dinan (2008). "Prolactin and dopamine: what is the connection? A review article." J Psychopharmacol **22**(2 Suppl): 12-19.

Fog, J. U., H. Khoshbouei, M. Holy, W. A. Owens, C. B. Vaegter, N. Sen, Y. Nikandrova, E. Bowton, D. G. McMahon, R. J. Colbran, L. C. Daws, H. H. Sitte, J. A. Javitch, A. Galli

and U. Gether (2006). "Calmodulin kinase II interacts with the dopamine transporter C terminus to regulate amphetamine-induced reverse transport." Neuron **51**(4): 417-429.

Foletti, D. L., R. Lin, M. A. Finley and R. H. Scheller (2000). "Phosphorylated syntaxin 1 is localized to discrete domains along a subset of axons." J Neurosci **20**(12): 4535-4544.

Friggi-Grelin, F., H. Coulom, M. Meller, D. Gomez, J. Hirsh and S. Birman (2003). "Targeted gene expression in Drosophila dopaminergic cells using regulatory sequences from tyrosine hydroxylase." J Neurobiol **54**(4): 618-627.

Gabriel, L. R., S. Wu, P. Kearney, K. D. Bellve, C. Standley, K. E. Fogarty and H. E. Melikian (2013). "Dopamine transporter endocytic trafficking in striatal dopaminergic neurons: differential dependence on dynamin and the actin cytoskeleton." J Neurosci **33**(45): 17836-17846.

Gadow, K. D., C. J. Devincent, D. M. Olvet, V. Pisarevskaya and E. Hatchwell (2010). "Association of DRD4 polymorphism with severity of oppositional defiant disorder, separation anxiety disorder and repetitive behaviors in children with autism spectrum disorder." Eur J Neurosci **32**(6): 1058-1065.

Gadow, K. D., C. J. DeVincent and J. Pomeroy (2006). "ADHD symptom subtypes in children with pervasive developmental disorder." J Autism Dev Disord **36**(2): 271-283.

Gadow, K. D., J. Roohi, C. J. DeVincent and E. Hatchwell (2008). "Association of ADHD, tics, and anxiety with dopamine transporter (DAT1) genotype in autism spectrum disorder." J Child Psychol Psychiatry **49**(12): 1331-1338.

Genomes Project, Consortium, G. R. Abecasis, A. Auton, L. D. Brooks, M. A. DePristo, R. M. Durbin, R. E. Handsaker, H. M. Kang, G. T. Marth and G. A. McVean (2012). "An integrated map of genetic variation from 1,092 human genomes." Nature **491**(7422): 56-65.

Gerhardt, G. A. and A. F. Hoffman (2001). "Effects of recording media composition on the responses of Nafion-coated carbon fiber microelectrodes measured using high-speed chronoamperometry." J Neurosci Methods **109**(1): 13-21.

Giambalvo, C. T. (1992). "Protein kinase C and dopamine transport--1. Effects of amphetamine in vivo." Neuropharmacology **31**(12): 1201-1210.

Giros, B. and M. G. Caron (1993). "Molecular characterization of the dopamine transporter." Trends Pharmacol Sci **14**(2): 43-49.

Giros, B., M. Jaber, S. R. Jones, R. M. Wightman and M. G. Caron (1996). "Hyperlocomotion and indifference to cocaine and amphetamine in mice lacking the dopamine transporter." Nature **379**(6566): 606-612.

Gnegy, M. E., H. Khoshbouei, K. A. Berg, J. A. Javitch, W. P. Clarke, M. Zhang and A. Galli (2004). "Intracellular Ca2+ regulates amphetamine-induced dopamine efflux and currents mediated by the human dopamine transporter." Mol Pharmacol **66**(1): 137-143.

Goldstein, S. and A. J. Schwebach (2004). "The comorbidity of Pervasive Developmental Disorder and Attention Deficit Hyperactivity Disorder: results of a retrospective chart review." J Autism Dev Disord **34**(3): 329-339.

Grunhage, F., T. G. Schulze, D. J. Muller, M. Lanczik, E. Franzek, M. Albus, M. Borrmann-Hassenbach, M. Knapp, S. Cichon, W. Maier, M. Rietschel, P. Propping and M. M. Nothen (2000). "Systematic screening for DNA sequence variation in the coding region of the human dopamine transporter gene (DAT1)." Mol Psychiatry **5**(3): 275-282.

Gu, H., S. C. Wall and G. Rudnick (1994). "Stable expression of biogenic amine transporters reveals differences in inhibitor sensitivity, kinetics, and ion dependence." J Biol Chem **269**(10): 7124-7130.

Guptaroy, B., M. Zhang, E. Bowton, F. Binda, L. Shi, H. Weinstein, A. Galli, J. A. Javitch, R. R. Neubig and M. E. Gnegy (2009). "A Juxtamembrane Mutation in the N-Terminus of the Dopamine Transporter Induces Preference for an Inward-Facing Conformation." Mol Pharmacol.

Hamilton, P. J., A. N. Belovich, G. Khelashvili, C. Saunders, K. Erreger, J. A. Javitch, H. H. Sitte, H. Weinstein, H. J. Matthies and A. Galli (2014). "PIP2 regulates psychostimulant behaviors through its interaction with a membrane protein." Nat Chem Biol **10**(7): 582-589.

Hamilton, P. J., N. G. Campbell, S. Sharma, K. Erreger, F. Herborg Hansen, C. Saunders, A. N. Belovich, Nih Arra Autism Sequencing Consortium, M. A. Sahai, E. H. Cook, U. Gether, H. S. McHaourab, H. J. Matthies, J. S. Sutcliffe and A. Galli (2013). "De novo mutation in the dopamine transporter gene associates dopamine dysfunction with autism spectrum disorder." Mol Psychiatry **18**(12): 1315-1323.

Hansen, F. H., T. Skjorringe, S. Yasmeen, N. V. Arends, M. A. Sahai, K. Erreger, T. F. Andreassen, M. Holy, P. J. Hamilton, V. Neergheen, M. Karlsborg, A. H. Newman, S. Pope, S. J. Heales, L. Friberg, I. Law, L. H. Pinborg, H. H. Sitte, C. Loland, L. Shi, H. Weinstein, A. Galli, L. E. Hjermind, L. B. Moller and U. Gether (2014). "Missense dopamine transporter mutations associate with adult parkinsonism and ADHD." J Clin Invest **124**(7): 3107-3120.

Hettinger, J. A., X. Liu, M. L. Hudson, A. Lee, I. L. Cohen, R. C. Michaelis, C. E. Schwartz, S. M. Lewis and J. J. Holden (2012). "DRD2 and PPP1R1B (DARPP-32) polymorphisms independently confer increased risk for autism spectrum disorders and additively predict affected status in male-only affected sib-pair families." Behav Brain Funct **8**: 19.

Hettinger, J. A., X. Liu, C. E. Schwartz, R. C. Michaelis and J. J. Holden (2008). "A DRD1 haplotype is associated with risk for autism spectrum disorders in male-only affected sib-pair families." Am J Med Genet B Neuropsychiatr Genet **147B**(5): 628-636.

Hilgemann, D. W. and R. Ball (1996). "Regulation of cardiac Na+,Ca2+ exchange and KATP potassium channels by PIP2." Science **273**(5277): 956-959.

Hirling, H. and R. H. Scheller (1996). "Phosphorylation of synaptic vesicle proteins: modulation of the alpha SNAP interaction with the core complex." Proc Natl Acad Sci U S A **93**(21): 11945-11949.

Hoffman, A. F. and G. A. Gerhardt (1999). "Differences in pharmacological properties of dopamine release between the substantia nigra and striatum: an in vivo electrochemical study." J Pharmacol Exp Ther **289**(1): 455-463.

Hoogman, M., M. Onnink, R. Cools, E. Aarts, C. Kan, A. Arias Vasquez, J. Buitelaar and B. Franke (2013). "The dopamine transporter haplotype and reward-related striatal responses in adult ADHD." Eur Neuropsychopharmacol **23**(6): 469-478.

Hope, H. R. and L. J. Pike (1996). "Phosphoinositides and phosphoinositide-utilizing enzymes in detergent-insoluble lipid domains." Mol Biol Cell **7**(6): 843-851.

Hosenbocus, S. and R. Chahal (2012). "A review of executive function deficits and pharmacological management in children and adolescents." J Can Acad Child Adolesc Psychiatry **21**(3): 223-229.

Hostetler, C. M., S. L. Harkey, T. B. Krzywosinski, B. J. Aragona and K. L. Bales (2011). "Neonatal exposure to the D1 agonist SKF38393 inhibits pair bonding in the adult prairie vole." Behav Pharmacol **22**(7): 703-710.

Hsia, Y., A. Y. Wong, D. G. Murphy, E. Simonoff, J. K. Buitelaar and I. C. Wong (2014). "Psychopharmacological prescriptions for people with autism spectrum disorder (ASD): a multinational study." Psychopharmacology (Berl) **231**(6): 999-1009.

Humphrey, W., A. Dalke and K. Schulten (1996). "VMD: visual molecular dynamics." J Mol Graph **14**(1): 33-38, 27-38.

Iossifov, I., M. Ronemus, D. Levy, Z. Wang, I. Hakker, J. Rosenbaum, B. Yamrom, Y. H. Lee, G. Narzisi, A. Leotta, J. Kendall, E. Grabowska, B. Ma, S. Marks, L. Rodgers, A. Stepansky, J. Troge, P. Andrews, M. Bekritsky, K. Pradhan, E. Ghiban, M. Kramer, J. Parla, R. Demeter, L. L. Fulton, R. S. Fulton, V. J. Magrini, K. Ye, J. C. Darnell, R. B. Darnell, E.

R. Mardis, R. K. Wilson, M. C. Schatz, W. R. McCombie and M. Wigler (2012). "De novo gene disruptions in children on the autistic spectrum." Neuron **74**(2): 285-299.

Iwata, S., G. H. Hewlett and M. E. Gnegy (1997). "Amphetamine increases the phosphorylation of neuromodulin and synapsin I in rat striatal synaptosomes." Synapse **26**(3): 281-291.

Jackson, M. J. and P. J. Garrod (1978). "Plasma zinc, copper, and amino acid levels in the blood of autistic children." J Autism Child Schizophr **8**(2): 203-208.

Jardetzky, O. (1966). "Simple allosteric model for membrane pumps." Nature **211**(5052): 969-970.

Jeschke, G., A. Koch, U. Jonas and A. Godt (2002). "Direct conversion of EPR dipolar time evolution data to distance distributions." J Magn Reson **155**(1): 72-82.

Jeschke, G. and Y. Polyhach (2007). "Distance measurements on spin-labelled biomacromolecules by pulsed electron paramagnetic resonance." Phys Chem Chem Phys **9**(16): 1895-1910.

Johnson, L. A., B. Guptaroy, D. Lund, S. Shamban and M. E. Gnegy (2005). "Regulation of amphetamine-stimulated dopamine efflux by protein kinase C beta." J Biol Chem.

Jones, S. R., R. R. Gainetdinov, R. M. Wightman and M. G. Caron (1998). "Mechanisms of amphetamine action revealed in mice lacking the dopamine transporter." J Neurosci **18**(6): 1979-1986.

Kadamur, G. and E. M. Ross (2013). "Mammalian phospholipase C." Annu Rev Physiol **75**: 127-154.

Kahlig, K. M., F. Binda, H. Khoshbouei, R. D. Blakely, D. G. McMahon, J. A. Javitch and A. Galli (2005). "Amphetamine induces dopamine efflux through a dopamine transporter channel." Proc Natl Acad Sci U S A **102**(9): 3495-3500.

Kahlig, K. M., B. J. Lute, Y. Wei, C. J. Loland, U. Gether, J. A. Javitch and A. Galli (2006). "Regulation of dopamine transporter trafficking by intracellular amphetamine." Mol Pharmacol **70**(2): 542-548.

Kantor, L. and M. E. Gnegy (1998). "Protein kinase C inhibitors block amphetamine-mediated dopamine release in rat striatal slices." J Pharmacol Exp Ther **284**(2): 592-598.

Kantor, L., M. Zhang, B. Guptaroy, Y. H. Park and M. E. Gnegy (2004). "Repeated amphetamine couples norepinephrine transporter and calcium channel activities in PC12 cells." J Pharmacol Exp Ther **311**(3): 1044-1051.

Khelashvili, G., A. Galli and H. Weinstein (2012). "Phosphatidylinositol 4,5-biphosphate (PIP(2)) lipids regulate the phosphorylation of syntaxin N-terminus by modulating both its position and local structure." Biochemistry **51**(39): 7685-7698.

Khelashvili, G., D. Harries and H. Weinstein (2009). "Modeling membrane deformations and lipid demixing upon protein-membrane interaction: the BAR dimer adsorption." Biophys J **97**(6): 1626-1635.

Khelashvili, G., H. Weinstein and D. Harries (2008). "Protein diffusion on charged membranes: a dynamic mean-field model describes time evolution and lipid reorganization." Biophys J **94**(7): 2580-2597.

Khoshbouei, H., N. Sen, B. Guptaroy, L. Johnson, D. Lund, M. E. Gnegy, A. Galli and J. A. Javitch (2004). "N-terminal phosphorylation of the dopamine transporter is required for amphetamine-induced efflux." PLoS Biol **2**(3): E78.

Khoshbouei, H., H. Wang, J. D. Lechleiter, J. A. Javitch and A. Galli (2003). "Amphetamine-induced dopamine efflux. A voltage-sensitive and intracellular Na+-dependent mechanism." J Biol Chem **278**(14): 12070-12077.

Kiessling, V., C. Wan and L. K. Tamm (2009). "Domain coupling in asymmetric lipid bilayers." Biochim Biophys Acta **1788**(1): 64-71.

Kniazeff, J., L. Shi, C. J. Loland, J. A. Javitch, H. Weinstein and U. Gether (2008). "An intracellular interaction network regulates conformational transitions in the dopamine transporter." J Biol Chem **283**(25): 17691-17701.

Kohls, G., M. T. Perino, J. M. Taylor, E. N. Madva, S. J. Cayless, V. Troiani, E. Price, S. Faja, J. D. Herrington and R. T. Schultz (2013). "The nucleus accumbens is involved in both the pursuit of social reward and the avoidance of social punishment." Neuropsychologia **51**(11): 2062-2069.

Kohls, G., H. Thonessen, G. K. Bartley, N. Grossheinrich, G. R. Fink, B. Herpertz-Dahlmann and K. Konrad (2014). "Differentiating neural reward responsiveness in autism versus ADHD." Dev Cogn Neurosci **10C**: 104-116.

Krishnamurthy, H. and E. Gouaux (2012). "X-ray structures of LeuT in substrate-free outward-open and apo inward-open states." Nature **481**(7382): 469-474.

Kristensen, A. S., J. Andersen, T. N. Jorgensen, L. Sorensen, J. Eriksen, C. J. Loland, K. Stromgaard and U. Gether (2011). "SLC6 neurotransmitter transporters: structure, function, and regulation." Pharmacol Rev **63**(3): 585-640.

Krueger, B. K. (1990). "Kinetics and block of dopamine uptake in synaptosomes from rat caudate nucleus." J Neurochem **55**(1): 260-267.

Kume, K., S. Kume, S. K. Park, J. Hirsh and F. R. Jackson (2005). "Dopamine is a regulator of arousal in the fruit fly." J Neurosci **25**(32): 7377-7384.

Kurian, M. A., Y. Li, J. Zhen, E. Meyer, N. Hai, H. J. Christen, G. F. Hoffmann, P. Jardine, A. von Moers, S. R. Mordekar, F. O'Callaghan, E. Wassmer, E. Wraige, C. Dietrich, T. Lewis, K. Hyland, S. Heales, Jr., T. Sanger, P. Gissen, B. E. Assmann, M. E. Reith and E. R. Maher (2011). "Clinical and molecular characterisation of hereditary dopamine transporter deficiency syndrome: an observational cohort and experimental study." Lancet Neurol **10**(1): 54-62.

Kurian, M. A., J. Zhen, S. Y. Cheng, Y. Li, S. R. Mordekar, P. Jardine, N. V. Morgan, E. Meyer, L. Tee, S. Pasha, E. Wassmer, S. J. Heales, P. Gissen, M. E. Reith and E. R. Maher

(2009). "Homozygous loss-of-function mutations in the gene encoding the dopamine transporter are associated with infantile parkinsonism-dystonia." J Clin Invest **119**(6): 1595-1603.

Langen, M., D. Bos, S. D. Noordermeer, H. Nederveen, H. van Engeland and S. Durston (2014). "Changes in the development of striatum are involved in repetitive behavior in autism." Biol Psychiatry **76**(5): 405-411.

Lee, K. H., M. Y. Kim, D. H. Kim and Y. S. Lee (2004). "Syntaxin 1A and receptor for activated C kinase interact with the N-terminal region of human dopamine transporter." Neurochem Res **29**(7): 1405-1409.

Leviel, V. (2011). "Dopamine release mediated by the dopamine transporter, facts and consequences." J Neurochem **118**(4): 475-489.

Levy, D., M. Ronemus, B. Yamrom, Y. H. Lee, A. Leotta, J. Kendall, S. Marks, B. Lakshmi, D. Pai, K. Ye, A. Buja, A. Krieger, S. Yoon, J. Troge, L. Rodgers, I. Iossifov and M. Wigler (2011). "Rare de novo and transmitted copy-number variation in autistic spectrum disorders." Neuron **70**(5): 886-897.

Leyfer, O. T., S. E. Folstein, S. Bacalman, N. O. Davis, E. Dinh, J. Morgan, H. Tager-Flusberg and J. E. Lainhart (2006). "Comorbid psychiatric disorders in children with autism: interview development and rates of disorders." J Autism Dev Disord **36**(7): 849-861.

Li, S. O., J. L. Wang, G. Bjorklund, W. N. Zhao and C. H. Yin (2014). "Serum copper and zinc levels in individuals with autism spectrum disorders." Neuroreport **25**(15): 1216-1220.

Lim, E. T., S. Raychaudhuri, S. J. Sanders, C. Stevens, A. Sabo, D. G. MacArthur, B. M. Neale, A. Kirby, D. M. Ruderfer, M. Fromer, M. Lek, L. Liu, J. Flannick, S. Ripke, U. Nagaswamy, D. Muzny, J. G. Reid, A. Hawes, I. Newsham, Y. Wu, L. Lewis, H. Dinh, S. Gross, L. S. Wang, C. F. Lin, O. Valladares, S. B. Gabriel, M. dePristo, D. M. Altshuler, S. M. Purcell, Nhlbi Exome Sequencing Project, M. W. State, E. Boerwinkle, J. D. Buxbaum, E. H. Cook, R. A. Gibbs, G. D. Schellenberg, J. S. Sutcliffe, B. Devlin, K. Roeder and M. J. Daly (2013). "Rare complete knockouts in humans: population distribution and significant role in autism spectrum disorders." Neuron **77**(2): 235-242.

Lin, A., A. Rangel and R. Adolphs (2012). "Impaired learning of social compared to monetary rewards in autism." Front Neurosci **6**: 143.

Liu, L., A. Sabo, B. M. Neale, U. Nagaswamy, C. Stevens, E. Lim, C. A. Bodea, D. Muzny, J. G. Reid, E. Banks, H. Coon, M. Depristo, H. Dinh, T. Fennel, J. Flannick, S. Gabriel, K. Garimella, S. Gross, A. Hawes, L. Lewis, V. Makarov, J. Maguire, I. Newsham, R. Poplin, S. Ripke, K. Shakir, K. E. Samocha, Y. Wu, E. Boerwinkle, J. D. Buxbaum, E. H. Cook, Jr., B. Devlin, G. D. Schellenberg, J. S. Sutcliffe, M. J. Daly, R. A. Gibbs and K. Roeder (2013). "Analysis of rare, exonic variation amongst subjects with autism spectrum disorders and population controls." PLoS Genet **9**(4): e1003443.

Loland, C. J., L. Norregaard and U. Gether (1999). "Defining proximity relationships in the tertiary structure of the dopamine transporter. Identification of a conserved glutamic acid as a third coordinate in the endogenous Zn(2+)-binding site." J Biol Chem **274**(52): 36928-36934.

Loland, C. J., L. Norregaard, T. Litman and U. Gether (2002). "Generation of an activating Zn(2+) switch in the dopamine transporter: mutation of an intracellular tyrosine constitutively alters the conformational equilibrium of the transport cycle." Proc Natl Acad Sci U S A **99**(3): 1683-1688.

Lord, C., S. Risi, L. Lambrecht, E. H. Cook, Jr., B. L. Leventhal, P. C. DiLavore, A. Pickles and M. Rutter (2000). "The autism diagnostic observation schedule-generic: a standard measure of social and communication deficits associated with the spectrum of autism." J Autism Dev Disord **30**(3): 205-223.

Lord, C., M. Rutter and A. Le Couteur (1994). "Autism Diagnostic Interview-Revised: a revised version of a diagnostic interview for caregivers of individuals with possible pervasive developmental disorders." J Autism Dev Disord **24**(5): 659-685.

Mackerell, A. D., Jr., M. Feig and C. L. Brooks, 3rd (2004). "Extending the treatment of backbone energetics in protein force fields: limitations of gas-phase quantum mechanics in reproducing protein conformational distributions in molecular dynamics simulations." J Comput Chem **25**(11): 1400-1415.

Mahajan, R., M. P. Bernal, R. Panzer, A. Whitaker, W. Roberts, B. Handen, A. Hardan, E. Anagnostou, J. Veenstra-VanderWeele and Committee Autism Speaks Autism Treatment Network Psychopharmacology (2012). "Clinical practice pathways for evaluation and medication choice for attention-deficit/hyperactivity disorder symptoms in autism spectrum disorders." Pediatrics **130 Suppl 2**: S125-138.

Matson, J. L., R. D. Rieske and L. W. Williams (2013). "The relationship between autism spectrum disorders and attention-deficit/hyperactivity disorder: an overview." Res Dev Disabil **34**(9): 2475-2484.

Matthies, H. J. and K. Broadie (2003). "Techniques to dissect cellular and subcellular function in the Drosophila nervous system." Methods Cell Biol **71**: 195-265.

Matthies, H. J., Q. Han, A. Shields, J. Wright, J. L. Moore, D. G. Winder, A. Galli and R. D. Blakely (2009). "Subcellular localization of the antidepressant-sensitive norepinephrine transporter." BMC Neurosci **10**: 65.

Mazei-Robison, M. S. and R. D. Blakely (2005). "Expression studies of naturally occurring human dopamine transporter variants identifies a novel state of transporter inactivation associated with Val382Ala." Neuropharmacology **49**(6): 737-749.

Mazei-Robison, M. S., E. Bowton, M. Holy, M. Schmudermaier, M. Freissmuth, H. H. Sitte, A. Galli and R. D. Blakely (2008). "Anomalous dopamine release associated with a human dopamine transporter coding variant." J Neurosci **28**(28): 7040-7046.

Mazei-Robison, M. S., R. S. Couch, R. C. Shelton, M. A. Stein and R. D. Blakely (2005). "Sequence variation in the human dopamine transporter gene in children with attention deficit hyperactivity disorder." Neuropharmacology **49**(6): 724-736.

McHaourab, H. S., Y. L. Lin and B. W. Spiller (2012). "Crystal structure of an activated variant of small heat shock protein Hsp16.5." Biochemistry **51**(25): 5105-5112.

McHaourab, H. S., P. R. Steed and K. Kazmier (2011). "Toward the fourth dimension of membrane protein structure: insight into dynamics from spin-labeling EPR spectroscopy." Structure **19**(11): 1549-1561.

McLaughlin, S. and D. Murray (2005). "Plasma membrane phosphoinositide organization by protein electrostatics." Nature **438**(7068): 605-611.

McLaughlin, S., J. Wang, A. Gambhir and D. Murray (2002). "PIP(2) and proteins: interactions, organization, and information flow." Annu Rev Biophys Biomol Struct **31**: 151-175.

Miller, E. K. and J. D. Cohen (2001). "An integrative theory of prefrontal cortex function." Annu Rev Neurosci **24**: 167-202.

Nakamura, K., A. Anitha, K. Yamada, M. Tsujii, Y. Iwayama, E. Hattori, T. Toyota, S. Suda, N. Takei, Y. Iwata, K. Suzuki, H. Matsuzaki, M. Kawai, Y. Sekine, K. J. Tsuchiya, G. Sugihara, Y. Ouchi, T. Sugiyama, T. Yoshikawa and N. Mori (2008). "Genetic and expression analyses reveal elevated expression of syntaxin 1A (STX1A) in high functioning autism." Int J Neuropsychopharmacol **11**(8): 1073-1084.

Nakamura, K., Y. Iwata, A. Anitha, T. Miyachi, T. Toyota, S. Yamada, M. Tsujii, K. J. Tsuchiya, Y. Iwayama, K. Yamada, E. Hattori, H. Matsuzaki, K. Matsumoto, K. Suzuki, S. Suda, K. Takebayashi, N. Takei, H. Ichikawa, T. Sugiyama, T. Yoshikawa and N. Mori (2011). "Replication study of Japanese cohorts supports the role of STX1A in autism susceptibility." Prog Neuropsychopharmacol Biol Psychiatry **35**(2): 454-458.

Nakamura, K., Y. Sekine, Y. Ouchi, M. Tsujii, E. Yoshikawa, M. Futatsubashi, K. J. Tsuchiya, G. Sugihara, Y. Iwata, K. Suzuki, H. Matsuzaki, S. Suda, T. Sugiyama, N. Takei and N. Mori (2010). "Brain serotonin and dopamine transporter bindings in adults with high-functioning autism." Arch Gen Psychiatry **67**(1): 59-68.

Neale, B. M., Y. Kou, L. Liu, A. Ma'ayan, K. E. Samocha, A. Sabo, C. F. Lin, C. Stevens, L. S. Wang, V. Makarov, P. Polak, S. Yoon, J. Maguire, E. L. Crawford, N. G. Campbell, E. T. Geller, O. Valladares, C. Schafer, H. Liu, T. Zhao, G. Cai, J. Lihm, R. Dannenfelser, O. Jabado, Z. Peralta, U. Nagaswamy, D. Muzny, J. G. Reid, I. Newsham, Y. Wu, L. Lewis, Y. Han, B. F. Voight, E. Lim, E. Rossin, A. Kirby, J. Flannick, M. Fromer, K. Shakir, T. Fennell, K. Garimella, E. Banks, R. Poplin, S. Gabriel, M. DePristo, J. R. Wimbish, B. E. Boone, S. E. Levy, C. Betancur, S. Sunyaev, E. Boerwinkle, J. D. Buxbaum, E. H. Cook, Jr., B. Devlin, R. A. Gibbs, K. Roeder, G. D. Schellenberg, J. S. Sutcliffe and M. J. Daly (2012). "Patterns and rates of exonic de novo mutations in autism spectrum disorders." Nature **485**(7397): 242-245.

Nemoda, Z., A. Szekely and M. Sasvari-Szekely (2011). "Psychopathological aspects of dopaminergic gene polymorphisms in adolescence and young adulthood." Neurosci Biobehav Rev **35**(8): 1665-1686.

Nguyen, M., A. Roth, E. J. Kyzar, M. K. Poudel, K. Wong, A. M. Stewart and A. V. Kalueff (2014). "Decoding the contribution of dopaminergic genes and pathways to autism spectrum disorder (ASD)." Neurochem Int **66**: 15-26.

Nieminen-von Wendt, T. S., L. Metsahonkala, T. A. Kulomaki, S. Aalto, T. H. Autti, R. Vanhala, O. Eskola, J. Bergman, J. A. Hietala and L. O. von Wendt (2004). "Increased presynaptic dopamine function in Asperger syndrome." Neuroreport **15**(5): 757-760.

Norregaard, L., D. Frederiksen, E. O. Nielsen and U. Gether (1998). "Delineation of an endogenous zinc-binding site in the human dopamine transporter." EMBO J **17**(15): 4266-4273.

Novak, G., T. Fan, B. F. O'Dowd and S. R. George (2013). "Striatal development involves a switch in gene expression networks, followed by a myelination event: implications for neuropsychiatric disease." Synapse **67**(4): 179-188.

O'Roak, B. J., L. Vives, S. Girirajan, E. Karakoc, N. Krumm, B. P. Coe, R. Levy, A. Ko, C. Lee, J. D. Smith, E. H. Turner, I. B. Stanaway, B. Vernot, M. Malig, C. Baker, B. Reilly, J. M. Akey, E. Borenstein, M. J. Rieder, D. A. Nickerson, R. Bernier, J. Shendure and E. E. Eichler (2012). "Sporadic autism exomes reveal a highly interconnected protein network of de novo mutations." Nature **485**(7397): 246-250.

Palmiter, R. D. (2008). "Dopamine signaling in the dorsal striatum is essential for motivated behaviors: lessons from dopamine-deficient mice." Ann N Y Acad Sci **1129**: 35-46.

Pendleton, R. G., A. Rasheed, T. Sardina, T. Tully and R. Hillman (2002). "Effects of tyrosine hydroxylase mutants on locomotor activity in Drosophila: a study in functional genomics." Behav Genet **32**(2): 89-94.

Penmatsa, A., K. H. Wang and E. Gouaux (2013). "X-ray structure of dopamine transporter elucidates antidepressant mechanism." Nature **503**(7474): 85-90.

Pifl, C., H. Drobny, H. Reither, O. Hornykiewicz and E. A. Singer (1995). "Mechanism of the dopamine-releasing actions of amphetamine and cocaine: plasmalemmal dopamine transporter versus vesicular monoamine transporter." Mol Pharmacol **47**(2): 368-373.

Pinto, D., A. T. Pagnamenta, L. Klei, R. Anney, D. Merico, R. Regan, J. Conroy, T. R. Magalhaes, C. Correia, B. S. Abrahams, J. Almeida, E. Bacchelli, G. D. Bader, A. J. Bailey, G. Baird, A. Battaglia, T. Berney, N. Bolshakova, S. Bolte, P. F. Bolton, T. Bourgeron, S. Brennan, J. Brian, S. E. Bryson, A. R. Carson, G. Casallo, J. Casey, B. H. Chung, L. Cochrane, C. Corsello, E. L. Crawford, A. Crossett, C. Cytrynbaum, G. Dawson, M. de Jonge, R. Delorme, I. Drmic, E. Duketis, F. Duque, A. Estes, P. Farrar, B. A. Fernandez, S. E. Folstein, E. Fombonne, C. M. Freitag, J. Gilbert, C. Gillberg, J. T. Glessner, J. Goldberg, A. Green, J. Green, S. J. Guter, H. Hakonarson, E. A. Heron, M. Hill, R. Holt, J. L. Howe, G. Hughes, V. Hus, R. Igliozzi, C. Kim, S. M. Klauck, A. Kolevzon, O. Korvatska, V. Kustanovich, C. M. Lajonchere, J. A. Lamb, M. Laskawiec, M. Leboyer, A. Le Couteur, B. L. Leventhal, A. C. Lionel, X. Q. Liu, C. Lord, L. Lotspeich, S. C. Lund, E. Maestrini, W. Mahoney, C. Mantoulan, C. R. Marshall, H. McConachie, C. J. McDougle, J. McGrath, W. M. McMahon, A. Merikangas, O. Migita, N. J. Minshew, G. K. Mirza, J. Munson, S. F. Nelson, C. Noakes, A. Noor, G. Nygren, G. Oliveira, K. Papanikolaou, J. R. Parr, B. Parrini, T. Paton, A. Pickles, M. Pilorge, J. Piven, C. P. Ponting, D. J. Posey, A. Poustka, F. Poustka, A. Prasad, J. Ragoussis, K. Renshaw, J. Rickaby, W. Roberts, K. Roeder, B. Roge, M. L. Rutter, L. J. Bierut, J. P. Rice, J. Salt, K. Sansom, D. Sato, R. Segurado, A. F. Sequeira, L. Senman, N. Shah, V. C. Sheffield, L. Soorya, I. Sousa, O. Stein, N. Sykes, V. Stoppioni, C. Strawbridge, R. Tancredi, K.

Tansey, B. Thiruvahindrapduram, A. P. Thompson, S. Thomson, A. Tryfon, J. Tsiantis, H. Van Engeland, J. B. Vincent, F. Volkmar, S. Wallace, K. Wang, Z. Wang, T. H. Wassink, C. Webber, R. Weksberg, K. Wing, K. Wittemeyer, S. Wood, J. Wu, B. L. Yaspan, D. Zurawiecki, L. Zwaigenbaum, J. D. Buxbaum, R. M. Cantor, E. H. Cook, H. Coon, M. L. Cuccaro, B. Devlin, S. Ennis, L. Gallagher, D. H. Geschwind, M. Gill, J. L. Haines, J. Hallmayer, J. Miller, A. P. Monaco, J. I. Nurnberger, Jr., A. D. Paterson, M. A. Pericak-Vance, G. D. Schellenberg, P. Szatmari, A. M. Vicente, V. J. Vieland, E. M. Wijsman, S. W. Scherer, J. S. Sutcliffe and C. Betancur (2010). "Functional impact of global rare copy number variation in autism spectrum disorders." Nature **466**(7304): 368-372.

Pizzo, A. B., C. S. Karam, Y. Zhang, C. L. Ma, B. D. McCabe and J. A. Javitch (2014). "Amphetamine-induced behavior requires CaMKII-dependent dopamine transporter phosphorylation." Mol Psychiatry **19**(3): 279-281.

Pizzo, A. B., C. S. Karam, Y. Zhang, H. Yano, R. J. Freyberg, D. S. Karam, Z. Freyberg, A. Yamamoto, B. D. McCabe and J. A. Javitch (2013). "The membrane raft protein Flotillin-1 is essential in dopamine neurons for amphetamine-induced behavior in Drosophila." Mol Psychiatry **18**(7): 824-833.

Qian, Y., M. Chen, H. Forssberg and R. Diaz Heijtz (2013). "Genetic variation in dopamine-related gene expression influences motor skill learning in mice." Genes Brain Behav **12**(6): 604-614.

Quick, M. W. (2002). "Role of syntaxin 1A on serotonin transporter expression in developing thalamocortical neurons." Int J Dev Neurosci **20**(3-5): 219-224.

Quick, M. W. (2003). "Regulating the conducting states of a mammalian serotonin transporter." Neuron **40**(3): 537-549.

Quick, M. W. (2006). "The role of SNARE proteins in trafficking and function of neurotransmitter transporters." Handb Exp Pharmacol(175): 181-196.

Rasmussen, T. N., P. Plenge, T. Bay, J. Egebjerg and U. Gether (2009). "A single nucleotide polymorphism in the human serotonin transporter introduces a new site for N-linked glycosylation." Neuropharmacology **57**(3): 287-294.

Reiersen, A. M. and A. A. Todorov (2011). "Association between DRD4 genotype and Autistic Symptoms in DSM-IV ADHD." J Can Acad Child Adolesc Psychiatry **20**(1): 15-21.

Rickhag, M., F. H. Hansen, G. Sorensen, K. N. Strandfelt, B. Andresen, K. Gotfryd, K. L. Madsen, I. Vestergaard-Klewe, I. Ammendrup-Johnsen, J. Eriksen, A. H. Newman, E. M. Fuchtbauer, J. Gomeza, D. P. Woldbye, G. Wortwein and U. Gether (2013). "A C-terminal PDZ domain-binding sequence is required for striatal distribution of the dopamine transporter." Nat Commun **4**: 1580.

Rickman, C. and R. R. Duncan "Munc18/Syntaxin interaction kinetics control secretory vesicle dynamics." J Biol Chem **285**(6): 3965-3972.

Risi, S., C. Lord, K. Gotham, C. Corsello, C. Chrysler, P. Szatmari, E. H. Cook, Jr., B. L. Leventhal and A. Pickles (2006). "Combining information from multiple sources in the diagnosis of autism spectrum disorders." J Am Acad Child Adolesc Psychiatry **45**(9): 1094-1103.

Robbins, J., S. J. Marsh and D. A. Brown (2006). "Probing the regulation of M (Kv7) potassium channels in intact neurons with membrane-targeted peptides." J Neurosci **26**(30): 7950-7961.

Robertson, S. D., H. J. Matthies and A. Galli (2009). "A closer look at amphetamine-induced reverse transport and trafficking of the dopamine and norepinephrine transporters." Mol Neurobiol **39**(2): 73-80.

Roman, T., L. A. Rohde and M. H. Hutz (2004). "Polymorphisms of the dopamine transporter gene: influence on response to methylphenidate in attention deficit-hyperactivity disorder." Am J Pharmacogenomics **4**(2): 83-92.

Ronald, A. and R. A. Hoekstra (2011). "Autism spectrum disorders and autistic traits: a decade of new twin studies." Am J Med Genet B Neuropsychiatr Genet **156B**(3): 255-274.

Ronald, A., E. Simonoff, J. Kuntsi, P. Asherson and R. Plomin (2008). "Evidence for overlapping genetic influences on autistic and ADHD behaviours in a community twin sample." J Child Psychol Psychiatry **49**(5): 535-542.

Ruiz-Montasell, B., F. Aguado, G. Majo, E. R. Chapman, J. M. Canals, J. Marsal and J. Blasi (1996). "Differential distribution of syntaxin isoforms 1A and 1B in the rat central nervous system." Eur J Neurosci **8**(12): 2544-2552.

Sali, A. and T. L. Blundell (1993). "Comparative protein modelling by satisfaction of spatial restraints." J Mol Biol **234**(3): 779-815.

Sanders, S. J., A. G. Ercan-Sencicek, V. Hus, R. Luo, M. T. Murtha, D. Moreno-De-Luca, S. H. Chu, M. P. Moreau, A. R. Gupta, S. A. Thomson, C. E. Mason, K. Bilguvar, P. B. Celestino-Soper, M. Choi, E. L. Crawford, L. Davis, N. R. Wright, R. M. Dhodapkar, M. DiCola, N. M. DiLullo, T. V. Fernandez, V. Fielding-Singh, D. O. Fishman, S. Frahm, R. Garagaloyan, G. S. Goh, S. Kammela, L. Klei, J. K. Lowe, S. C. Lund, A. D. McGrew, K. A. Meyer, W. J. Moffat, J. D. Murdoch, B. J. O'Roak, G. T. Ober, R. S. Pottenger, M. J. Raubeson, Y. Song, Q. Wang, B. L. Yaspan, T. W. Yu, I. R. Yurkiewicz, A. L. Beaudet, R. M. Cantor, M. Curland, D. E. Grice, M. Gunel, R. P. Lifton, S. M. Mane, D. M. Martin, C. A. Shaw, M. Sheldon, J. A. Tischfield, C. A. Walsh, E. M. Morrow, D. H. Ledbetter, E. Fombonne, C. Lord, C. L. Martin, A. I. Brooks, J. S. Sutcliffe, E. H. Cook, Jr., D. Geschwind, K. Roeder, B. Devlin and M. W. State (2011). "Multiple recurrent de novo CNVs, including duplications of the 7q11.23 Williams syndrome region, are strongly associated with autism." Neuron **70**(5): 863-885.

Sanders, S. J., M. T. Murtha, A. R. Gupta, J. D. Murdoch, M. J. Raubeson, A. J. Willsey, A. G. Ercan-Sencicek, N. M. DiLullo, N. N. Parikshak, J. L. Stein, M. F. Walker, G. T. Ober, N. A. Teran, Y. Song, P. El-Fishawy, R. C. Murtha, M. Choi, J. D. Overton, R. D. Bjornson, N. J. Carriero, K. A. Meyer, K. Bilguvar, S. M. Mane, N. Sestan, R. P. Lifton, M. Gunel, K. Roeder, D. H. Geschwind, B. Devlin and M. W. State (2012). "De novo mutations revealed by whole-exome sequencing are strongly associated with autism." Nature **485**(7397): 237-241.

Schiavo, G., C. C. Shone, M. K. Bennett, R. H. Scheller and C. Montecucco (1995). "Botulinum neurotoxin type C cleaves a single Lys-Ala bond within the carboxyl-terminal region of syntaxins." J Biol Chem **270**(18): 10566-10570.

Scott-Van Zeeland, A. A., M. Dapretto, D. G. Ghahremani, R. A. Poldrack and S. Y. Bookheimer (2010). "Reward processing in autism." Autism Res **3**(2): 53-67.

Sebat, J., B. Lakshmi, D. Malhotra, J. Troge, C. Lese-Martin, T. Walsh, B. Yamrom, S. Yoon, A. Krasnitz, J. Kendall, A. Leotta, D. Pai, R. Zhang, Y. H. Lee, J. Hicks, S. J. Spence, A. T. Lee, K. Puura, T. Lehtimaki, D. Ledbetter, P. K. Gregersen, J. Bregman, J. S. Sutcliffe, V. Jobanputra, W. Chung, D. Warburton, M. C. King, D. Skuse, D. H. Geschwind, T. C. Gilliam, K. Ye and M. Wigler (2007). "Strong association of de novo copy number mutations with autism." Science **316**(5823): 445-449.

Seeman, P. and H. B. Niznik (1990). "Dopamine receptors and transporters in Parkinson's disease and schizophrenia." FASEB J **4**(10): 2737-2744.

Shan, J., J. A. Javitch, L. Shi and H. Weinstein (2011). "The substrate-driven transition to an inward-facing conformation in the functional mechanism of the dopamine transporter." PLoS One **6**(1): e16350.

Sharp, K. A. and B. Honig (1990). "Electrostatic interactions in macromolecules: theory and applications." Annu Rev Biophys Biophys Chem **19**: 301-332.

Sherry, S. T., M. H. Ward, M. Kholodov, J. Baker, L. Phan, E. M. Smigielski and K. Sirotkin (2001). "dbSNP: the NCBI database of genetic variation." Nucleic Acids Res **29**(1): 308-311.

Sitte, H. H., S. Huck, H. Reither, S. Boehm, E. A. Singer and C. Pifl (1998). "Carrier-mediated release, transport rates, and charge transfer induced by amphetamine, tyramine, and

dopamine in mammalian cells transfected with the human dopamine transporter." J Neurochem **71**(3): 1289-1297.

Siuta, M. A., S. D. Robertson, H. Kocalis, C. Saunders, P. J. Gresch, V. Khatri, C. Shiota, J. P. Kennedy, C. W. Lindsley, L. C. Daws, D. B. Polley, J. Veenstra-Vanderweele, G. D. Stanwood, M. A. Magnuson, K. D. Niswender and A. Galli (2010). "Dysregulation of the norepinephrine transporter sustains cortical hypodopaminergia and schizophrenia-like behaviors in neuronal rictor null mice." PLoS Biol **8**(6): e1000393.

Sorkina, T., J. Caltagarone and A. Sorkin (2013). "Flotillins regulate membrane mobility of the dopamine transporter but are not required for its protein kinase C dependent endocytosis." Traffic **14**(6): 709-724.

Staal, W. G., M. de Krom and M. V. de Jonge (2012). "Brief report: the dopamine-3-receptor gene (DRD3) is associated with specific repetitive behavior in autism spectrum disorder (ASD)." J Autism Dev Disord **42**(5): 885-888.

Stanwood, G. D. and P. Levitt (2007). "Prenatal exposure to cocaine produces unique developmental and long-term adaptive changes in dopamine D1 receptor activity and subcellular distribution." J Neurosci **27**(1): 152-157.

Stockner, T., T. R. Montgomery, O. Kudlacek, R. Weissensteiner, G. F. Ecker, M. Freissmuth and H. H. Sitte (2013). "Mutational analysis of the high-affinity zinc binding site validates a refined human dopamine transporter homology model." PLoS Comput Biol **9**(2): e1002909.

Sturm, H., E. Fernell and C. Gillberg (2004). "Autism spectrum disorders in children with normal intellectual levels: associated impairments and subgroups." Dev Med Child Neurol **46**(7): 444-447.

Sucic, S., S. Dallinger, B. Zdrazil, R. Weissensteiner, T. N. Jorgensen, M. Holy, O. Kudlacek, S. Seidel, J. H. Cha, U. Gether, A. H. Newman, G. F. Ecker, M. Freissmuth and H. H. Sitte "The N terminus of monoamine transporters is a lever required for the action of amphetamines." J Biol Chem **285**(14): 10924-10938.

Sudhof, T. C. and J. E. Rothman (2009). "Membrane fusion: grappling with SNARE and SM proteins." Science **323**(5913): 474-477.

Suh, B. C. and B. Hille (2008). "PIP2 is a necessary cofactor for ion channel function: how and why?" Annu Rev Biophys **37**: 175-195.

Sulzer, D., T. K. Chen, Y. Y. Lau, H. Kristensen, S. Rayport and A. Ewing (1995). "Amphetamine redistributes dopamine from synaptic vesicles to the cytosol and promotes reverse transport." J Neurosci **15**(5 Pt 2): 4102-4108.

Sulzer, D., M. S. Sonders, N. W. Poulsen and A. Galli (2005). "Mechanisms of neurotransmitter release by amphetamines: a review." Prog Neurobiol **75**(6): 406-433.

Sung, U. and R. D. Blakely (2007). "Calcium-dependent interactions of the human norepinephrine transporter with syntaxin 1A." Mol Cell Neurosci **34**(2): 251-260.

Tassone, F., L. Qi, W. Zhang, R. L. Hansen, I. N. Pessah and I. Hertz-Picciotto (2011). "MAOA, DBH, and SLC6A4 variants in CHARGE: a case-control study of autism spectrum disorders." Autism Res **4**(4): 250-261.

Teng, F. Y., Y. Wang and B. L. Tang (2001). "The syntaxins." Genome Biol **2**(11): REVIEWS3012.

Van Esch, H., M. Bauters, J. Ignatius, M. Jansen, M. Raynaud, K. Hollanders, D. Lugtenberg, T. Bienvenu, L. R. Jensen, J. Gecz, C. Moraine, P. Marynen, J. P. Fryns and G. Froyen (2005). "Duplication of the MECP2 region is a frequent cause of severe mental retardation and progressive neurological symptoms in males." Am J Hum Genet **77**(3): 442-453.

van Rheenen, J., E. M. Achame, H. Janssen, J. Calafat and K. Jalink (2005). "PIP2 signaling in lipid domains: a critical re-evaluation." EMBO J **24**(9): 1664-1673.

Varnai, P. and T. Balla (1998). "Visualization of phosphoinositides that bind pleckstrin homology domains: calcium- and agonist-induced dynamic changes and relationship to myo-[3H]inositol-labeled phosphoinositide pools." J Cell Biol **143**(2): 501-510.

Varnai, P., X. Lin, S. B. Lee, G. Tuymetova, T. Bondeva, A. Spat, S. G. Rhee, G. Hajnoczky and T. Balla (2002). "Inositol lipid binding and membrane localization of isolated pleckstrin homology (PH) domains. Studies on the PH domains of phospholipase C delta 1 and p130." J Biol Chem **277**(30): 27412-27422.

Volkow, N. D., L. Chang, G. J. Wang, J. S. Fowler, D. Franceschi, M. Sedler, S. J. Gatley, E. Miller, R. Hitzemann, Y. S. Ding and J. Logan (2001). "Loss of dopamine transporters in methamphetamine abusers recovers with protracted abstinence." J Neurosci **21**(23): 9414-9418.

Volkow, N. D., G. J. Wang, M. W. Fischman, R. W. Foltin, J. S. Fowler, N. N. Abumrad, S. Vitkun, J. Logan, S. J. Gatley, N. Pappas, R. Hitzemann and C. E. Shea (1997). "Relationship between subjective effects of cocaine and dopamine transporter occupancy." Nature **386**(6627): 827-830.

Volkow, N. D., G. J. Wang, J. Newcorn, F. Telang, M. V. Solanto, J. S. Fowler, J. Logan, Y. Ma, K. Schulz, K. Pradhan, C. Wong and J. M. Swanson (2007). "Depressed dopamine activity in caudate and preliminary evidence of limbic involvement in adults with attention-deficit/hyperactivity disorder." Arch Gen Psychiatry **64**(8): 932-940.

Wall, D. P., R. Dally, R. Luyster, J. Y. Jung and T. F. Deluca (2012). "Use of artificial intelligence to shorten the behavioral diagnosis of autism." PLoS One **7**(8): e43855.

Wall, S. C., H. Gu and G. Rudnick (1995). "Biogenic amine flux mediated by cloned transporters stably expressed in cultured cell lines: amphetamine specificity for inhibition and efflux." Mol Pharmacol **47**(3): 544-550.

Wang, D., S. L. Deken, T. L. Whitworth and M. W. Quick (2003). "Syntaxin 1A inhibits GABA flux, efflux, and exchange mediated by the rat brain GABA transporter GAT1." Mol Pharmacol **64**(4): 905-913.

Wang, J. and D. A. Richards (2012). "Segregation of PIP2 and PIP3 into distinct nanoscale regions within the plasma membrane." Biol Open **1**(9): 857-862.

Wang, J. W., E. S. Beck and B. D. McCabe (2012). "A modular toolset for recombination transgenesis and neurogenetic analysis of Drosophila." PLoS One **7**(7): e42102.

Weiss, L. A., Y. Shen, J. M. Korn, D. E. Arking, D. T. Miller, R. Fossdal, E. Saemundsen, H. Stefansson, M. A. Ferreira, T. Green, O. S. Platt, D. M. Ruderfer, C. A. Walsh, D. Altshuler, A. Chakravarti, R. E. Tanzi, K. Stefansson, S. L. Santangelo, J. F. Gusella, P. Sklar, B. L. Wu, M. J. Daly and Consortium Autism (2008). "Association between microdeletion and microduplication at 16p11.2 and autism." N Engl J Med **358**(7): 667-675.

Whorton, M. R. and R. MacKinnon (2011). "Crystal structure of the mammalian GIRK2 K+ channel and gating regulation by G proteins, PIP2, and sodium." Cell **147**(1): 199-208.

Wicker-Thomas, C. and M. Hamann (2008). "Interaction of dopamine, female pheromones, locomotion and sex behavior in Drosophila melanogaster." J Insect Physiol **54**(10-11): 1423-1431.

Wise, R. A. (1998). "Drug-activation of brain reward pathways." Drug Alcohol Depend **51**(1-2): 13-22.

Wolfson, W. (2007). "Boston Autism Consortium searches for genetic clues to autism's puzzle." Chem Biol **14**(2): 117-118.

Yamashita, A., S. K. Singh, T. Kawate, Y. Jin and E. Gouaux (2005). "Crystal structure of a bacterial homologue of Na+/Cl--dependent neurotransmitter transporters." Nature **437**(7056): 215-223.

Yoo, H. J., I. H. Cho, M. Park, S. Y. Yang and S. A. Kim (2013). "Association of the catechol-o-methyltransferase gene polymorphisms with Korean autism spectrum disorders." J Korean Med Sci **28**(9): 1403-1406.

Yoshida, Y. and T. Uchiyama (2004). "The clinical necessity for assessing Attention Deficit/Hyperactivity Disorder (AD/HD) symptoms in children with high-functioning Pervasive Developmental Disorder (PDD)." Eur Child Adolesc Psychiatry **13**(5): 307-314.

Yu, Q., C. M. Teixeira, D. Mahadevia, Y. Huang, D. Balsam, J. J. Mann, J. A. Gingrich and M. S. Ansorge (2014). "Dopamine and serotonin signaling during two sensitive developmental periods differentially impact adult aggressive and affective behaviors in mice." Mol Psychiatry **19**(6): 688-698.

Zhao, Y., D. S. Terry, L. Shi, M. Quick, H. Weinstein, S. C. Blanchard and J. A. Javitch (2011). "Substrate-modulated gating dynamics in a Na+-coupled neurotransmitter transporter homologue." Nature **474**(7349): 109-113.

Zou, P. and H. S. McHaourab (2010). "Increased sensitivity and extended range of distance measurements in spin-labeled membrane proteins: Q-band double electron-electron resonance and nanoscale bilayers." Biophys J **98**(6): L18-20.